Part I

Between Maxwell and Shannon

1

The Digital Communications Point of View

When detailing how to dimension a transceiver, it can seem natural to first clarify what is expected from such a system. This means understanding both the minimum set of functions that need to be implemented in a transceiver line-up as well as the minimum performance expected from them. In practice, these requirements come from different topics which can be sorted into three groups. We can indeed refer to the signal processing associated with the modulations encountered in digital communications, to the physics of the medium used for the propagation of the information, and to the organization of wireless networks when considering a transceiver that belongs to such system, or alternatively its coexistence with such systems.

The last two topics are discussed in Chapter 2 and Chapter 3 respectively, while this chapter focuses on the consequences for transceiver architectures of the signal processing associated with the digital communications. In that perspective, a first set of functions to be embedded in such a system can be derived from the inspection of the relationship that holds between the modulating waveforms used in this area and the corresponding modulated RF signals to be propagated in the channel medium.

As a side effect, this approach enables us to understand how information that needs a complex baseband modulating signal to be represented can be carried by a simple real valued RF signal, thus leading to the key concept of the complex envelope. It is interesting to see that this concept allows us to define correctly classical quantities used to characterize RF signals and noise, in addition to its usefulness for performing analytical derivations. It is therefore used extensively throughout this book.

Finally, in this chapter we also review some particular modulation schemes that are representative of the different statistics that can be encountered in classical wireless standards. These schemes are then used as examples to illustrate subsequent derivations in this book.

Wireless Transceiver Architecture: Bridging RF and Digital Communications, First Edition. Pierre Baudin.

1.1 Bandpass Signal Representation

1.1.1 RF Signal Complex Modulation

Digital modulating waveforms in their most general form are represented by a complex signal function of time in digital communications books [1]. But, even if we understand that this complex signal allows us to increase the number of bits per second that can be transmitted by working on symbols using this two-dimensional space, a question remains. The final RF signal that carries the information, like the RF current or voltage generated at the transmitter (TX) output, is a real valued signal like any physical quantity that can be measured. Accordingly, we may wonder how the information that needs a complex signal to be represented can be carried by such an RF signal. Any RF engineer would respond by saying that an electromagnetic wave has an amplitude and a phase that can be modulated independently. Nevertheless, we can anticipate the discussion in Chapter 2, and in particular in Section 2.1.2, by saying that there is nothing in the electromagnetic theory that requires this particular structure for the time dependent part of the electromagnetic field. In fact, the right argument remains that this time dependent part, like any real valued signal, can be represented by two independent quantities that can be interpreted as its instantaneous amplitude and its instantaneous phase as long as it is a *bandpass* signal. Here, "bandpass signal" means that the spectral content of the signal has no low frequency component that spreads down to the zero frequency. In other words, the spectrum of the RF signal considered, whose positive and negative sidebands are assumed centered around $\pm\omega_c$, must be non-vanishing only for angular frequencies in $[-\omega_u - \omega_c, -\omega_c + \omega_l] \cup [+\omega_c - \omega_l, +\omega_c + \omega_u]$, with ω_c, ω_l and ω_u defined as positive quantities, and with $\omega_c > \omega_l$.

To understand this behavior, let us consider the complex baseband signal $\tilde{s}(t)$ expressed as

$$\tilde{s}(t) = p(t) + \mathrm{j}q(t), \tag{1.1}$$

where $p(t)$ and $q(t)$ are respectively the real and imaginary parts of this complex signal. We can assume that the spectrum of this signal spreads over $[-\omega_l, +\omega_u]$. Such baseband signals with a non-vanishing DC component in their spectrum are called *lowpass* signals in contrast to the bandpass signals as given above. If we now wish to shift the spectrum of this signal around the central carrier angular frequency $+\omega_c$, we have to convolve its spectrum with the Dirac delta distribution $\delta(\omega - \omega_c)$. In the time domain, this means multiplying the signal by the Fourier transform of this Dirac delta distribution, i.e. the complex exponential $e^{+j\omega_c t}$ [2]. This results in the complex signal $s_a(t)$ defined by

$$s_a(t) = \tilde{s}(t)e^{+j\omega_c t} = (p(t) + \mathrm{j}q(t))e^{+j\omega_c t}. \tag{1.2}$$

Suppose now that we take the real part of this signal. Using

$$e^{+j\omega t} = \cos(\omega t) + \mathrm{j}\sin(\omega t), \tag{1.3}$$

we get the classical form of the resulting RF signal $s(t)$ we are looking for,

$$s(t) = \mathrm{Re}\{s_a(t)\} = p(t)\cos(\omega_c t) - q(t)\sin(\omega_c t). \tag{1.4}$$

But what is interesting to see is that even if we took only the real part of the upconverted initial complex lowpass signal transposed around $+\omega_{\mathrm{c}}$, we have no loss of information compared to the initial complex baseband signal as long as $\omega_{\mathrm{c}} > \omega_{\mathrm{l}}$. Indeed, under that condition, the original complex modulating waveform $\tilde{s}(t)$ can be reconstructed from the bandpass RF real signal $s(t)$.

To understand this, let us first consider the spectral content of the resulting bandpass signal $s(t)$. What would be a good mathematical tool to choose for the spectral analysis? Dealing with digital modulations that are randomly modulated most of the time, the natural choice would be to use the stochastic approach to derive the signal power spectral density. The problem with this approach is that the power spectral density (PSD) of a signal is only linked to the modulus of the Fourier transform of the original signal. It thus leads to a loss of information compared to the time domain signal. As a result, in some cases of interest in this book, we need to keep the simple Fourier transform representation in order to be able to discuss the phase relationship between different sidebands present in the spectrum. Here, by “sideband” we mean a non-vanishing portion of spectrum of finite frequency support. This phase relationship is indeed required to understand the underlying phenomenon involved in concepts as reviewed in this chapter, but also in Chapter 6, for instance, when dealing with frequency conversion and image rejection. The existence of such Fourier transforms can be justified thanks to the practical finite temporal support of the signals of interest that ensures a finite energy. This is indeed the practical use case when dealing with the post-processing of a finite duration measurement or simulation result. The signals we deal with are therefore assumed to have a finite temporal support and a finite energy, i.e. they are assumed to belong to $L^2[0, T]$, the space of square-integrable functions over the bounded interval $[0, T]$. Nevertheless, when dealing with a randomly modulated signal, this approach means that we consider only the spectral properties of a single realization of the process of interest. Thus, even if this direct Fourier analysis is suitable for discussing some signal processing operations involved in transceivers, the power spectral analysis should be considered when possible for taking into account the statistical properties of the modulating process of interest, as done in “Power spectral density” (Section 1.1.3).

Let us therefore derive the Fourier transform of $s(t)$. As the aim is to make the link between the spectral representation of $s(t)$ and that of $\tilde{s}(t)$, we can first expand the relationship between $s(t)$ and the complex signal $s_{\mathrm{a}}(t)$ given by equation (1.4). To do so, we use the general property that for any complex number $\tilde{s}(t)$, we have

$$\mathrm{Re}\{\tilde{s}(t)\} = \frac{1}{2}(\tilde{s}(t) + \tilde{s}^*(t)), \tag{1.5}$$

where $\tilde{s}^*(t)$ stands for the complex conjugate of $\tilde{s}(t)$. This means that we can write

$$s(t) = \mathrm{Re}\{s_{\mathrm{a}}(t)\} = \frac{1}{2}(s_{\mathrm{a}}(t) + s_{\mathrm{a}}^*(t)). \tag{1.6}$$

Using the relationship between $s_{\mathrm{a}}(t)$ and $\tilde{s}(t)$ given by equation (1.2), we finally get that

$$s(t) = \frac{1}{2}\tilde{s}(t)\mathrm{e}^{+\mathrm{j}\omega_{\mathrm{c}}t} + \frac{1}{2}\tilde{s}^*(t)\mathrm{e}^{-\mathrm{j}\omega_{\mathrm{c}}t}. \tag{1.7}$$

It now remains to take the Fourier transform of this signal. For that, we can use two properties of the Fourier transform. The first states that for any signal, $\tilde{s}(t)$, the Fourier transform of the complex conjugate, $\tilde{s}^*(t)$, of such a signal can be related to that of $\tilde{s}(t)$ through

$$\begin{aligned}\mathcal{F}_{\{\tilde{s}^*(t)\}}(\omega) &= \int_{-\infty}^{+\infty} \tilde{s}^*(t)\mathrm{e}^{-\mathrm{j}\omega t}\mathrm{d}t \\ &= \left[\int_{-\infty}^{+\infty} \tilde{s}(t)\mathrm{e}^{+\mathrm{j}\omega t}\mathrm{d}t\right]^* \\ &= \left[\mathcal{F}_{\{\tilde{s}(t)\}}(-\omega)\right]^*. \end{aligned} \tag{1.8}$$

We observe that this derivation remains valid when $\tilde{s}(t)$ reduces to a real signal $s(t)$. In that case, having $s^*(t) = s(t)$ leads to having $S^*(-\omega) = S(\omega)$. We then recover the classical property of real signals, i.e. the Hermitian symmetry of their spectrum. Then we can use the property that the Fourier transform of a product of signals is equal to the convolution of the Fourier transforms of each signal. Indeed, we get that

$$\begin{aligned}\mathcal{F}_{\{\tilde{s}_1(t)\tilde{s}_2(t)\}}(\omega) &= \int_{-\infty}^{+\infty} \tilde{s}_1(t)\tilde{s}_2(t)\mathrm{e}^{-\mathrm{j}\omega t}\mathrm{d}t \\ &= \int_{-\infty}^{+\infty} \tilde{S}_1(\omega') \int_{-\infty}^{+\infty} \tilde{s}_2(t)\mathrm{e}^{-\mathrm{j}(\omega-\omega')t}\mathrm{d}t\mathrm{d}\omega' \\ &= \int_{-\infty}^{+\infty} \tilde{S}_1(\omega')\tilde{S}_2(\omega-\omega')\mathrm{d}\omega', \end{aligned} \tag{1.9}$$

i.e. that

$$\mathcal{F}_{\{\tilde{s}_1(t)\tilde{s}_2(t)\}}(\omega) = \mathcal{F}_{\{\tilde{s}_1(t)\}}(\omega) \star \mathcal{F}_{\{\tilde{s}_2(t)\}}(\omega). \tag{1.10}$$

Thus, using the two properties above, we get that the Fourier transform of equation (1.7) reduces to

$$S(\omega) = \frac{1}{2}\tilde{S}(\omega) \star \delta(\omega - \omega_\mathrm{c}) + \frac{1}{2}\tilde{S}^*(-\omega) \star \delta(\omega + \omega_\mathrm{c}), \tag{1.11}$$

where[1] $\tilde{S}(\omega)$ stands for the Fourier transform of $\tilde{s}(t)$ and where the Dirac delta distribution is the Fourier transform of the complex exponential. As this distribution is even, i.e. we have $\delta(\omega + \omega_\mathrm{c}) = \delta(-\omega - \omega_\mathrm{c})$, the spectrum of $s(t)$ can be expressed as the sum of two components as illustrated in Figure 1.1. The first component corresponds to the positive frequencies part, denoted $S_+(\omega)$, and is referred to as the positive sideband of the spectrum of $s(t)$. The second component corresponds to the negative part of the spectrum, $S_-(\omega)$, and is therefore referred to as the negative sideband of the spectrum of $s(t)$. As $s(t)$ is assumed to be bandpass, there is

[1] Recall our convention in this book that $\tilde{S}(\omega)$ stands for the spectral domain representation of the complex envelope $\tilde{s}(t)$ and not for the complex envelope of the signal $S(\omega)$.

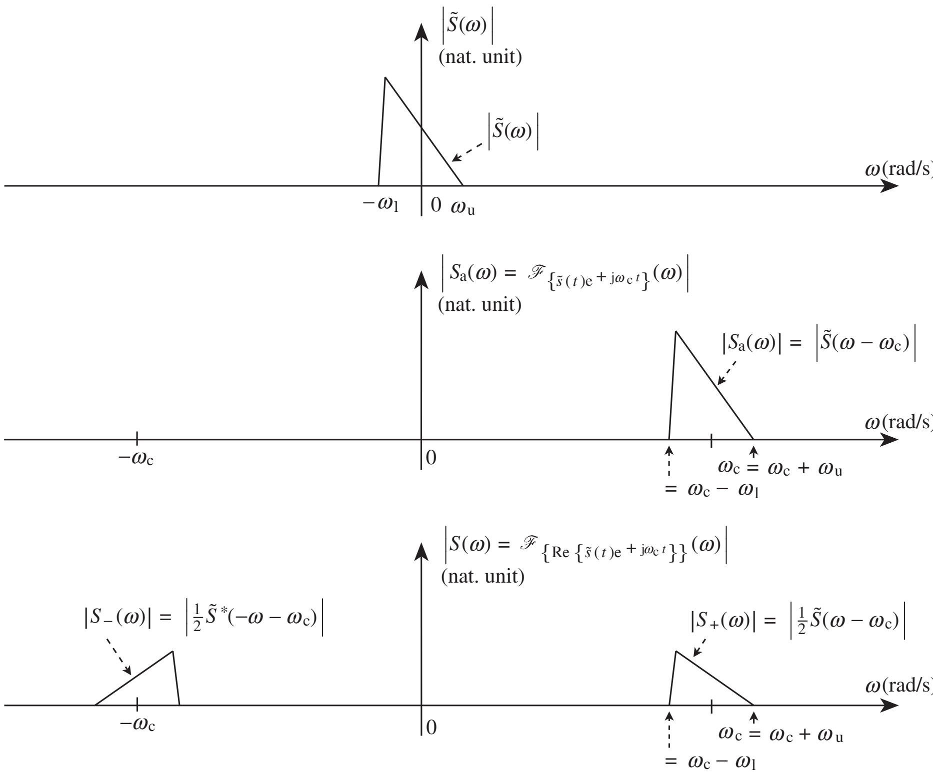

Figure 1.1 Spectral domain representation of the complex modulation of a real bandpass RF signal – The information linked to a complex lowpass signal, whose spectrum does not fulfill Hermitian symmetry (top), can be carried by a real bandpass signal as long as the intermediate complex upconverted signal is such that its spectrum does not spread toward zero frequency (middle), i.e. as long as $\omega_c > \omega_l$. In that case, the two sidebands of the spectrum of the resulting real bandpass signal do not overlap (bottom).

no overlap between those sidebands. They are thus defined without ambiguity from equation (1.11) as

$$\begin{aligned} S(\omega) &= \frac{1}{2}\tilde{S}(\omega - \omega_c) + \frac{1}{2}\tilde{S}^*(-\omega - \omega_c) \\ &= S_+(\omega) + S_-(\omega), \end{aligned} \tag{1.12}$$

where

$$S_+(\omega) = \frac{1}{2}\tilde{S}(\omega - \omega_c), \tag{1.13a}$$

$$S_-(\omega) = \frac{1}{2}\tilde{S}^*(-\omega - \omega_c). \tag{1.13b}$$

As expected for a real signal, the spectrum of $s(t)$ fulfills Hermitian symmetry as we have $S_-(\omega) = S_+^*(-\omega)$. Reconsidering our derivation so far, we thus see that $S_+(\omega)$ represents the spectrum of the initial complex signal $\tilde{s}(t)$ transposed around $+\omega_c$, whereas $S_-(\omega)$ represents the spectrum of the complex conjugate of the initial complex signal, i.e. of $\tilde{s}^*(t)$, transposed around $-\omega_c$. We therefore see that the action of taking the real part of $s_a(t)$ leads to a symmetrization of the spectrum by creating a negative part of the spectrum that is a flipped copy of its positive part. What is interesting to remark is that even if the resulting real RF signal spectrum fulfills Hermitian symmetry, the portion that lies in the positive frequencies part still represents precisely the initial complex lowpass signal spectrum. Consequently, as long as the resulting signal $s(t)$ is bandpass the two sidebands of its spectrum do not overlap. The initial complex lowpass signal can thus be reconstructed, theoretically without distortion, by downconversion to baseband of the positive sideband of the passband signal.

As a consequence of the concepts presented so far, we can see that in a transceiver, as long as we are dealing with a lowpass representation of a complex modulating waveform, $\tilde{s}(t)$, we need to work with two analog real quantities to represent, for instance, its real and imaginary parts $p(t)$ and $q(t)$. However, this is not required when working on the corresponding modulated real bandpass signal for which a representation using a single analog signal is always possible with no loss of information. We also mention that the real and imaginary parts are classically labeled $p(t)$ and $q(t)$, as used in this book, or alternatively as $i(t)$ and $q(t)$. The origin of these labels is that $p(t)$ or $i(t)$ stand for the in-phase component and $q(t)$ stands for the in-quadrature component of the bandpass signal as those lowpass modulating signals are carried by cosine and sine waveforms that are effectively in quadrature.

1.1.2 Complex Envelope Concept

We saw in Section 1.1.1 that a real bandpass RF signal can be modulated in such a way that it carries information that needs a complex lowpass modulating signal, i.e. two independent real baseband signals, to be represented. We can now go through the reverse process and examine how to reconstruct the equivalent complex lowpass modulating signal that represents the modulation of a given bandpass RF signal $s(t)$.

For that purpose, we can retain the approach of Section 1.1.1, i.e. assume that it is the positive sideband of $s(t)$ that is an image of the spectrum of the original complex lowpass modulating waveform. Let us first define the complex signal $s_a(t)$ whose spectral representation $S_a(\omega)$ is equal to twice the positive sideband of $s(t)$, i.e. such that

$$S_a(\omega) = 2\mathrm{U}(\omega)S(\omega), \tag{1.14}$$

where U(.) stands for the Heaviside step function. Here, the factor 2 is used for the sake of consistency with the definition introduced in Section 1.1.1. The signal $s_a(t)$ defined as such is said to be the *analytic* signal associated with $s(t)$. Based on its definition, we clearly get that this signal is unique, which is an important difference compared to the complex envelope concept defined later on. We observe that the term “analytic” is used for a signal whose spectrum is null for negative frequencies. This is thus the equivalent, in the spectral domain, of the causality concept encountered in the time domain. In order to recover the complex modulating waveform we are looking for, it thus remains to downconvert this analytic signal toward the zero frequency. In that perspective, it remains of interest to consider a time domain representation of $s_a(t)$. In doing so, rather than directly taking the inverse Fourier transform of equation (1.14), it is convenient to remark that an alternative expression for $S_a(\omega)$ is

$$\begin{aligned} S_a(\omega) &= S(\omega) + \mathrm{sign}\{\omega\}S(\omega) \\ &= S(\omega) + \mathrm{j}(-\mathrm{j}\,\mathrm{sign}\{\omega\})S(\omega), \end{aligned} \tag{1.15}$$

where sign{.} denotes the sign function. This expression is in fact the direct transcription of the cancellation of the negative part of the spectrum of $s(t)$ for expressing $s_a(t)$. If we now transpose this equation in the time domain, this signal can then be expressed as

$$s_a(t) = s(t) + \mathrm{j}\hat{s}(t), \tag{1.16}$$

where $\hat{s}(t)$ represents the signal resulting from the filtering of $s(t)$ by the filter whose transfer function can be expressed in the frequency domain as

$$-\mathrm{j}\,\mathrm{sign}\{\omega\} = \begin{cases} -\mathrm{j} & \text{when } \omega > 0, \\ 0 & \text{when } \omega = 0, \\ \mathrm{j} & \text{when } \omega < 0. \end{cases} \tag{1.17}$$

At this stage, it may be of interest to remark that this filter simply behaves as a $\pi/2$ phase shifter when acting on a bandpass signal. This can be highlighted by considering, for instance, its effect on a pure sine wave such as $s(t) = \cos(\omega_c t)$. Expanding the cosine function as the sum of two complex exponentials results in

$$\cos(\omega_c t) = \frac{1}{2}\left(e^{\mathrm{j}\omega_c t} + e^{-\mathrm{j}\omega_c t}\right). \tag{1.18}$$

Thus, considering the effect of the transfer function given by equation (1.17), we get that the first complex exponential, $e^{\mathrm{j}\omega_c t}$, changes to $-\mathrm{j}e^{\mathrm{j}\omega_c t}$ and the second one, $e^{-\mathrm{j}\omega_c t}$, changes to $\mathrm{j}e^{-\mathrm{j}\omega_c t}$. The signal recovered at the filter output is therefore the sine wave:

$$\sin(\omega_c t) = \frac{1}{2\mathrm{j}}\left(e^{\mathrm{j}\omega_c t} - e^{-\mathrm{j}\omega_c t}\right). \tag{1.19}$$

Given that $\sin(\omega t) = \cos(\omega t - \pi/2)$, we thus recover the expected behavior of a $\pi/2$ phase shifter. This effect can in fact be confirmed for any bandpass signals by reconsidering equation (1.17). Indeed, given that $\mathrm{j} = e^{\mathrm{j}\pi/2}$, we get that this filter simply subtracts a constant $\pi/2$ phase offset from all the frequency components of the input signal lying at positive frequencies and adds the same $\pi/2$ phase offset to all the components lying at negative frequencies, thus confirming the behavior of an ideal $\pi/2$ phase shifter. The transfer function of this filter can also be transposed in the time domain, thus leading to the implementation of a Hilbert transform corresponding to the convolution of the input signal with the distribution principal value of $1/(\pi t)$ [2]. The filter impulse response can thus be expressed in the distribution sense as

$$\hat{s}(t) = \text{pv}\left(\frac{1}{\pi t}\right) \star s(t) = \lim_{\epsilon \to 0} \frac{1}{\pi} \int_{|t'|>\epsilon} \frac{s(t-t')}{t'} \text{d}t', \tag{1.20}$$

where pv(.) stands for the Cauchy principal value.

Now that we have an expression for $s_\text{a}(t)$, it remains to downconvert this signal toward the zero frequency to recover the complex modulating waveform $\tilde{s}(t)$. This can be achieved by multiplying its time domain expression by the negative complex exponential $\text{e}^{-\text{j}\omega_\text{c} t}$ so that [2]

$$\tilde{s}(t) = s_\text{a}(t)\text{e}^{-\text{j}\omega_\text{c} t}. \tag{1.21}$$

Using equation (1.16) we then get that

$$\tilde{s}(t) = (s(t) + \text{j}\hat{s}(t))\text{e}^{-\text{j}\omega_\text{c} t}. \tag{1.22}$$

At first glance, the signal $\tilde{s}(t)$ defined this way matches the definition of the complex modulating waveform as defined in Section 1.1.1. This signal is called the complex envelope of the bandpass signal $s(t)$. The different steps for its construction are illustrated in the frequency domain in Figure 1.2. Alternatively, its real and imaginary parts, $p(t)$ and $q(t)$ respectively, can also be expressed in the time domain as functions of $s(t)$ and $\hat{s}(t)$ by expanding the above equation. This results in

$$p(t) = s(t)\cos(\omega_\text{c} t) + \hat{s}(t)\sin(\omega_\text{c} t), \tag{1.23a}$$

$$q(t) = \hat{s}(t)\cos(\omega_\text{c} t) - s(t)\sin(\omega_\text{c} t). \tag{1.23b}$$

Reconsidering our definitions so far, we observe that we have called $\tilde{s}(t)$ *the* complex envelope of the bandpass signal $s(t)$. But we should in fact say that $\tilde{s}(t)$ is *a* complex envelope of $s(t)$. Indeed, we defined the lowpass signal $\tilde{s}(t)$ by the downconversion of the analytic signal $s_\text{a}(t)$ around the zero frequency. This notion of "around" the zero frequency is somewhat imprecise. The point for the definition of this downconversion is only that the resulting signal must have a non-vanishing DC component in order to be effectively lowpass. We can thus define as many complex envelopes as we want for a given bandpass signal, depending on the chosen angular frequency ω_c used for the downconversion of its associated analytic signal. We see that this definition necessarily leads to an interesting relationship between the different complex envelopes that can be defined for a given bandpass signal. Indeed, considering for instance the complex envelopes $\tilde{s}_1(t)$ and $\tilde{s}_2(t)$ as defined through the downconversion of the analytic signal $s_\text{a}(t)$ using $\omega_{\text{c}1}$ and $\omega_{\text{c}2}$ respectively, we get that

$$\tilde{s}_1(t) = s_\text{a}(t)\text{e}^{-\text{j}\omega_{\text{c}1} t}, \tag{1.24a}$$

$$\tilde{s}_2(t) = s_\text{a}(t)\text{e}^{-\text{j}\omega_{\text{c}2} t}. \tag{1.24b}$$

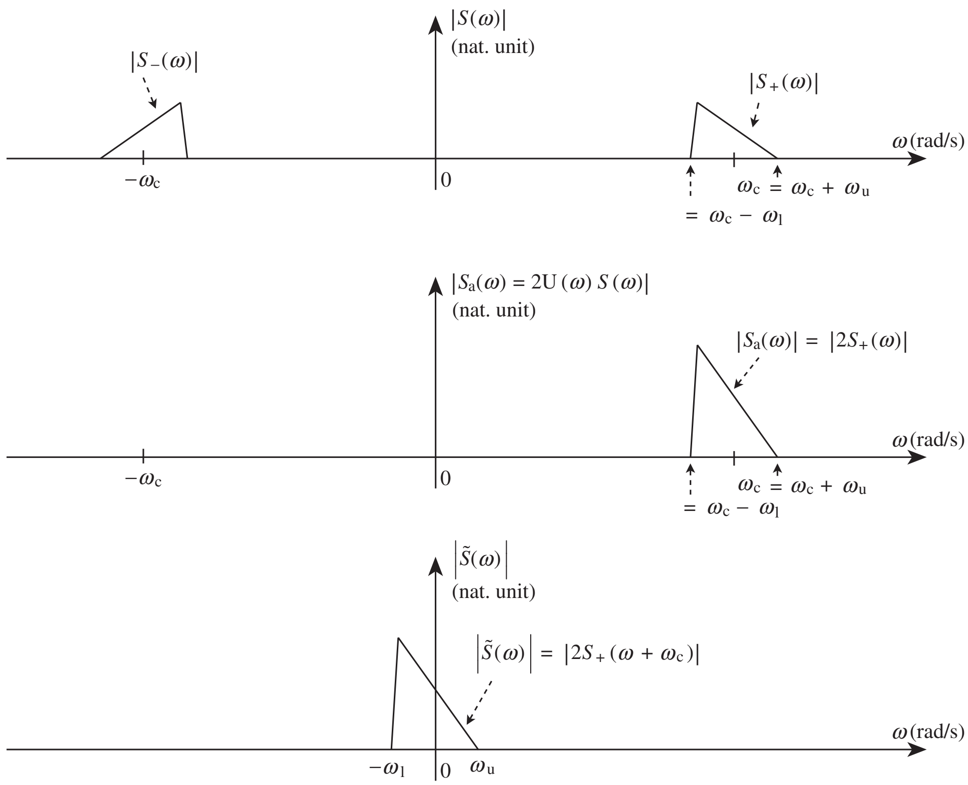

Figure 1.2 Illustration in the frequency domain of the complex envelope derivation of a bandpass RF signal – The analytic signal associated with a bandpass RF signal (top) is defined by considering twice its positive sideband (middle). The complex envelope then results from the downconversion to baseband of this analytic signal (bottom).

We thus have

$$\tilde{s}_1(t) = \tilde{s}_2(t)e^{-j(\omega_{c1}-\omega_{c2})t}. \tag{1.25}$$

Consequently, all the complex envelopes representing a given bandpass signal necessarily have the same modulus. There is only a continuous phase rotation difference between them. This property is important, as in transceiver budgets we often use such complex envelopes to perform analytic signal power evaluation for the purpose of signal to noise power ratio (SNR) budgets. And as illustrated for instance in "Average power" (Section 1.1.3) or throughout Chapter 5, it is the modulus of those complex envelopes that is involved in such evaluations. It is therefore good to see that the quantities involved in those derivations are well defined whatever the complex envelope considered. However, in digital communications, we generally do not have this kind of ambiguity in the selection of the center angular frequency used for the definition of the complex envelopes we deal with. Indeed, for reasons discussed in "Impact of spectral symmetry on top of stationarity" (Section 1.1.3), the complex lowpass modulating waveforms that are classically used in wireless systems almost always have a symmetrical PSD around the zero frequency, as illustrated for instance in Section 1.3. Thus, the angular frequency of the corresponding center of symmetry in the spectrum of the modulated RF bandpass signals remains a natural choice for the definition of the corresponding complex envelope.

Reconsidering our derivations so far, we see that we have derived an expression for the complex envelopes in their Cartesian form, i.e. through their real and imaginary parts $p(t)$ and $q(t)$. But, as for any complex number, we can instead use a polar representation. Denoting by $\rho(t)$ and $\phi(t)$ respectively the modulus and phase of the complex number $\tilde{s}(t)$, we can write

$$\tilde{s}(t) = p(t) + \mathrm{j}q(t) = \rho(t)\mathrm{e}^{\mathrm{j}\phi(t)}. \tag{1.26}$$

In this expression and throughout the rest of this book we assume that $\rho(t)$ is a positive quantity. This is indeed required in order to define $\phi(t)$ without ambiguity. Thus by using the Cartesian or polar representation of $\tilde{s}(t)$, we can derive two different (albeit equivalent) analytical expressions for the corresponding bandpass RF signal $s(t)$. Indeed, since by equations (1.2) and (1.4) we have that

$$s(t) = \mathrm{Re}\{s_\mathrm{a}(t)\} = \mathrm{Re}\left\{\tilde{s}(t)\mathrm{e}^{\mathrm{j}\omega_\mathrm{c}t}\right\}, \tag{1.27}$$

we can write, using either representation of $\tilde{s}(t)$,

$$s(t) = \mathrm{Re}\left\{(p(t) + \mathrm{j}q(t))\mathrm{e}^{\mathrm{j}\omega_\mathrm{c}t}\right\} = p(t)\cos(\omega_\mathrm{c}t) - q(t)\sin(\omega_\mathrm{c}t), \tag{1.28a}$$

$$= \mathrm{Re}\left\{\rho(t)\mathrm{e}^{\mathrm{j}(\omega_\mathrm{c}t+\phi(t))}\right\} = \rho(t)\cos(\omega_\mathrm{c}t + \phi(t)). \tag{1.28b}$$

We can thus see that the modulus of the complex envelope represents the amplitude part of the modulation of the corresponding bandpass RF signal, while its argument represents the phase/frequency part. In that sense, it is often said that an RF signal is complex modulated when it is both amplitude and phase/frequency modulated. We see here that this statement is not directly related to the nature of the corresponding complex envelope. The latter can only be a real signal for a pure amplitude modulation. A phase/frequency modulation is still said to be a real modulation scheme, whereas the corresponding complex envelope is truly complex, even if with a constant modulus. In practice a real modulation corresponds to a modulating signal that can be represented by a single real signal, i.e. either $\rho(t)$ or $\phi(t)$, regardless of the mathematical nature of the complex envelope. In this book we therefore reserve the term "complex modulated RF signals" for signals that are both amplitude and phase modulated.

In conclusion we highlight that, as illustrated in the next sections, the concept of the complex envelope is of particular importance as this lowpass signal embeds all the statistical characteristics of interest of the modulated bandpass RF signal it represents. We can thus say that from the signal processing point of view, the transceiver architecture reduces to how to upconvert or recover a given complex envelope while minimizing its degradation due to implementation limitations. We can also point out that such complex envelopes have additional practical advantages over the use of real bandpass signal representations when performing analytical derivations. The root cause for this comes from its complex nature that can allow for more straightforward analytical derivations. This behavior is illustrated for instance in Chapter 5 where the complex envelope polar notation allows easy analytical derivations when dealing with nonlinearity due to the fact that trigonometric polynomials are naturally linearized compared to power of sine and cosine functions. This complex nature is

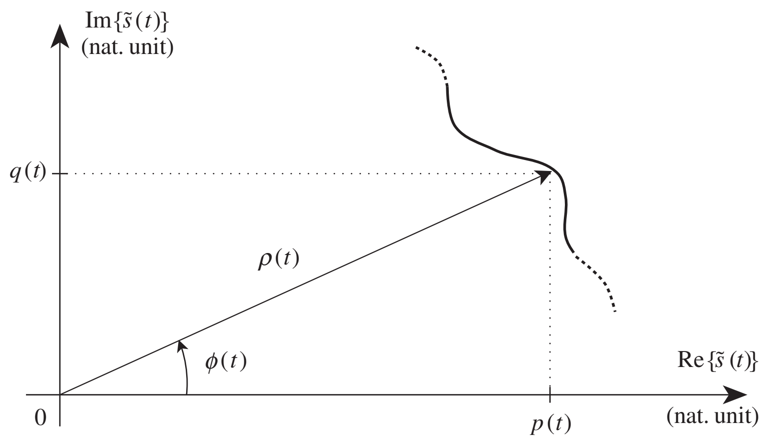

Figure 1.3 Complex envelope and corresponding trajectory representation in the complex plane – The complex envelope as well as the analytic signal concept allow vectorial representations for complex RF modulated signals. It can be seen as a generalization of the Fresnel representation used for continuous waves. The set of points that successively represent, in time, the complex envelope values, i.e. the extremity of its representative vector in the complex plane, define the trajectory of the modulation.

also of interest as it allows useful vectorial representations of signals in the complex plane. As shown in Figure 1.3, we are dealing here with a generalization of the Fresnel representation used for continuous waves. This approach leads to simple vectorial interpretations of analytical derivations that are often not so obvious to interpret directly. Furthermore, considering a simple practical modulating waveform, we get that the corresponding complex envelope describes a curve in the complex plane as a function of time. This curve represents what is called the trajectory associated with the modulating waveform. This trajectory in fact results from the pulse shaping filtering of the original sequence of symbols. If this pulse shaping filter does not introduce intersymbol interference (ISI), the trajectory simply links the symbols represented as a constellation in the complex plane. Some trajectory examples are shown in Section 1.3. Finally, we get that complex envelopes and the associated analytic signal concept allow us to correctly define the quantities of interest for characterizing RF signals, as illustrated in the following sections.

1.1.3 Bandpass Signals vs. Complex Envelopes

Due to the importance of the complex envelope concept introduced in the previous section, it is of interest to consider the characteristics of such complex lowpass signals in more detail, in particular with respect to the characteristics of the real bandpass signals they represent.

Positive vs. Negative Sidebands

Returning the definition of the complex envelope $\tilde{s}(t)$ of a real bandpass signal $s(t)$ given in Section 1.1.2, we see that we considered the positive sideband, i.e. the positive part of the spectrum, of that signal to define the associated analytic signal, $s_\mathrm{a}(t)$, the complex envelope being the downconversion of this analytic signal toward baseband. Practically speaking, this definition necessarily leads to the use of the negative complex exponential, i.e. the complex exponential with a negative angular frequency $e^{-j\omega_c t}$, for the ideal implementation of the downconversion processing of $s_a(t)$, as illustrated by equation (1.21). Conversely, it is thus the positive complex exponential, i.e. the complex exponential with a positive angular frequency $e^{+j\omega_c t}$, that was considered for the upconversion of an initial complex lowpass envelope in order to generate the corresponding modulated real bandpass signal according to equation (1.27). We might wonder whether we could consider the opposite choice for the complex exponentials. We observe that the processing corresponding to $\mathrm{Re}\{\tilde{s}(t)e^{-j\omega_c t}\}$ would result in a real bandpass signal that has the same spectral location as that corresponding to our definition so far. This would result in different characteristics for the resulting modulated signals.

By way of illustration, let us consider a first bandpass signal $s_1(t)$ resulting from the upconversion of the complex lowpass signal $\tilde{s}(t)$ following our legacy definition, i.e. using the positive complex exponential $e^{+j\omega_c t}$. According to Section 1.1.2, $s_1(t)$ can be written as

$$s_1(t) = \mathrm{Re}\left\{\tilde{s}(t)e^{+j\omega_c t}\right\}. \tag{1.29}$$

For our analysis, it is of interest to decompose this bandpass signal as the sum of two time domain bandpass signals that correspond to the two sidebands present in its spectrum, i.e. the positive one lying around $+\omega_c$ and the negative one lying around $-\omega_c$. We can use equation (1.5) to expand the real part in the above expression as

$$s_1(t) = \frac{1}{2}\tilde{s}^*(t)e^{-j\omega_c t} + \frac{1}{2}\tilde{s}(t)e^{+j\omega_c t}. \tag{1.30}$$

As expected, we recover a bandpass signal that is the sum of the upconversion of $\tilde{s}(t)$ around $+\omega_c$, and the upconversion of its complex conjugate $\tilde{s}^*(t)$ around $-\omega_c$. Those two bandpass signals centered around symmetric angular frequencies with respect to the zero frequency are obviously complex valued, but also complex conjugates to each other. This is indeed required in order to have the spectrum of the real valued signal $s_1(t)$ that exhibits Hermitian symmetry, as can be seen by taking the Fourier transform of the above expression. Using equation (1.8), we get that

$$S_1(\omega) = \frac{1}{2}\tilde{S}^*(-\omega - \omega_c) + \frac{1}{2}\tilde{S}(\omega - \omega_c). \tag{1.31}$$

We thus see that the sideband centered on $-\omega_c$ is a flipped copy of that corresponding to $\tilde{s}(t)$.

Let us now consider the upconversion of $\tilde{s}(t)$ using the negative complex exponential $e^{-j\omega_c t}$. This results in a second real bandpass signal $s_2(t)$ that can be expressed as

$$\begin{aligned} s_2(t) &= \mathrm{Re}\left\{\tilde{s}(t)e^{-j\omega_c t}\right\} \\ &= \frac{1}{2}\tilde{s}(t)e^{-j\omega_c t} + \frac{1}{2}\tilde{s}^*(t)e^{+j\omega_c t}, \end{aligned} \tag{1.32}$$

and whose representation in the frequency domain is given by

$$S_2(\omega) = \frac{1}{2}\tilde{S}(\omega + \omega_c) + \frac{1}{2}\tilde{S}^*(-\omega + \omega_c). \tag{1.33}$$

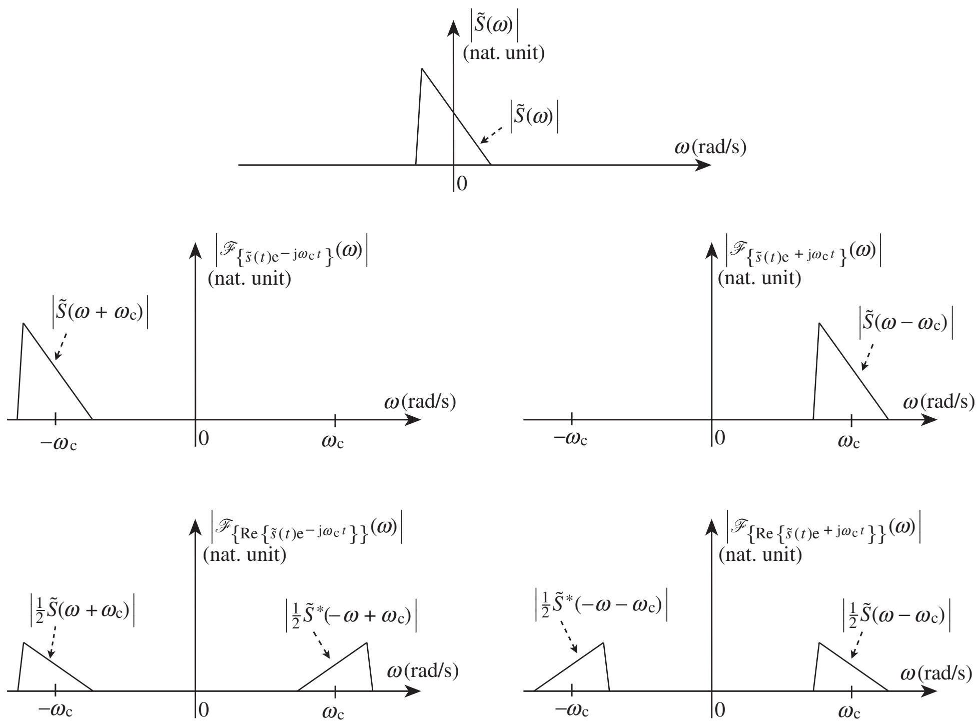

Figure 1.4 Spectral domain representation of the complex envelope frequency upconversion and resulting RF bandpass signal – Depending on the sign of the complex exponential, $e^{+j\omega_c t}$ (middle right) or $e^{-j\omega_c t}$ (middle left), used for the frequency upconversion, the same complex lowpass envelope (top) results in different RF bandpass signals. In the first case, the positive sideband of the resulting spectrum corresponds to the spectrum of the original complex envelope (bottom right) whereas in the second case, it corresponds to a flipped copy of it (bottom left).

Comparing this expression with equation (1.31), we see that we now face an inversion of the positive and negative sidebands of the spectrum of $s_2(t)$ with respect to those of $s_1(t)$, as illustrated in Figure 1.4. Reconsidering this figure and equation (1.32), we can moreover see that $s_2(t)$ can alternatively be interpreted as the result of the upconversion of the complex lowpass signal $\tilde{s}^*(t)$ using the positive complex exponential $e^{+j\omega_c t}$.

The same kind of comment applies when considering the downconversion operation performed to recover the complex envelope of a given bandpass signal. Indeed, depending on whether we use the negative or the positive complex exponential to perform the operation, we obtain through this processing either the positive or the negative sideband of the original bandpass signal. Moreover, depending on whether the bandpass signal considered for such downconversion has been originally generated by the upconversion of an initial complex envelope through the use of the negative or the positive complex exponential, we can finally recover at the output of the downconversion process the sideband that corresponds to the complex conjugate of the initially upconverted complex envelope. In fact, this is not so problematic as it is just a matter of a complex conjugate operation in the complex envelope and hence of managing the sign of the $q(t)$ modulating component. We then get that the choice of sideband transmitted on the positive part of the resulting RF bandpass signal spectrum can be simply made through this $q(t)$ sign selection. We observe that for a given standardized modulation scheme definition, the convention is often that the positive sideband of the resulting bandpass signal corresponds to $\tilde{s}(t) = p(t) + \mathrm{j}q(t)$ and the negative sideband to its complex conjugate. Consequently, in this book we mostly assume that theoretical upconversions are implemented using the positive complex exponential $\mathrm{e}^{+\mathrm{j}\omega_c t}$ and reciprocal downconversions with the corresponding negative complex exponential, $\mathrm{e}^{-\mathrm{j}\omega_c t}$. Trickier configurations can occur in practical architecture choices. In some transceiver implementations we can indeed consider successive up- or downconversions based on the selection of different sidebands to be transposed each time. This may be the case in order to optimize the frequency planning of the transceiver through the use of supradyne or infradyne conversions. This topic is discussed in Chapter 6 when dealing with more general real and complex frequency conversions.

Power Spectral Density

So far, we have used Fourier transforms directly to examine the spectral representation of a given signal. As discussed in Section 1.1.1, this was done with the aim of keeping the good phase relationship between the signal sidebands and thus interpreting the behavior of a signal processing function in the frequency domain. However, for digital modulation schemes generated through random data bits, the Fourier transform only provides a frequency representation of a given realization of the modulating process over a finite time frame. It is thus of interest to derive the PSD of those randomly modulated waveforms, taking into account their statistical properties. Given that the complex envelope $\tilde{s}(t)$ of an RF bandpass signal $s(t)$ contains all its statistical information, it is of interest to examine the link between the power spectral densities of these two signals.

The simplest way to proceed is to derive the autocorrelation function of $s(t)$ in order to take its Fourier transform [3, 4]. We suppose that we are dealing with stationary bandpass signals, at least up to second order. This is an assumption we can rely on in most cases for processes we have to deal with in wireless transceivers, as discussed in Appendix 2. Assuming the ergodicity of the modulating process, we get that the autocorrelation function of $s(t)$, defined by

$$\gamma_{s\times s}(t_1, t_2) = \lim_{\substack{\tau_1 \to -\infty \\ \tau_2 \to +\infty}} \frac{1}{\tau_2 - \tau_1} \int_{\tau_1}^{\tau_2} s(t - t_1)s(t - t_2)\mathrm{d}t, \tag{1.34}$$

can be evaluated as

$$\gamma_{s\times s}(t_1, t_2) = \mathbb{E}\left\{s_{t_1} s_{t_2}\right\}. \tag{1.35}$$

Here $\mathbb{E}\{.\}$ stands for the stochastic expectation value and s_t for the random variable corresponding to the sample of $s(t)$ at time t. In order to go further, we can then use the fact that $s(t)$ is related to its complex envelope $\tilde{s}(t)$, assumed defined as centered around the angular frequency ω_c, according to equation (1.7). As a result, the above expectation can be written as

$$\gamma_{s\times s}(t_1, t_2) = \frac{1}{4}\mathbb{E}\left\{\left(\tilde{s}_{t_1}\mathrm{e}^{\mathrm{j}\omega_c t_1} + \tilde{s}^*_{t_1}\mathrm{e}^{-\mathrm{j}\omega_c t_1}\right)\left(\tilde{s}_{t_2}\mathrm{e}^{\mathrm{j}\omega_c t_2} + \tilde{s}^*_{t_2}\mathrm{e}^{-\mathrm{j}\omega_c t_2}\right)\right\}. \tag{1.36}$$

After expansion, we finally get that

$$\begin{aligned}\gamma_{s\times s}(t_1, t_2) = {} & \frac{1}{4}\mathbb{E}\left\{\tilde{s}_{t_1}\tilde{s}^*_{t_2}\right\}\mathrm{e}^{\mathrm{j}\omega_c(t_1-t_2)} + \frac{1}{4}\mathbb{E}\left\{\tilde{s}^*_{t_1}\tilde{s}_{t_2}\right\}\mathrm{e}^{-\mathrm{j}\omega_c(t_1-t_2)} \\ & + \frac{1}{2}\mathrm{Re}\left\{\mathbb{E}\left\{\tilde{s}_{t_1}\tilde{s}_{t_2}\right\}\mathrm{e}^{\mathrm{j}\omega_c(t_1+t_2)}\right\}.\end{aligned} \tag{1.37}$$

As discussed in Appendix 2, a side effect of the stationarity of $s(t)$, at least up to second order, is that any of its complex envelopes must fulfill equation (A2.11). We thus get in particular that $\mathbb{E}\left\{\tilde{s}_{t_1}\tilde{s}_{t_2}\right\} = 0$, and that the autocorrelation of $s(t)$ finally reduces to

$$\gamma_{s\times s}(t_1, t_2) = \gamma_{s\times s}(\tau) = \frac{1}{4}\gamma_{\tilde{s}\times\tilde{s}}(\tau)\mathrm{e}^{\mathrm{j}\omega_c\tau} + \frac{1}{4}\gamma_{\tilde{s}\times\tilde{s}}(-\tau)\mathrm{e}^{-\mathrm{j}\omega_c\tau}. \tag{1.38}$$

with $\tau = t_1 - t_2$.

We can then derive the PSD of $s(t)$ by taking the Fourier transform of this autocorrelation function.[2] For this, we can use the Fourier transform property, valid for all signals real or complex, that links the Fourier transform of a signal with that of its time reversal copy according to

$$\begin{aligned}\mathcal{F}_{\{\tilde{s}(-t)\}}(\omega) &= \int_{-\infty}^{+\infty}\tilde{s}(-t)\mathrm{e}^{-\mathrm{j}\omega t}\mathrm{d}t \\ &= \int_{-\infty}^{+\infty}\tilde{s}(t)\mathrm{e}^{-\mathrm{j}(-\omega)t}\mathrm{d}t \\ &= \mathcal{F}_{\{\tilde{s}(t)\}}(-\omega).\end{aligned} \tag{1.39}$$

Thus, using this property while taking the Fourier transform of equation (1.38) finally results in

$$\Gamma_{s\times s}(\omega) = \frac{1}{4}\Gamma_{\tilde{s}\times\tilde{s}}(\omega - \omega_c) + \frac{1}{4}\Gamma_{\tilde{s}\times\tilde{s}}(-\omega - \omega_c). \tag{1.40}$$

[2] Here and in the rest of this book, we follow the signal processing approach for the definition of the PSD, i.e. we implicitly assume that we are working with normalized impedances when dealing with analog quantities for $s(t)$. Otherwise, as illustrated in Section 2.2.3, a factor $\mathrm{Re}\{1/Z_0\}$ should appear when $s(t)$ represents a voltage over an impedance Z_0. In the same way, a factor $\mathrm{Re}\{Z_0\}$ should appear when $s(t)$ represents a current across Z_0. But in most formulas derived in this book, only relative power quantities are involved so that such normalization factors cancel, as illustrated for instance in Chapter 5, in "Characterization of RF device nonlinearity" (Section 5.1.2). Nevertheless, for the derivation of the absolute PSD of an analog quantity across a given load, the reader needs to add the corresponding impedance term compared to the results derived in this book.

As might be expected for the modulated bandpass RF signal $s(t)$ that corresponds to the frequency upconversion of the lowpass modulating signal $\tilde{s}(t)$, its PSD is simply proportional to that of $\tilde{s}(t)$ once transposed around the angular frequencies $\pm\omega_c$. Here, we recover that the resulting sideband of the spectrum lying at negative frequencies is the flipped version of the original lowpass signal spectrum, i.e. a transposition of $\Gamma_{\tilde{s}\times\tilde{s}}(-\omega)$ around $-\omega_c$. As highlighted in earlier sections, this behavior is related to the Hermitian symmetry that must be retrieved on the Fourier transform of any real signal. We also observe that each sideband of the PSD of the bandpass signal $s(t)$, i.e. both that centered on $+\omega_c$ and that centered on $-\omega_c$, is one fourth that of its complex envelope. This means that the integration of the PSD of such sideband corresponds to one half the original complex envelope signal power. As discussed in "Average power" later in this section, this can be linked to the convention followed in this book for the definition of this complex lowpass signal that is defined as twice the positive sideband of the original bandpass signal it represents.

Impact of Stationarity

In the previous section, we assumed the bandpass signal $s(t)$ to be stationary in order to derive its PSD. However, we did not examine all the resulting characteristics of the spectrum for such stationarity. In particular, in the light of the derivations performed in Appendix 2, we get that the stationarity of $s(t)$ implies that all of its complex envelopes $\tilde{s}(t)$ satisfy equation (A2.11), i.e.

$$\gamma_{\tilde{s}\times\tilde{s}^*}(\tau) = 0. \tag{1.41}$$

We can then expand this equation in terms of the real and imaginary parts of $\tilde{s}(t) = p(t) + \mathrm{j}q(t)$ following equation (A1.46b). Referring to equation (A2.13a), we then get that

$$\gamma_{p\times p}(\tau) = \gamma_{q\times q}(\tau). \tag{1.42}$$

Now taking the Fourier transform of this equation leads to

$$\Gamma_{p\times p}(\omega) = \Gamma_{q\times q}(\omega). \tag{1.43}$$

We thus recover the remarkable result that the stationarity of $s(t)$ implies that the real and imaginary parts of any of its complex envelopes have the same PSD. We observe that this result is related to the discussion in Appendix 2 that gives more insight into the conditions required to achieve the generation of an RF bandpass signal that is stationary.

Impact of Spectral Symmetry on Top of Stationarity

Let us now go a step further and suppose that on top of dealing with a stationary bandpass signal $s(t)$, at least up to second order, we also face an even symmetry in the PSD of either of its sidebands when inspected independently of the other one. Referring to equation (1.40), we get that the spectral shape of the sidebands of such bandpass signal is proportional to that of any of its complex envelopes. We thus get for instance that a symmetry regarding the zero frequency in the spectrum of such complex envelope, let say $\tilde{s}(t)$, necessarily corresponds to a symmetry regarding ω_c of the positive sideband of $s(t)$, ω_c being the center angular frequency chosen for the definition of $\tilde{s}(t)$. The point is that such a characteristic leads to interesting properties.

In order to examine this, let us assume that the PSD of $\tilde{s}(t)$ exhibits an even symmetry, i.e. is such that

$$\Gamma_{\tilde{s}\times\tilde{s}}(\omega) = \Gamma_{\tilde{s}\times\tilde{s}}(-\omega). \tag{1.44}$$

At the same time, we know from the results derived in Appendix 1 that the PSD of any process is necessarily a real valued function. Thus the relationship

$$\Gamma_{\tilde{s}\times\tilde{s}}(\omega) = \Gamma^{*}_{\tilde{s}\times\tilde{s}}(\omega) \tag{1.45}$$

always holds. From the above two equations, we can thus deduce that the complex envelope considered fulfills

$$\Gamma^{*}_{\tilde{s}\times\tilde{s}}(\omega) = \Gamma_{\tilde{s}\times\tilde{s}}(-\omega). \tag{1.46}$$

This means that the even symmetry in the PSD of $\tilde{s}(t)$ leads to a quantity that exhibits Hermitian symmetry. Thus, recalling the property discussed during the derivation of equation (1.8), we can deduce that the autocorrelation function of $\tilde{s}(t)$, $\gamma_{\tilde{s}\times\tilde{s}}(\tau)$, is necessarily a real valued function. So its imaginary part must be null. We then deduce from equation (A1.46a) that

$$\gamma_{p\times q}(-\tau) - \gamma_{p\times q}(\tau) = 0. \tag{1.47}$$

On the other hand, we get that any complex envelope of a stationary bandpass signal necessarily fulfills equation (1.41). Using equation (A1.46b) to expand $\gamma_{\tilde{s}\times\tilde{s}^{*}}(\tau)$ in terms of the real and imaginary parts of $\tilde{s}(t) = p(t) + \mathrm{j}q(t)$, we then get that

$$\gamma_{p\times q}(-\tau) + \gamma_{p\times q}(\tau) = 0. \tag{1.48}$$

From the above two equations, we thus deduce that

$$\gamma_{p\times q}(\tau) = \gamma_{q\times p}(\tau) = 0. \tag{1.49}$$

The real and imaginary parts of $\tilde{s}(t) = p(t) + \mathrm{j}q(t)$ are thus necessarily uncorrelated, even when considered at different times. This is obviously a new property as, according to Appendix 2, the stationarity of $s(t)$ implies that $p(t)$ and $q(t)$ are uncorrelated when considered at the same time t.

Conversely, considering a complex lowpass signal $\tilde{s}(t) = p(t) + \mathrm{j}q(t)$ such that equation (1.49) holds, we necessarily get that $\gamma_{\tilde{s}\times\tilde{s}}(\tau)$ is a real valued quantity by equation (A1.46a). It follows that the PSD of $\tilde{s}(t)$, which reduces to the Fourier transform of this autocorrelation function, satisfies Hermitian symmetry. But, given at the same time that this quantity is also real valued, we then recover the even spectral symmetry of this PSD, i.e. that $\Gamma_{\tilde{s}\times\tilde{s}}(\omega) = \Gamma_{\tilde{s}\times\tilde{s}}(-\omega)$. As highlighted at the beginning of the derivation, this symmetry property is thus necessarily recovered on the sidebands of the corresponding modulated bandpass signal $s(t)$ relative to the angular frequency ω_c used for the definition of the complex envelope $\tilde{s}(t)$. At the same time, we get that most of the modulating waveforms used in practical wireless standards are defined such that $\gamma_{p\times q}(\tau) = \gamma_{q\times p}(\tau) = 0$, as discussed in Appendix 2. This explains why this even spectral symmetry in the spectrum of modulated bandpass signals is encountered in most practical cases. In spite of this, we often represent the spectrum as asymmetrical throughout this book. This allows us to clearly highlight which sideband we are dealing with, i.e. whether the complex envelope we are dealing with is $\tilde{s}(t) = p(t) + \mathrm{j}q(t)$ or its complex conjugate $\tilde{s}^*(t) = p(t) - \mathrm{j}q(t)$ as discussed in "Positive vs. negative sidebands" earlier in this section. Given that those complex envelopes are complex conjugates to each other, it follows that their Fourier transforms are related as in equation (1.8), i.e. their magnitudes are symmetric to each other with respect to the zero frequency. Thus, representing them as asymmetrical allows us to distinguish easily between them, even if, when $p(t)$ and $q(t)$ are uncorrelated, the modulus of their Fourier transform, and thus their power spectral densities, are evenly symmetrical. In this last case, it is only the argument of their Fourier transform that remains an odd function of the frequency, and it is only the phase difference between them that distinguishes these sidebands.

We can even go a step further. Recall that for a stationary bandpass signal $s(t)$, the real and imaginary parts of any of its complex envelopes $\tilde{s}(t) = p(t) + \mathrm{j}q(t)$ necessarily have the same autocorrelation function as given by equation (1.42). Thus, if we now assume that we are also dealing with a signal whose spectrum exhibits the even symmetry discussed above, we necessarily have that $p(t)$ and $q(t)$ are also uncorrelated as given by equation (1.49). Based on those two results, equation (A1.46a) reduces to

$$\gamma_{\tilde{s}\times\tilde{s}}(\tau) = \gamma_{p\times p}(\tau) + \gamma_{q\times q}(\tau) = 2\gamma_{p\times p}(\tau) = 2\gamma_{q\times q}(\tau). \tag{1.50}$$

Now taking the Fourier transform of this equation, we finally obtain

$$\Gamma_{\tilde{s}\times\tilde{s}}(\omega) = \Gamma_{p\times p}(\omega) + \Gamma_{q\times q}(\omega) = 2\Gamma_{p\times p}(\omega) = 2\Gamma_{q\times q}(\omega). \tag{1.51}$$

We now see that $\tilde{s}(t)$ and thus $s(t)$ also have the same spectral shape as $p(t)$ and $q(t)$ when this spectrum is evenly symmetric regarding the carrier center angular frequency used to define the complex envelope. Practically speaking, this property is important not only for the study of modulated RF bandpass signals but also for RF bandpass noise, as discussed in Section 1.2. Indeed, the stationarity of an RF bandpass noise source allows us to link the PSD of the bandpass noise term $n(t)$ it delivers to its load, to the PSD of the real and imaginary parts of any of its complex envelopes $\tilde{n}(t)$. It is important to link the properties of the noise terms at the input and output of a complex frequency conversion, for instance.

Average Power

Let us now focus on the average power of a bandpass signal, or more precisely on the link between this quantity and the statistical properties of any of its complex envelopes. Let us consider the expression for the bandpass signal $s(t)$ as a function of its complex envelope $\tilde{s}(t)$, defined as centered around the carrier angular frequency ω_c. According to equation (1.27), this expression reduces to

$$s(t) = \mathrm{Re}\left\{\tilde{s}(t)\mathrm{e}^{+\mathrm{j}\omega_c t}\right\}. \tag{1.52}$$

In order to derive the average power of this signal, we can thus consider further either the direct time domain average or the stochastic approach. Under ergodicity, the two approaches are expected to give the same result. Here, we initially adopt the time domain average approach as it leads to an intuitive explanation for the result when considering the derivation in the frequency domain.

Let us therefore evaluate the long-term average power P_s of this bandpass signal as its root mean square (RMS) value. Considering the complex envelope $\tilde{s}(t)$ expressed in its polar form as $\tilde{s}(t) = \rho(t)\mathrm{e}^{\mathrm{j}\phi(t)}$, we can then write:[3]

$$P_s = \lim_{\substack{\tau_1 \to -\infty \\ \tau_2 \to +\infty}} \frac{1}{\tau_2 - \tau_1} \int_{\tau_1}^{\tau_2} [\rho(t)\cos(\omega_c t + \phi(t))]^2 \mathrm{d}t. \tag{1.53}$$

In order to evaluate this integral, we can linearize the cosine function using

$$\cos^2(\theta) = \frac{1 + \cos(2\theta)}{2}. \tag{1.54}$$

This leads to

$$\begin{aligned} P_s = & \lim_{\substack{\tau_1 \to -\infty \\ \tau_2 \to +\infty}} \frac{1}{\tau_2 - \tau_1} \int_{\tau_1}^{\tau_2} \frac{\rho^2(t)}{2} \mathrm{d}t \\ & + \lim_{\substack{\tau_1 \to -\infty \\ \tau_2 \to +\infty}} \frac{1}{\tau_2 - \tau_1} \int_{\tau_1}^{\tau_2} \frac{\rho^2(t)}{2} \cos(2\omega_c t + 2\phi(t))\mathrm{d}t. \end{aligned} \tag{1.55}$$

The first term on the right-hand side obviously depends only on the amplitude part of the modulating signal, i.e. on the modulus of the complex envelope $\tilde{s}(t)$. More precisely, it is equal to half the RMS value of the modulus of this complex envelope. We remark that it reduces to the classical value $\rho^2/2$ when dealing with a constant amplitude bandpass signal. And given that it directly gives the average power of this particular bandpass signal, we can then guess that the second term in the above expression is null. This is indeed true as long as the spectrum of $\tilde{s}(t)$ can be assumed narrowband with respect to the carrier angular frequency ω_c. In other words, if the spectrum of $\tilde{s}(t)$ lies over the frequency band $[-\Omega/2, \Omega/2]$, we need $\Omega \ll \omega_c$.

We first interpret this condition in the time domain. As can be seen in the left part of Figure 1.5, as long as the time domain variations of $\rho^2(t)$ are weak over a period $2\pi/\omega_c$ of the carrier, the integral of $\rho^2(t)\cos(2\omega_c t + 2\phi(t))$ over this period is necessarily almost null.

[3] As highlighted in "Power spectral density" earlier in this section, we adopt the signal processing approach for this definition as this expression implicitly assumes that we are working with normalized impedances when dealing with analog quantities for $s(t)$.

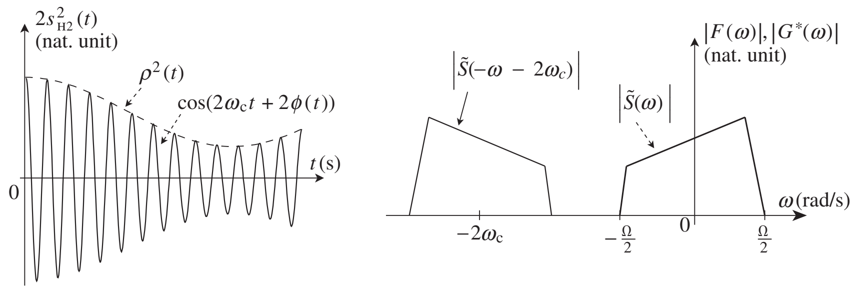

Figure 1.5 Illustration in the frequency and time domain of the bandpass signal average power estimation mechanism – The long-term average power estimation of $s(t) = \rho(t)\cos(\omega_c t + \phi(t))$ involves the time average of the high-frequency term $\rho^2(t)\cos(2\omega_c t + 2\phi(t))$ (left). This contribution is expected to be negligible as can be seen in the spectral domain (right). If we refer to equation (1.60), it indeed involves the averaging of the product of two non-overlapping spectrum, $F(\omega) = \tilde{S}(\omega)$ and $G^*(\omega) = \tilde{S}(-\omega - 2\omega_c)$.

We can thus expect that the overall integral toward infinity is also almost null, or at least negligible regarding the first term of equation (1.55). This condition can be interpreted more clearly in the frequency domain. Now we may need to consider Fourier transforms of the corresponding signals. As discussed in Section 1.1.1, for that to be possible we can initially assume a signal corresponding to an observation over a finite duration, for instance limited to $[0, T]$, of a realization of the modulating process. Under that assumption, we can rewrite the second term of equation (1.55) as

$$I = \frac{1}{2T}\int_0^T \rho^2(t)\cos(2\omega_c t + 2\phi(t))\mathrm{d}t. \tag{1.56}$$

This quantity can then be expressed in terms of the complex envelope $\tilde{s}(t)$ through the use of equation (1.52). This leads to

$$I = \frac{1}{2T}\mathrm{Re}\left\{\int_0^T \tilde{s}^2(t)\mathrm{e}^{\mathrm{j}2\omega_c t}\mathrm{d}t\right\}. \tag{1.57}$$

With $\tilde{s}(t)$ vanishing outside $[0, T]$, this integral can be extended toward infinity:

$$I = \frac{1}{2T}\mathrm{Re}\left\{\int_{-\infty}^{+\infty} \tilde{s}(t)\left[\tilde{s}^*(t)\mathrm{e}^{-\mathrm{j}2\omega_c t}\right]^* \mathrm{d}t\right\}. \tag{1.58}$$

Then, using the Fourier transform property, which states that

$$\int_{-\infty}^{+\infty} f(t)g^*(t)\mathrm{d}t = \frac{1}{2\pi}\int_{-\infty}^{+\infty} F(\omega)G^*(\omega)\mathrm{d}f, \tag{1.59}$$

we finally get that I is proportional to

$$\mathrm{Re}\left\{ \int \tilde{S}(\omega)\tilde{S}(-\omega - 2\omega_c)\mathrm{d}\omega \right\}, \tag{1.60}$$

where $\tilde{S}(\omega)$ stands for the Fourier transform of the complex envelope $\tilde{s}(t)$. As can be understood by inspecting the representation shown in Figure 1.5, we then get that for ω_c high enough with respect to Ω, the spectra involved in that equation are non-overlapping. We can thus expect that their product is null, as is the above integral. We must mention that having assumed a finite temporal support over $[0, T]$ for the time domain signals, their spectra necessarily spread toward infinity. On the other hand, we get that their asymptotic behavior is also necessarily decreasing in order to have an overall power that remains finite. This means that the above integral necessarily tends to zero as ω_c becomes higher and higher compared to Ω. We thus see that the second term of the right-hand side of equation (1.55) necessarily remains negligible compared to the first. As a result, the power of the modulated bandpass signal $s(t)$ can effectively be estimated as half the RMS value of the modulus of its complex envelope according to

$$P_s = \lim_{\substack{\tau_1 \to -\infty \\ \tau_2 \to +\infty}} \frac{1}{\tau_2 - \tau_1} \int_{\tau_1}^{\tau_2} \frac{\rho^2(t)}{2}\mathrm{d}t. \tag{1.61}$$

Then, assuming the ergodicity of the process we are dealing with, we can rewrite this result as

$$P_s = \frac{\mathbb{E}\left\{\rho_t^2\right\}}{2}, \tag{1.62}$$

so that under stationarity we finally get

$$P_s = \frac{\mathbb{E}\{\rho^2\}}{2}. \tag{1.63}$$

Alternatively, given that $\tilde{s}(t)$ is a lowpass process, we remark that its power is simply given by $\mathbb{E}\{\tilde{s}\tilde{s}^*\} = \mathbb{E}\{\rho^2\}$. We can therefore write

$$P_s = \frac{\mathbb{E}\{\rho^2\}}{2} = \frac{1}{2}P_{\tilde{s}}. \tag{1.64}$$

The long-term average power of a bandpass signal $s(t)$ is therefore equal to half the long-term average power of its lowpass complex envelope $\tilde{s}(t)$. This factor $1/2$ is in fact related to the definition used in this book for the complex envelope as already discussed in Section 1.1.3. In the same way, as reviewed in Section 1.1.2, we may recall that we can define as many complex envelopes as we want for a given bandpass signal. All those complex envelopes necessarily have the same modulus if we refer to equation (1.25). We thus get that the quantity defined by equation (1.61) or (1.64) necessarily remains well defined whatever the complex envelope considered to perform the derivation.

In conclusion, it is of interest to highlight the link that holds between the average power of the bandpass signal $s(t)$ and the average power of the real and imaginary parts of one of its complex envelopes $\tilde{s}(t) = p(t) + \mathrm{j}q(t)$. Using equation (A1.39), we can immediately write under stationarity that

$$P_s = \frac{1}{2}P_{\tilde{s}} = \frac{1}{2}\mathbb{E}\{\tilde{s}\tilde{s}^*\} = \frac{1}{2}\gamma_{\tilde{s}\times\tilde{s}}(0). \tag{1.65}$$

This result can be expanded in terms of the autocorrelation functions of the real and imaginary parts of the complex envelope $\tilde{s}(t)$ by using equation (A1.46a). This finally leads to

$$P_s = \frac{1}{2}\gamma_{\tilde{s}\times\tilde{s}}(0) = \frac{1}{2}[\gamma_{p\times p}(0) + \gamma_{q\times q}(0)]. \tag{1.66}$$

We can thus sum the average power of the in-phase and in-quadrature components, $p(t)$ and $q(t)$ respectively, to get twice the average power of the corresponding bandpass signal $s(t)$. This property remains valid for $p(t)$ and $q(t)$ whether correlated or not. The deep reason for this is that the bandpass signal $s(t)$ is constructed through the sum of orthogonal waveforms that carry the information of $p(t)$ and $q(t)$. Thus, whatever the correlation behavior of $p(t)$ and $q(t)$, the powers of the orthogonal waveforms that carry their information sum together during the derivation of the power of the final bandpass RF signal.

Peak to Average Power Ratio and Crest Factor

Two quantities are of particular interest for the characterization of the waveforms that are processed in a transceiver: the peak to average power ratio (PAPR) and the crest factor (CF). Although the purpose of those two quantities is to characterize the amplitude variations of a given signal, they are up to a point related to different problems in the dimensioning of transceivers.

For instance, the PAPR of a bandpass signal $s(t)$ of the form $\rho(t)\cos(\omega_c t + \phi(t))$ is defined as the ratio between its peak and average power. Although this definition may look clear enough at first glance, it remains of interest to discuss what we call peak power in the wireless transceiver perspective. In so doing, we may anticipate the discussion in Chapter 5 as the analytical derivations performed in this chapter clearly highlight that it is the square of the magnitude of the modulating waveform, i.e. $\rho^2(t)$, that is involved in the formulations related to RF compression. We can then understand that when talking about the instantaneous power variations of a bandpass RF signal, we are in fact talking about the variations linked to the modulation part only of the signal. Consequently, the peak power involved in the PAPR definition reduces to a peak average power of the bandpass modulated signal $s(t)$ over a duration short enough that the characteristics of the modulation remain almost constant, but long enough that many carrier periods have occurred. Classically, this duration can be assumed in the range of a data symbol.

We can now derive an analytical expression for the PAPR of $s(t)$ assuming that its spectrum spreads over a bandwidth of width Ω such that $\Omega \ll \omega_c$; that is, assuming that $s(t)$ is narrowband, we can directly reuse the material derived in the previous section to express its average power P_s through equation (1.61). In order to derive the PAPR of this signal, it thus remains to derive an expression for its peak power. We therefore reconsider the expansion of $s^2(t)$ as

$$s^2(t) = \frac{\rho^2(t)}{2} + \frac{\rho^2(t)}{2}\cos(2\omega_c t + 2\phi(t)). \tag{1.67}$$

The first term is linked to the modulation process only, and the second term is a high frequency component. The latter term thus vanishes when averaged. In the present case, the power variations we are looking for can be estimated through an average of this instantaneous power over a short duration $\tau_2 - \tau_1$ that is in the range of the data symbol, say $2\pi/\Omega$. Thus, given that the modulation scheme is assumed narrowband regarding the carrier frequency, we necessarily get that at least a few carrier periods occur during $\tau_2 - \tau_1$. This means that as long as the averaging period is short enough that the modulation scheme amplitude does not vary much, but long enough to have an averaging of the carrier over few periods, we can write

$$p_1(t) = \frac{1}{\tau_2 - \tau_1}\int_{t+\tau_1}^{t+\tau_2} \frac{\rho^2(t')}{2}\mathrm{d}t' \approx \frac{\tau_2 - \tau_1}{\tau_2 - \tau_1}\frac{\rho^2(t)}{2} = \frac{\rho^2(t)}{2}, \tag{1.68a}$$

$$p_2(t) = \frac{1}{\tau_2 - \tau_1}\int_{t+\tau_1}^{t+\tau_2} \frac{\rho^2(t')}{2}\cos\left(2\omega_c t' + 2\phi(t')\right)\mathrm{d}t' \approx 0. \tag{1.68b}$$

We then get that the second contribution $p_2(t)$ is almost null, whereas the first term is still proportional to the instantaneous power of the modulating waveform. As a result, the instantaneous power variations $p(t)$ linked only to the envelope contributions can be estimated as

$$p(t) = p_1(t) + p_2(t) \approx \frac{\rho^2(t)}{2}. \tag{1.69}$$

We can thus express the PAPR as the ratio between the peak value of $p(t)$ and the average power P_s given by equation (1.61). This results in

$$PAPR = \frac{\max_t\{\rho^2(t)\}}{\overline{\rho^2(t)}}, \tag{1.70}$$

where $\overline{(.)}$ denotes the time average and $\max\{.\}$ the maximum value. Since we consider $\rho(t)$ to be a positive quantity, and due to the fact that the square function is strictly monotonic for such a positive quantity, the maximum of the square is therefore equal to the square of the maximum. Thus, denoting by ρ_{pk} the peak value of $\rho(t)$, we simply get that

$$PAPR = \frac{\rho_{\mathrm{pk}}^2}{\overline{\rho^2(t)}} \tag{1.71}$$

or, in decibels,

$$PAPR|_{\mathrm{dB}} = 10\log_{10}(PAPR) = 10\log_{10}\left(\frac{\rho_{\mathrm{pk}}^2}{\overline{\rho^2(t)}}\right). \tag{1.72}$$

Up to now, we have adopted a deterministic approach to the derivation of the PAPR quantity through time averaging. But, dealing with randomly modulated signals, we can transpose those definitions using stochastic concepts. Under ergodicity and assuming the stationarity of those processes, which is a reasonable assumption in the wireless transceiver area as discussed in Appendix 2, we can write the above expressions as

$$PAPR = \frac{\rho_{\mathrm{pk}}^2}{\mathbb{E}\{\rho^2\}}, \tag{1.73a}$$

$$PAPR|_{\mathrm{dB}} = 10\log_{10}\left(\frac{\rho_{\mathrm{pk}}^2}{\mathbb{E}\{\rho^2\}}\right). \tag{1.73b}$$

The peak value ρ_{pk} of $\rho(t)$ may thus be defined in turn in a probabilistic way. In that case, this peak value can be defined such that a given percentage of the realizations of ρ are lower than ρ_{pk}. In practice the value of 99.9% is often used for the definition. Having that ρ is a positive quantity, we thus get

$$F(\rho_{\mathrm{pk}}) = \int_{-\infty}^{\rho_{\mathrm{pk}}} p(\rho)\mathrm{d}\rho = \int_{0}^{\rho_{\mathrm{pk}}} p(\rho)\mathrm{d}\rho = 0.999. \tag{1.74}$$

Here, $p(\rho)$ stands for the probability density function (PDF) of ρ and thus $F(\rho)$ for its cumulative distribution function (CDF). Obviously, the definition using the complementary cumulative distribution function (CCDF), $F_{\mathrm{c}}(\rho_{\mathrm{pk}})$, can be used instead. This leads to

$$F_{\mathrm{c}}(\rho_{\mathrm{pk}}) = \int_{\rho_{\mathrm{pk}}}^{+\infty} p(\rho)\mathrm{d}\rho = 0.001. \tag{1.75}$$

We observe that effective modulating waveforms necessarily remain bounded in amplitude whatever the pattern of modulating bits that is used. Thus, an upper bound is always well defined for the amplitude of those waveforms. But for some schemes this kind of maximum value can occur with a very low probability. In that case, it may be of interest to adopt a statistical approach in order not to overdimension the data path only for events with no significant contributions to overall system performance. The orthogonal frequency division multiplexing (OFDM) signals introduced in “OFDM” (Section 1.3.3) are a good example of this.

Let us now focus on the CF. This quantity is classically defined as the peak amplitude of a given waveform over its RMS value. As a result, we can write the crest factor CF of the signal $s(t)$ as

$$CF = \frac{s_{\mathrm{pk}}}{\sqrt{\overline{s^2(t)}}}, \tag{1.76}$$

with $s_{\mathrm{pk}} = \max\{s(t)\}$ the peak value of $s(t)$. Alternatively, it can be expressed in decibels as

$$CF|_{\mathrm{dB}} = 20\log_{10}(CF) = 20\log_{10}\left(\frac{s_{\mathrm{pk}}}{\sqrt{\overline{s^2(t)}}}\right). \tag{1.77}$$

As was done for the PAPR, under ergodicity and still assuming the stationarity of the processes we are dealing with, we can transpose those expressions to the stochastic case:

$$CF = \frac{s_{\mathrm{pk}}}{\sqrt{\mathbb{E}\{s^2\}}}, \tag{1.78a}$$

$$CF|_{\mathrm{dB}} = 20\log_{10}\left(\frac{s_{\mathrm{pk}}}{\sqrt{\mathbb{E}\{s^2\}}}\right), \tag{1.78b}$$

where the signal peak value depends on a chosen bound for the CDF of the signal as discussed above. Compared to the definition of the PAPR, the CF is not related to the instantaneous power of the considered signal but directly to its amplitude. Thus, according to our discussion so far, we may initially expect the CF to be more useful for characterizing lowpass signals than RF bandpass ones. As illustrated, for instance in Chapter 7, the CF of baseband modulating waveforms indeed drives the scaling of those signals along the data path in order to avoid any potential saturation. Nevertheless, even if the CF is more suited to addressing lowpass signal problems, there is nothing to prevent its use in deriving bandpass signals. For instance, a continuous wave (CW) signal has both a PAPR of 1, i.e. 0 dB, and a CF of $\sqrt{2}$, i.e. 3 dB. In terms of physical interpretation of those results, it may be of interest to highlight that the deep reason for this ratio of $\sqrt{2}$ between those quantities in the present case comes from the fact that the PAPR focuses on the power variations, i.e. on the variations of the complex envelope only, whereas the CF takes into account the variations of the overall signal, i.e. including those of the sinusoidal carrier. Thus, it is natural to wonder if this ratio of $\sqrt{2}$ cannot be generalized to any bandpass signal $s(t)$. We can consider the following expression for its complex envelope $\tilde{s}(t)$:

$$\tilde{s}(t) = p(t) + \mathrm{j}q(t) = \rho(t)e^{\mathrm{j}\phi(t)}. \tag{1.79}$$

We can then write

$$|\tilde{s}(t)|^2 = \rho^2(t) = p^2(t) + q^2(t). \tag{1.80}$$

Using the stochastic approach, this means that under stationarity we can transpose equation (1.66) as

$$\mathbb{E}\{\rho^2\} = \mathbb{E}\{p^2\} + \mathbb{E}\{q^2\}. \tag{1.81}$$

But, as discussed in "Impact of stationarity" earlier in this section, the stationarity of $s(t)$ also leads to having the same power for $p(t)$ and $q(t)$. We can thus write

$$\mathbb{E}\{\rho^2\} = 2\mathbb{E}\{p^2\} = 2\mathbb{E}\{q^2\}. \tag{1.82}$$

On the other hand, from a statistical point of view we can expect that the maximum value that $p(t)$ or $q(t)$ can reach is of the same order of magnitude as the maximum value of $\rho(t)$. We can indeed assume in most cases that the maximum value of $\rho(t)$ occurs when the contributions of one of the signals $p(t)$ or $q(t)$ is negligible with regard to the other. Thus, comparing equations (1.73a) and (1.78a), we see that we can approximate for most bandpass signals the result that was exact for CW, i.e. that

$$CF_{\mathrm{p}} = CF_{\mathrm{q}} \approx \sqrt{2PAPR_{\rho}}, \tag{1.83}$$

or, in decibels,

$$CF_{\mathrm{p}}\big|_{\mathrm{dB}} = CF_{\mathrm{q}}\big|_{\mathrm{dB}} \approx PAPR_{\rho}\big|_{\mathrm{dB}} + 3, \tag{1.84}$$

In those equations, CF_{p} and CF_{q} stand respectively for the CF of the real and imaginary parts $p(t)$ and $q(t)$ of the complex envelope that describes the modulating waveform considered, and $PAPR_{\rho}$ for the PAPR of the corresponding bandpass RF modulated signal. This behavior is confirmed by the examples detailed in Section 1.3.

Instantaneous Amplitude and Instantaneous Frequency

Let us now clarify two other concepts classically associated with bandpass RF signals, namely their instantaneous amplitude and their instantaneous phase or frequency. At first glance, we might be tempted to say that these quantities are quite straightforward to define. Indeed, considering, for instance, a modulated bandpass signal that can be written using equation (1.28b) in the form $s(t) = \rho(t)\cos(\omega_{\mathrm{c}}t + \phi(t))$, we could obviously call $\rho(t)$ the instantaneous amplitude of $s(t)$ and $\omega_{\mathrm{c}}t + \phi(t)$ as the instantaneous phase of $s(t)$. Nevertheless, we might wonder whether this analytical expression for $s(t)$ is unique and thus whether the resulting expressions for its instantaneous amplitude and phase are also unique. Moreover, considering the situation where $s(t)$ is a bandpass signal for which no particular analytical expression of this form is available, we can guess what is the correct way to define and derive those quantities.

Let us first focus on the problem of uniqueness by considering the definition of the instantaneous frequency. Recall that the concept of frequency in itself is naturally associated with Fourier analysis. Perhaps we can rely on this theoretical tool to formalize the instantaneous frequency concept we are looking for. Unfortunately, in order to correctly evaluate the angular frequency of a CW in the form

$$s_{\mathrm{cw}}(t) = \rho\cos(\omega_{\mathrm{c}}t), \tag{1.85}$$

we require an infinite duration of observation. Practically speaking, this is the cost of having infinite integration bounds in the integral of the Fourier transform. As soon as we try to "locate" the frequency content of a signal in the time domain we get a limitation in terms of frequency resolution related to the Heisenberg uncertainty principle. This limitation shows that Fourier analysis may not be the right tool for the definition of an *instantaneous* frequency. We can look at another approach when considering a generalization of the above CW signal with an arbitrary time dependent phase $\varphi(t)$ in the form

$$s_{\mathrm{PM}}(t) = \rho \cos(\varphi(t)). \tag{1.86}$$

Looking at the analytical expression for this constant amplitude signal, it seems natural to define its instantaneous frequency, $f(t)$, as

$$f(t) = \frac{1}{2\pi}\frac{\mathrm{d}\varphi(t)}{\mathrm{d}t}. \tag{1.87}$$

This definition indeed leads to no ambiguity in the definition of $f(t)$ and gives good results when applied to a CW signal such as $s_{\mathrm{CW}}(t)$. Nevertheless, a problem occurs if we now consider a general bandpass signal,

$$s(t) = \rho(t) \cos(\varphi(t)), \tag{1.88}$$

that is now also amplitude modulated. In this latter case the direct application of equation (1.87) gives a result that is not unique. This can be seen by considering a time dependent function $\xi(t)$, such that $0 < \xi(t) < 1$, that allows $s(t)$ to be rewritten as

$$s(t) = \frac{\rho(t)}{\xi(t)}\xi(t) \cos(\varphi(t)), \tag{1.89}$$

or alternatively, in a form more suited to our purposes, as

$$s(t) = \rho'(t) \cos(\varphi'(t)), \tag{1.90}$$

with

$$\rho'(t) = \rho(t)/\xi(t), \tag{1.91a}$$

$$\varphi'(t) = \arccos(\xi(t) \cos(\varphi(t))). \tag{1.91b}$$

We thus get two different analytical expressions for the same bandpass signal $s(t)$. The direct application of equation (1.87) to those expressions therefore results in two different expressions for the instantaneous frequency of $s(t)$. Obviously, this is unsatisfactory.

Nowadays, the most commonly used definition for the instantaneous frequency of a bandpass signal is that given by Ville in 1948 [5]. This definition involves the analytic signal associated with the considered bandpass signal according to the definition given in Section 1.1.2. Indeed, reconsidering the former CW signal $s_{\mathrm{CW}}(t)$, we can see that by using equations (1.16) and (1.17) we can express its analytic signal, $s_{\mathrm{CW,a}}(t)$, as

$$s_{\mathrm{CW,a}}(t) = \rho e^{j\omega_c t}. \tag{1.92}$$

We can therefore conclude that the angular frequency of $s_{\mathrm{CW}}(t)$ matches the rotation angular speed of the vectorial representation in the complex plane of $s_{\mathrm{CW,a}}(t)$. What is interesting in this way of proceeding is that the analytic signal derived from any real bandpass signal is unique. It can therefore be used for the generalization of the concept of instantaneous frequency without ambiguity. Thus, we can use equations (1.27) and (1.5) to express the bandpass signal $s(t)$ as a function of its analytic signal $s_{\mathrm{a}}(t)$:

$$s(t) = \mathrm{Re}\{s_{\mathrm{a}}(t)\} = \frac{1}{2}\left(s_{\mathrm{a}}(t) + s_{\mathrm{a}}^*(t)\right). \tag{1.93}$$

Then, given that $s_{\mathrm{a}}(t)$ and $s_{\mathrm{a}}^*(t)$ have the same modulus but opposite arguments, we can represent those quantities in the complex plane as vectors of the same magnitude but symmetrical with regard to the real axis. As expected, and as shown in Figure 1.6, their sum therefore remains a real quantity equal to twice the value of $s(t)$. Practically speaking, we thus get that the instantaneous phase $\varphi(t)$ of $s(t)$ can be defined as the argument of $s_{\mathrm{a}}(t)$ or equivalently its instantaneous frequency, $f(t)$, as the angular velocity of the representation in the complex plane of this analytic signal. In the same way, the instantaneous amplitude $\rho(t)$ of $s(t)$ can be defined without ambiguity as the modulus of $s_{\mathrm{a}}(t)$. In terms of analytical expressions, we obtain

$$f(t) = \frac{1}{2\pi}\frac{\mathrm{d}\varphi(t)}{\mathrm{d}t} = \frac{1}{2\pi}\frac{\mathrm{d}\arg\{s_{\mathrm{a}}(t)\}}{\mathrm{d}t}, \tag{1.94a}$$

$$\rho(t) = |s_{\mathrm{a}}(t)|. \tag{1.94b}$$

For our purposes, it is of interest to link those quantities to the characteristics of the complex envelopes of the bandpass signals we are dealing with. Let us therefore suppose

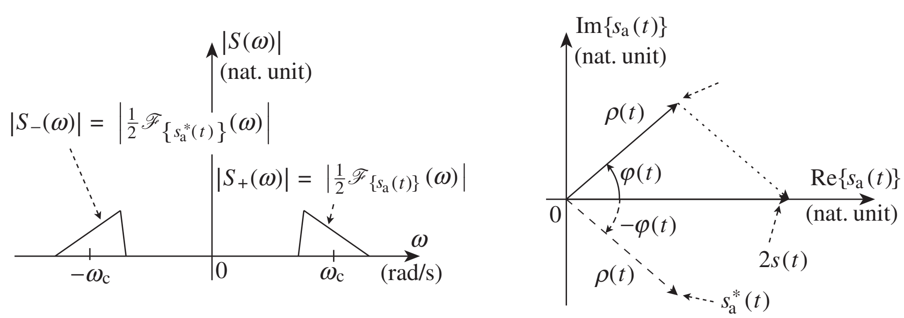

Figure 1.6 Instantaneous amplitude and phase definition of a real bandpass signal through its associated analytic signal – A real bandpass signal, $s(t)$, can be decomposed as half the sum of its analytic signal, $s_{\mathrm{a}}(t)$, and its complex conjugate according to equation (1.93). In this decomposition, the analytic signal is linked to the signal corresponding to the positive sideband of $s(t)$ and its complex conjugate to the signal corresponding to the negative sideband (left). The representation in the complex plane of those signals illustrates the definition of the instantaneous amplitude, $\rho(t)$, and phase, $\varphi(t)$, of $s(t)$ as the modulus and argument of $s_{\mathrm{a}}(t)$, respectively (right).

that $\tilde{s}(t) = \rho(t)\,\mathrm{e}^{\mathrm{j}\phi(t)}$ is the complex envelope defined as centered around ω_c of $s(t)$. Inverting equation (1.21), we immediately get the following expression for the analytic signal $s_\mathrm{a}(t)$ associated with $s(t)$:

$$s_\mathrm{a}(t) = \tilde{s}(t)\mathrm{e}^{\mathrm{j}\omega_\mathrm{c}t} = \rho(t)\,\mathrm{e}^{\mathrm{j}(\omega_\mathrm{c}t+\phi(t))}. \tag{1.95}$$

The instantaneous phase of $s(t)$ can then be expressed as

$$\begin{aligned}\varphi(t) = \arg\{s_\mathrm{a}(t)\} &= \omega_\mathrm{c}t + \arg\{\tilde{s}(t)\}\\ &= \omega_\mathrm{c}t + \phi(t),\end{aligned} \tag{1.96}$$

and its instantaneous frequency as

$$\begin{aligned}f(t) = \frac{1}{2\pi}\frac{\mathrm{d}\arg\{s_\mathrm{a}(t)\}}{\mathrm{d}t} &= \frac{1}{2\pi}\left(\omega_\mathrm{c} + \frac{\mathrm{d}\arg\{\tilde{s}(t)\}}{\mathrm{d}t}\right)\\ &= \frac{1}{2\pi}\left(\omega_\mathrm{c} + \frac{\mathrm{d}\phi(t)}{\mathrm{d}t}\right).\end{aligned} \tag{1.97}$$

In the same way, its instantaneous amplitude can then be expressed as

$$\rho(t) = |s_\mathrm{a}(t)| = |\tilde{s}(t)|. \tag{1.98}$$

Thus the instantaneous frequency of an RF bandpass signal is precisely the sum of the carrier frequency and the normalized time derivative of the phase of its complex envelope that is defined as centered around this carrier frequency. This instantaneous frequency is thus related to the angular rate at which the complex envelope describes the modulation trajectory in the complex plane. As a side effect, it also allows us to understand how the spectral limitation of the modulating signal impacts the speed at which the vector representing the complex envelope can go from a data symbol representation to another one in the complex plane, and thus impacts the relationship between the data symbol rate and the instantaneous frequency variations of the resulting modulated bandpass signal.

Following those definitions, it may be of interest to recall that an infinity of complex envelopes can be defined for a given bandpass signal, as discussed in Section 1.1.2 “Complex envelope concept” (Section 1.1.2). Nevertheless, all these complex envelopes are derived from the same unique analytic signal, so that they all fulfill equation (1.25). As a result, the above relationships linking the instantaneous amplitude and phase or frequency to the characteristics of the complex envelopes result in well-defined quantities.

In conclusion, it may be of interest to illustrate the concepts discussed so far in this section with an example. In Section 1.3.3 we examine the characteristics of a wideband code division multiple access (WCDMA) modulated bandpass signal, $s(t)$, in two different configurations. In the first, the carrier angular frequency ω_c is low enough that it is of the same order of magnitude as the modulation spectrum width even though still ensuring the bandpass condition. Thus, given that the spectrum of a WCDMA modulation spreads in a frequency bandwidth slightly lower than $[-1/(2T_\mathrm{c}), 1/(2T_\mathrm{c})]$, where T_c represents the chip rate as detailed in “Code

Division Multiple Access" in Section 1.3.3, we can select ω_c as equal to $0.8 \times 2\pi/T_c$ for our example. In the second configuration, the carrier angular frequency is high enough that $s(t)$ can be considered as narrowband. We can select, for instance, ω_c as equal to $4 \times 2\pi/T_c$. As illustrated in Figure 1.7, we then get in the first situation that the frequency of occurrence of the instantaneous amplitude variations is of the same order of magnitude as those of the carrier. As a result, the definition of an instantaneous amplitude and phase or frequency of $s(t)$ is not so obvious just from the time domain representation of $s(t)$. In contrast, as soon as ω_c increases compared to the modulating bandwidth, the shape of $s(t)$ clearly matches that of a CW signal whose amplitude and frequency are slowly varying according to its instantaneous amplitude and frequency. Nevertheless, it is interesting to notice that the modulus and phase of the analytic signal of $s(t)$ lead to an unambiguous definition for those quantities in both cases. Moreover, we recover that whatever the chosen carrier angular frequency, all the resulting bandpass signals necessarily have the same instantaneous amplitude. The same holds for their instantaneous frequency variations when considered relative to their carrier frequencies.

1.2 Bandpass Noise Representation

The complex envelope is a valuable concept in performing analytical derivations for transceiver budgets, and we now focus on extending it to bandpass noise. Or rather, we now focus on the additional properties of complex envelopes for bandpass noise as the complex envelope, originally introduced for bandpass deterministic signals in Section 1.1.2, has already been implicitly extended to bandpass stochastic processes when considering modulated bandpass signals. Practically speaking, we consider that each realization of a given bandpass process is also bandpass. We can thus define a complex envelope associated with each of its realizations, thus in turn allowing us to define the complex envelope as a stochastic process.

There are new features of complex envelopes to consider when dealing with bandpass noises as classically encountered in practical wireless transceiver implementations. For instance, we get that the distribution of most such bandpass noises is Gaussian, which leads to interesting characteristics for their complex envelopes. Furthermore, those bandpass noises can often be seen as additive with regard to the signal being processed along the line-up. In that case, the bandpass behavior of both the noise and the signal allows for an interesting decomposition of the noise in terms of amplitude and phase noise, i.e. in terms of noise components that corrupt the instantaneous amplitude or the instantaneous phase respectively of the bandpass signal it adds to. Due to the importance of this decomposition in the field of transceivers, it is important to introduce it correctly based on the complex envelope concept.

Before going any further, however, we discuss the bandpass concept itself for noise signals as classically encountered in practical transceivers. Referring to the discussion at the beginning of Chapter 4, we get that noise components such as thermal noise have a spectrum that spreads up to a very high frequency. Although the bandpass concept requires only that the spectral extent has no power density at the zero frequency, it turns out that the noise processes we need to consider for the derivation of transceiver budgets often have limited bandwidth. Practically speaking, there are various reasons for that:

(i) On the receive side, we always get channel filters that select the desired signal. We thus get that the noise contributions that would lie outside their passband are canceled, or at

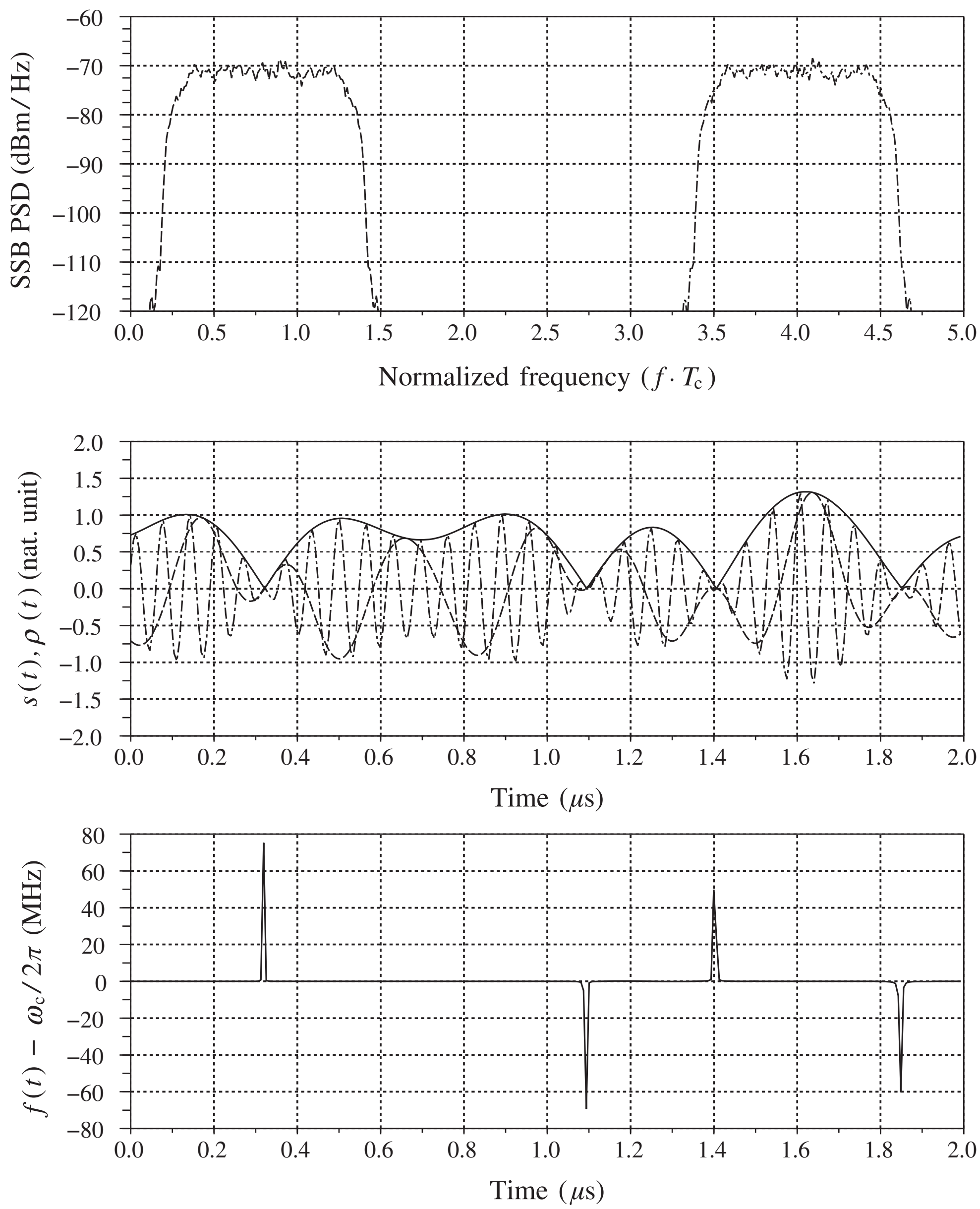

Figure 1.7 Bandpass signal and associated instantaneous amplitude and frequency – When the carrier frequency is set to $0.8/T_c$, where T_c is the chip rate, a WCDMA bandpass signal has a spectrum with low frequency components (top, dashed). This results in a time domain waveform (middle, dashed) that does not highlight clearly the shape of the instantaneous amplitude waveform (middle, solid). This is not the case when the carrier frequency is set to $4/T_c$ (top, dot-dashed), which results in a clear shaping of the time domain waveform by the instantaneous amplitude (middle, dot-dashed). In these two cases, the bandpass signals have the same instantaneous amplitude (middle, solid) and the same instantaneous frequency variations around the carrier frequency (bottom).

least reduced to a negligible level. As a result, even when dealing with noises that are broadband in essence due to their physical origin, we can restrict their description to the fraction that lies within the receiver passband in order to perform the line-up budget. We observe that it leads to the concept of receiver noise bandwidth, which directly matches the receiver passband when dealing with a noise process that has a flat spectral density.

(ii) On the transmit side, we can invoke the same kind of argument. We observe, for instance, that analog reconstruction filters are often required in the line-up as discussed in Section 4.6. Any broadband noise contribution that experiences such filtering can thus be seen as a narrower bandpass noise at the output of the line-up.

We also observe that various noise contributions have a spectral extent naturally in the region of that of the signal being processed. This is the case, for instance, for the distortion terms that are generated from it through linear or nonlinear effects. In any case, the concept of the complex envelope is well suited for performing analytical derivations involving such noise contributions. Among other things, it allows interesting vectorial representations in the complex plane that illustrate underlying phenomena that are sometimes not immediately obvious.

1.2.1 Gaussian Components

Let us now detail some characteristics of complex envelopes of real bandpass noises that exhibit a Gaussian distribution – or, rather, of Gaussian bandpass processes in general. The Gaussian distribution is naturally associated with analog noises, the most famous being thermal noise as discussed in Chapter 4, and is encountered in many situations in practice, among them the following:

(i) The modulating waveforms used in some wideband wireless systems. As discussed in Section 1.3.3, the Gaussian distribution can be seen as a limit case for the distribution of most of the resulting modulated bandpass signal.

(ii) The wireless propagation channel in a mobile environment. As discussed in Chapter 2, the simplest propagation channel is the Rayleigh channel. In this channel model we have a Gaussian distribution for the bandpass signal that goes through it, thus resulting in a Rayleigh distribution for its instantaneous amplitude.

Looking at those various use cases, we can appreciate the importance of going through the statistical properties of the Gaussian real bandpass process and its associated complex envelopes.

Let us suppose that we are dealing with a Gaussian bandpass process $s(t)$ whose PSD spreads over a bandwidth $\delta\omega$ centered around ω_c as illustrated in Figure 1.8. Generally speaking, the term "Gaussian process" means that for any set of N samples of $s(t)$, taken at times $t_1, t_2, \ldots, t_N$, the vector $\left(s_{t_1}, s_{t_2}, \ldots, s_{t_N}\right)^T$ is a real normal random vector as defined in Appendix 3. Practically speaking, when it exists, the PDF of $\left(s_{t_1}, s_{t_2}, \ldots, s_{t_N}\right)^T$, $p(x_1, \ldots, x_N)$, has a multivariate normal distribution as given by equation (A3.2). Furthermore, correlations can exist between successive time samples due to the finite spectral bandwidth of the process.

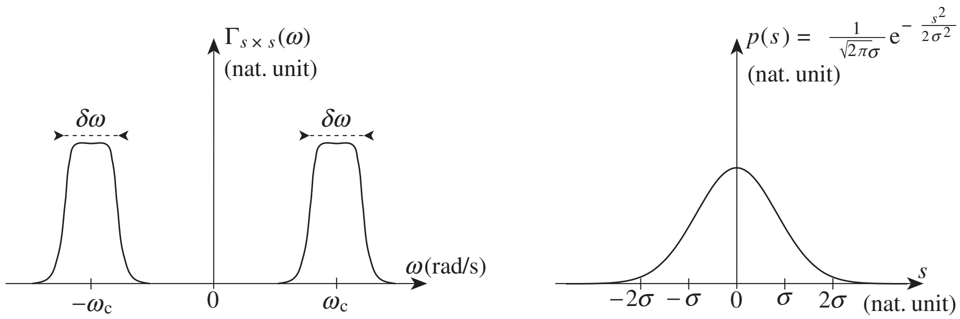

Figure 1.8 Power spectral density and probability density function of a real bandpass Gaussian process – A real Gaussian bandpass process, $s(t)$, has a PSD that is non-vanishing only over a finite frequency band, $\delta\omega$, that does not go down to the zero frequency (left). Due to the finite spectral width of the process, correlation terms can exist between successive time samples of the process. Considered at a given time t, the random variable s_t has a Gaussian distribution (right).

This simply means that the noise process we are considering is not white in the sense that its flat spectrum does not spread toward infinity. As a result, the covariance matrix $\mathbf{\Sigma}$, whose elements are given by equation (A3.6), can be non-diagonal. The PDF of a single sample random variable s_t reduces to a Gaussian distribution.

Let us now suppose that we are dealing with a centered and stationary bandpass process. This is indeed a reasonable assumption in the field of wireless transceivers. Practically speaking, it means we can assume that the PDF $p(s_t)$ of s_t is independent of t and that it takes the simple form

$$p(s_t) = p(s) = \frac{1}{\sqrt{2\pi}\sigma}e^{-\frac{s^2}{2\sigma^2}}, \tag{1.99}$$

with

$$\mathbb{E}\{s\} = 0, \tag{1.100a}$$

$$\mathbb{E}\{s^2\} = \sigma^2. \tag{1.100b}$$

As the realization $s(t)$ is bandpass, we can consider for it the complex envelope $\tilde{s}(t)$, defined as centered around the angular frequency ω_c. As a first step, let us consider a Cartesian representation of $\tilde{s}(t) = p\,(t) + \mathrm{j}q\,(t)$. This means that $s(t)$ can be expressed as

$$\begin{aligned} s(t) &= \mathrm{Re}\left\{\tilde{s}(t)e^{\mathrm{j}\omega_c t}\right\} \\ &= p\,(t)\cos(\omega_c t) - q\,(t)\sin(\omega_c t). \end{aligned} \tag{1.101}$$

On the other hand, we get that the stationarity of $s(t)$ leads to $\gamma_{\tilde{s}\times\tilde{s}^*}(\tau) = 0$ following the arguments in Appendix 2, and in particular equation (A2.11). This property, by which the complex normal random vector $\left(\tilde{s}_{t_1}, \tilde{s}_{t_2}, \dots, \tilde{s}_{t_N}\right)^{\mathrm{T}}$ is said to be circular, also leads to $p\,(t)$ and $q\,(t)$ being uncorrelated when considered at the same time, as given by equation (A2.13b) for

$\tau = 0$. Under our assumptions, the result is that p_t and q_t are independent, with a distribution given by [3, 4]

$$p(p_t) = p(p) = \frac{1}{\sqrt{2\pi}\sigma} \mathrm{e}^{-\frac{p^2}{2\sigma^2}}, \tag{1.102a}$$

$$p(q_t) = p(q) = \frac{1}{\sqrt{2\pi}\sigma} \mathrm{e}^{-\frac{q^2}{2\sigma^2}}, \tag{1.102b}$$

with

$$\mathbb{E}\{p\} = \mathbb{E}\{q\} = \mathbb{E}\{s\} = 0, \tag{1.103a}$$

$$\mathbb{E}\{p^2\} = \mathbb{E}\{q^2\} = \mathbb{E}\{s^2\} = \sigma^2. \tag{1.103b}$$

We thus get that the real and imaginary parts, $p(t)$ and $q(t)$, of the complex envelopes that represent a stationary and centered bandpass Gaussian process also have a centered Gaussian distribution with the same variance as the original bandpass process.

An additional interesting property for $p(t)$ and $q(t)$ occurs when $s(t)$ also exhibits a spectral symmetry with regard to the angular frequency chosen for the definition of its complex envelope $\tilde{s}(t) = p(t) + \mathrm{j}q(t)$ – or, more precisely, when its PSD is evenly symmetrical with regard to the frequency used to define the complex envelope $\tilde{s}(t)$. In that case, the results in "Impact of spectral symmetry on top of stationarity" (Section 1.1.3) apply and we get from equation (1.51) that

$$\Gamma_{\tilde{s}\times\tilde{s}}(\omega) = \Gamma_{p\times p}(\omega) + \Gamma_{q\times q}(\omega) = 2\Gamma_{p\times p}(\omega) = 2\Gamma_{q\times q}(\omega). \tag{1.104}$$

In that case, then, $p(t)$ and $q(t)$ have the same spectral shape as the original stationary bandpass process they represent. The converse situation is also obviously true. This means that the frequency upconversion of two stationary and centered lowpass processes with Gaussian distributions results in a bandpass process that also exhibits a Gaussian distribution. And when the two initial lowpass components are also uncorrelated, we get that the PSD of the resulting RF bandpass signal is the sum of the input ones.

Let us now focus on the characteristics of the polar form of the complex envelope $\tilde{s}(t) = p(t) + \mathrm{j}q(t) = \rho(t)\mathrm{e}^{\mathrm{j}\phi(t)}$. Assuming that we are dealing with a stationary and centered bandpass process, we have seen that $p(t)$ and $q(t)$ are lowpass processes such that p_t and q_t are also centered and have a Gaussian distribution. Under the same assumption, it can be shown that the magnitude $\rho(t)$ of the complex envelope $\tilde{s}(t)$ is such that ρ_t follows a Rayleigh distribution, i.e. that [3]

$$p(\rho_t) = p(\rho) = \frac{\rho}{\sigma^2} \mathrm{e}^{-\frac{\rho^2}{2\sigma^2}}. \tag{1.105}$$

In the same way, as illustrated in Figure 1.9, the phase $\phi(t)$ of $\tilde{s}(t)$ is necessarily uniformly distributed on $[0, 2\pi]$, i.e.

$$p(\phi_t) = p(\phi) = \frac{1}{2\pi}. \tag{1.106}$$

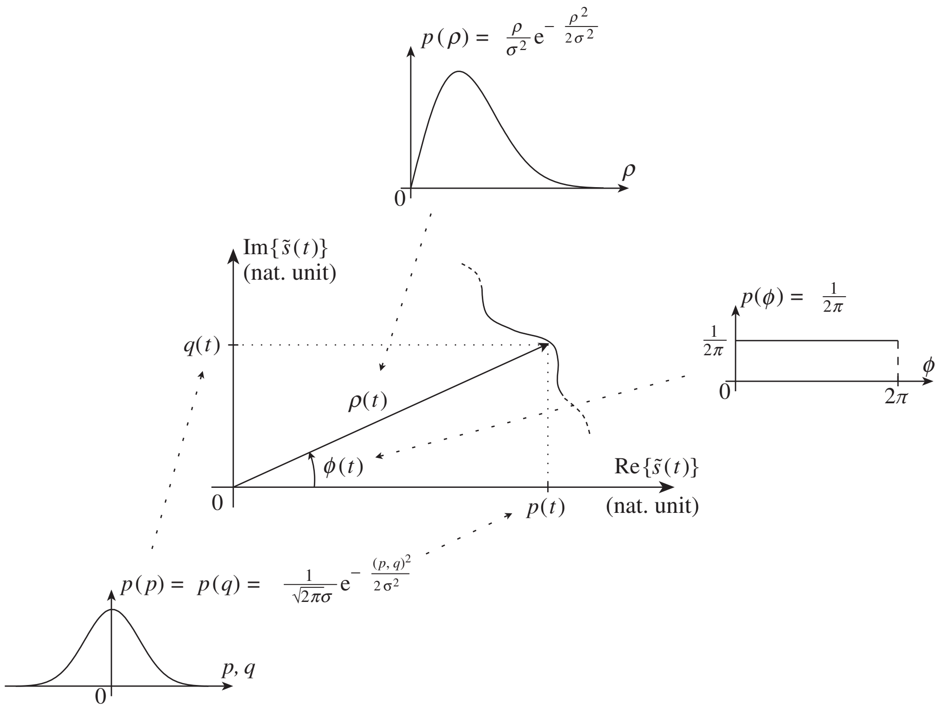

Figure 1.9 Statistical properties of the complex envelope of a stationary and centered bandpass Gaussian process – The complex envelope of a stationary and centered bandpass Gaussian process, whose PSD and PDF are of the form shown in Figure 1.8, has noticeable statistical properties: its real and imaginary parts also have a Gaussian distribution with the same variance as the original bandpass process, its modulus is Rayleigh distributed and its argument uniformly distributed over $[0, 2\pi]$. When considered at the same time, the modulus and argument are mutually independent.

Moreover, we get that the joint distribution of the random variables ρ_t and ϕ_t corresponding to two realizations of $\rho(t)$ and $\phi(t)$, when considered at the *same* time, is such that

$$p(\rho_t, \phi_t) = p(\rho_t)p(\phi_t). \tag{1.107}$$

Practically speaking, this means that the variables ρ_t and ϕ_t are independent when considered at the same time. Nevertheless, we have to keep in mind that this is true only when $p(t)$ and $q(t)$ are centered. Indeed, if

$$\mathbb{E}\{p\} = m_{\mathrm{p}}, \tag{1.108a}$$

$$\mathbb{E}\{q\} = m_{\mathrm{q}}, \tag{1.108b}$$

with

$$m_{\mathrm{p}} + \mathrm{j}m_{\mathrm{q}} = m e^{\mathrm{j}\theta}, \tag{1.109}$$

it can be shown that [3]

$$p(\rho_t, \phi_t) = \frac{1}{2\pi}\frac{\rho_t}{\sigma^2}\mathrm{e}^{-\frac{1}{2\sigma^2}\left(\rho_t^2 - 2\rho_t m\cos(\phi_t-\theta)+m^2\right)}, \tag{1.110}$$

which is a Rayleigh–Rice distribution. And if equation (1.107) no longer holds, then ρ_t and ϕ_t are no longer independent. However, as already highlighted, we can assume that all processes of interest in wireless transceivers are centered.

To conclude this section, we briefly review the moments of the modulus $\rho(t)$ of the complex envelope of such a Gaussian and centered bandpass process. Those moments will be needed to perform analytical derivations, for instance when dealing with nonlinear transfer functions, as is done in Chapter 5. From our discussion so far, we have that those moments are nothing more than those of the Rayleigh distribution. We can thus write that [1]

$$\mathbb{E}\{\rho^n\} = (2\sigma^2)^{n/2}\Gamma\left(1+\frac{n}{2}\right), \tag{1.111}$$

where $\Gamma(.)$ is the gamma function, which can be expressed for instance in its Euler integral form as [6]

$$\Gamma(z) = \int_0^{+\infty} t^{z-1}e^{-t}\mathrm{d}t. \tag{1.112}$$

One property of this function is that it reduces, for integers z, to a factorial expression:

$$\Gamma(z) = (z-1)! = (z-1)(z-2)\cdots 1. \tag{1.113}$$

Thus, for any even $n = 2k$, the moments of the Rayleigh distribution given by equation (1.111) reduce to

$$\mathbb{E}\{\rho^{2k}\} = (2\sigma^2)^k k!. \tag{1.114}$$

It is these even order moments that will later be of interest.

1.2.2 Phase Noise vs. Amplitude Noise

Let us now take another step forward in the description of how an additive bandpass noise corrupts a bandpass signal. Such bandpass noise can be decomposed into two terms that, under the assumption that the SNR is good enough, corrupt up to first order either the instantaneous amplitude or the instantaneous phase of the bandpass signal it is added to. Such decomposition is of particular interest in practice as there are times when only one of the two terms is involved in some of the mechanisms we deal with in the field of transceivers. One example is the transfer of the phase noise part of the local oscillator (LO) signal during a frequency transposition based on the use of mixers behaving as choppers, as discussed in Section 4.3.2. Another is the cancellation mechanism of the amplitude part of such an additive noise signal in nonlinear devices exhibiting compression behavior, as discussed in Sections 5.1.4 and 5.2.3.

Let us consider a real bandpass signal, $s_{\mathrm{w}}(t)$, resulting from the upconversion of the complex envelope

$$\tilde{s}_{\mathrm{w}}(t) = \rho_{\mathrm{w}}(t)\mathrm{e}^{\mathrm{j}\phi_{\mathrm{w}}(t)}, \tag{1.115}$$

around the center angular frequency ω_{c}. We can thus express $s_{\mathrm{w}}(t)$ as

$$s_{\mathrm{w}}(t) = \mathrm{Re}\left\{\tilde{s}_{\mathrm{w}}(t)\mathrm{e}^{\mathrm{j}\omega_{\mathrm{c}}t}\right\}. \tag{1.116}$$

Let us suppose that this signal is corrupted by an additive bandpass noise, $n(t)$, described by the complex envelope

$$\tilde{n}(t) = \rho_{\mathrm{n}}(t)\mathrm{e}^{\mathrm{j}\phi_{\mathrm{n}}(t)}, \tag{1.117}$$

also defined as centered around the *same* center frequency ω_{c}. We thus assume that $n(t)$ can be written as

$$n(t) = \mathrm{Re}\left\{\tilde{n}(t)\mathrm{e}^{\mathrm{j}\omega_{\mathrm{c}}t}\right\}. \tag{1.118}$$

Using these expressions, we can express the total signal $s(t)$, defined as the superposition of $s_{\mathrm{w}}(t)$ and $n(t)$, as

$$s(t) = s_{\mathrm{w}}(t) + n(t) = \mathrm{Re}\left\{(\tilde{s}_{\mathrm{w}}(t) + \tilde{n}(t))\mathrm{e}^{\mathrm{j}\omega_{\mathrm{c}}t}\right\}. \tag{1.119}$$

We then see that the complex envelope $\tilde{s}(t)$ of $s(t)$, when also defined as centered around ω_{c}, can be written as

$$\tilde{s}(t) = \tilde{s}_{\mathrm{w}}(t) + \tilde{n}(t). \tag{1.120}$$

Having defined those signals, we can now focus on the decomposition of $n(t)$. Let us consider the decomposition of its complex envelope, $\tilde{n}(t)$, as the sum of two terms

$$\tilde{n}(t) = \tilde{n}_{\|}(t) + \tilde{n}_{\perp}(t). \tag{1.121}$$

As illustrated in Figure 1.10, in this expression $\tilde{n}_{\|}(t)$ is defined as collinear to $\tilde{s}_{\mathrm{w}}(t)$ when represented in the complex plane, and $\tilde{n}_{\perp}(t)$ as orthogonal to it. Obviously, this definition requires that $\tilde{s}_{\mathrm{w}}(t)$ is non-vanishing in order to be able to define the direction of its representation in the complex plane. Unfortunately, practical modulating complex envelopes can exhibit such zero crossings, as illustrated in Section 1.3. However, when they occur, we can assume that it is only for a set of discrete instants in practice. We can thus assume that $\tilde{n}_{\|}(t)$ and $\tilde{n}_{\perp}(t)$ can still be defined at any time by continuity. The result is that we can in turn interpret $\tilde{n}_{\|}(t)$

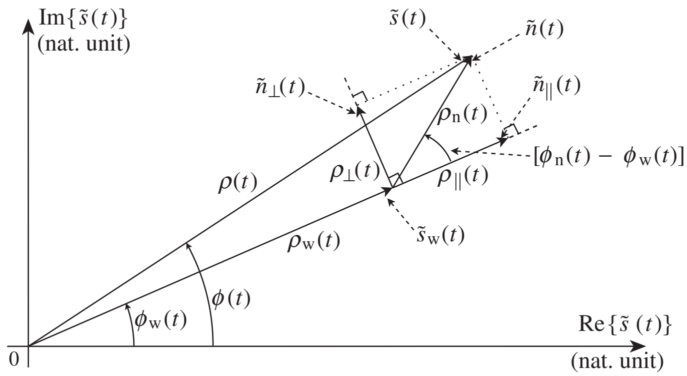

Figure 1.10 Additive bandpass noise decomposition in terms of amplitude and phase noise terms – The complex envelope of a bandpass noise, when defined as centered around the same center frequency as that considered for the definition of the complex envelope of a bandpass signal it is added to, can be decomposed into two components. The first, collinear to the signal complex envelope, represents a bandpass noise that corrupts, at first order, mainly its instantaneous amplitude. The second, orthogonal to it, represents a bandpass noise that corrupts, still at first order, mainly its instantaneous phase.

and $\tilde{n}_{\perp}(t)$ as the complex envelopes, still defined as centered around ω_{c}, of the bandpass noise processes $n_{\parallel}(t)$ and $n_{\perp}(t)$ that can be written as

$$n_{\parallel}(t) = \mathrm{Re}\left\{\tilde{n}_{\parallel}(t)e^{j\omega_{\mathrm{c}}t}\right\}, \tag{1.122a}$$

$$n_{\perp}(t) = \mathrm{Re}\left\{\tilde{n}_{\perp}(t)e^{j\omega_{\mathrm{c}}t}\right\}. \tag{1.122b}$$

Thus, given that all the complex envelopes we are dealing with are defined as centered around the same angular frequency, by substituting equation (1.121) into equation (1.118) and using the above definition we can write

$$\begin{aligned} n(t) &= \mathrm{Re}\left\{\tilde{n}(t)e^{j\omega_{\mathrm{c}}t}\right\} \\ &= n_{\parallel}(t) + n_{\perp}(t). \end{aligned} \tag{1.123}$$

We have thus decomposed the additive bandpass noise $n(t)$ as the sum of two bandpass terms that have interesting properties. This can be advantageously investigated by expressing the complex envelopes of those bandpass terms as a function of the characteristics of $\tilde{s}_{\mathrm{w}}(t)$ and $\tilde{n}(t)$. This can be done in a straightforward way following geometrical considerations that can be derived from the illustration in Figure 1.10. Based on this figure, we immediately have that

$$\tilde{n}_{\parallel}(t) = \rho_{\parallel}(t)\epsilon_{\parallel}(t)e^{j\phi_{\mathrm{w}}(t)} = \rho_{\epsilon\parallel}(t)e^{j\phi_{\mathrm{w}}(t)}, \tag{1.124a}$$

$$\tilde{n}_{\perp}(t) = \rho_{\perp}(t)\epsilon_{\perp}(t)e^{j(\phi_{\mathrm{w}}(t)+\pi/2)} = j\rho_{\epsilon\perp}(t)e^{j\phi_{\mathrm{w}}(t)}, \tag{1.124b}$$

where we have defined

$$\rho_{\|}(t) = \rho_{\mathrm{n}}(t)\ |\cos(\phi_{\mathrm{n}}(t) - \phi_{\mathrm{w}}(t))|, \tag{1.125a}$$

$$\rho_{\perp}(t) = \rho_{\mathrm{n}}(t)\ |\sin(\phi_{\mathrm{n}}(t) - \phi_{\mathrm{w}}(t))|, \tag{1.125b}$$

and

$$\epsilon_{\|}(t) = \mathrm{sign}\ \{\cos(\phi_{\mathrm{n}}(t) - \phi_{\mathrm{w}}(t))\}, \tag{1.126a}$$

$$\epsilon_{\perp}(t) = \mathrm{sign}\ \{\sin(\phi_{\mathrm{n}}(t) - \phi_{\mathrm{w}}(t))\}. \tag{1.126b}$$

The reason for this definition comes from the fact that, following our conventions, $\rho_{\|}(t)$ and $\rho_{\perp}(t)$ are positive quantities that represent moduli of complex envelopes. We thus introduce $\epsilon_{\|}(t)$ and $\epsilon_{\perp}(t)$, which can be only ±1, in order to represent the π phase shift of the arguments of $\tilde{n}_{\|}(t)$ and $\tilde{n}_{\perp}(t)$ depending on the relative instantaneous phase between $\tilde{s}_{\mathrm{w}}(t)$ and $\tilde{n}(t)$. However, as will be seen shortly, the quantities of interest for our derivations are $\rho_{\epsilon\|}(t)$ in equation (1.124a) and $\rho_{\epsilon\perp}(t)$ in equation (1.124b), defined as

$$\rho_{\epsilon\|}(t) = \rho_{\mathrm{n}}(t)\cos(\phi_{\mathrm{n}}(t) - \phi_{\mathrm{w}}(t)), \tag{1.127a}$$

$$\rho_{\epsilon\perp}(t) = \rho_{\mathrm{n}}(t)\sin(\phi_{\mathrm{n}}(t) - \phi_{\mathrm{w}}(t)). \tag{1.127b}$$

Based on this decomposition of $n(t)$, we can then go further in the interpretation of the degradation of $s_{\mathrm{w}}(t)$. We can express the modulus and argument of the complex envelope $\tilde{s}(t) = \rho(t)\mathrm{e}^{\mathrm{j}\phi(t)}$ of the total signal $s(t) = s_{\mathrm{w}}(t) + n(t)$ as a function of the characteristics of those two bandpass noises. For that purpose, we can consider both the decomposition of $\tilde{n}(t)$ given by equation (1.121), and the expressions for $\tilde{n}_{\|}(t)$ and $\tilde{n}_{\perp}(t)$ given by equation (1.124). Following the representation shown in Figure 1.10, we can then immediately write

$$\rho(t) = |\tilde{s}_{\mathrm{w}}(t) + \tilde{n}(t)| = \sqrt{\rho_{\mathrm{w}}^2(t) + 2\rho_{\epsilon\|}(t)\rho_{\mathrm{w}}(t) + \rho_{\mathrm{n}}^2(t)}, \tag{1.128a}$$

$$\phi(t) = \arg\{\tilde{s}_{\mathrm{w}}(t) + \tilde{n}(t)\} = \phi_{\mathrm{w}}(t) + \arctan\left\{\frac{\rho_{\epsilon\perp}(t)}{\rho_{\mathrm{w}}(t) + \rho_{\epsilon\|}(t)}\right\}, \tag{1.128b}$$

with $\rho_{\epsilon\|}(t)$ and $\rho_{\epsilon\perp}(t)$ given by equation (1.127). Obviously, this definition requires that $\tilde{s}_{\mathrm{w}}(t)$ is non-vanishing so that $\rho_{\mathrm{w}}(t) \neq 0$ so as to be able to define at least $\phi(t)$ correctly. Nevertheless, as highlighted previously, we can assume when dealing with practical modulations that this situation occurs only for a set of discrete instants. We can thus assume that we can define such a quantity at any time by continuity. Moreover, we can assume in many practical use cases that $\rho_{\mathrm{n}}(t) \ll \rho_{\mathrm{w}}(t)$. At first glance, we could consider linking this assumption to the fact of having a good enough SNR, i.e. to the assumption of having $\mathbb{E}\{\rho_{\mathrm{n}}^2\} \ll \mathbb{E}\{\rho_{\mathrm{w}}^2\}$ according to equation (1.64). This is unfortunately not true in all cases, as we have just recalled that practical modulating complex envelopes can have their instantaneous amplitude going down toward zero. This means that whatever their power, at some instant we can potentially have that the modulus of their complex envelope is lower than that of a bandpass noise it is added to. However, as the SNR increases, we can imagine that the set of instants for which this situation occurs diminishes. Furthermore, there are classical modulating waveforms for which the instantaneous amplitude has a lower bound. This is obviously the case for constant amplitude schemes, but is also the case for some complex modulations such as the modified 8PSK used in the GSM/EDGE standard and detailed in Section 1.3.2. For such a modulation, there is thus a minimum SNR for which the condition $\rho_n(t) \ll \rho_w(t)$ can be considered as true at any time. Finally, we recall that the classical use case for such decomposition of a bandpass noise corresponds to a signal that is nothing more than the LO waveform flowing from an RF synthesizer and used to drive a mixer for implementing a frequency transposition. In any case, given that $\rho_n(t) \ll \rho_w(t)$ holds, we can rely on a small angle approximation in our derivations so that the above expressions for $\rho(t)$ and $\phi(t)$ reduce to

$$\rho(t) = \rho_w(t) + n_\rho(t), \tag{1.129a}$$

$$\phi(t) = \phi_w(t) + n_\phi(t), \tag{1.129b}$$

with

$$n_\rho(t) \approx \rho_{\epsilon\|}(t), \tag{1.130a}$$

$$n_\phi(t) \approx \frac{\rho_{\epsilon\perp}(t)}{\rho_w(t)}. \tag{1.130b}$$

Under our present assumption, we thus get that up to first order $\rho_{\epsilon\|}(t)$ corrupts only the magnitude $\rho_w(t)$ of the signal complex envelope, i.e. the instantaneous amplitude of $s_w(t)$, whereas $\rho_{\epsilon\perp}(t)$ corrupts only the argument $\phi_w(t)$ of the signal complex envelope, i.e. the instantaneous frequency of $s_w(t)$. We also have an additive behavior for the terms $n_\rho(t)$ and $n_\phi(t)$ that can naturally be labeled as respectively the *amplitude noise* and the *phase noise* which corrupt respectively the instantaneous amplitude and the instantaneous phase of the signal.

We thus have two distinct, albeit equivalent, ways of describing the impact of the bandpass noise $n(t)$ on the bandpass signal $s_w(t)$ it is added to. On the one hand, we can keep the *additive* behavior of $n(t)$ regarding $s_w(t)$ while achieving its decomposition as the sum of $n_\|(t)$ and $n_\perp(t)$. Using equations (1.119) and (1.123), we can write $s(t)$ as

$$s(t) = s_w(t) + n_\|(t) + n_\perp(t). \tag{1.131}$$

Up to first order, i.e. given that $\rho_n(t) \ll \rho_w(t)$, we then get that $n_\|(t)$ and $n_\perp(t)$ corrupt either the instantaneous amplitude of $s_w(t)$ or its instantaneous phase or frequency. On the other hand, we can directly *embed* the noise terms in the components of the complex envelope of $s_w(t)$ in order to derive an expression for $s(t)$. In that case, with the small angle approximation, i.e. still assuming that $\rho_n(t) \ll \rho_w(t)$, we can use the expression for the complex envelope of $s(t)$ given by equation (1.129) to write

$$\tilde{s}(t) = (\rho_w(t) + n_\rho(t))e^{j(\phi_w(t)+n_\phi(t))}, \tag{1.132}$$

with $n_\rho(t)$ and $n_\phi(t)$ given by equation (1.130). In that case, $s(t)$ can be written as

$$\begin{aligned} s(t) &= \mathrm{Re}\left\{\tilde{s}(t)\mathrm{e}^{\mathrm{j}\omega_\mathrm{c}t}\right\} \\ &= (\rho_\mathrm{w}(t) + n_\rho(t))\cos(\omega_\mathrm{c}t + \phi_\mathrm{w}(t) + n_\phi(t)). \end{aligned} \tag{1.133}$$

Although the latter formulation hides the additive behavior of the original bandpass noise with regard to the signal, it is of interest for some practical analytical derivations. In any case, the two representations are strictly equivalent when they exist. The use of either one thus depends only on how easily derivations can be done with it. Nevertheless, despite this equivalence we need to keep in mind that there is a fundamental difference between the terms involved in the two different representations. On the one hand we are dealing with *bandpass* noise terms, $n_\parallel(t)$ and $n_\perp(t)$, directly related to the decomposition of the original bandpass noise $n(t)$. On the other hand, we have *lowpass* components, $n_\rho(t)$ and $n_\phi(t)$, which are involved in the modulus and argument of the complex envelope of the total signal $s(t)$.

To conclude this section, it is of interest to mention additional considerations that arise when the bandpass noise, implicitly assumed centered, also has a Gaussian distribution. In this case it is easy to derive the fraction of power of the bandpass noise that corrupts either the instantaneous amplitude of the signal or its instantaneous phase or frequency. Assuming we are dealing with stationary processes, we can express the power $P_{\mathrm{n}_\parallel}$ and $P_{\mathrm{n}_\perp}$ of the bandpass processes $n_\parallel(t)$ and $n_\perp(t)$ based on the expressions we have derived so far for their complex envelopes through the use of equation (1.64). Focusing first on the average power of $n_\parallel(t)$, given that $\epsilon_\parallel(t)$ can be only ± 1, from equations (1.124a) and (1.125a) we have that

$$P_{\mathrm{n}_\parallel} = \frac{\mathbb{E}\left\{\rho_\mathrm{n}^2\cos^2(\phi_\mathrm{n} - \phi_\mathrm{w})\right\}}{2}. \tag{1.134}$$

But, following the derivations performed in Section 1.2.1, we also get that the modulus and argument of the complex envelope of a stationary and centered Gaussian process are independent when considered at the same time. Because the wanted signal $s_\mathrm{w}(t)$ and the noise component $n(t)$ can also be assumed independent, we can therefore write

$$P_{\mathrm{n}_\parallel} = \frac{\mathbb{E}\left\{\rho_\mathrm{n}^2\right\}}{2}\mathbb{E}\left\{\cos^2(\phi_\mathrm{n} - \phi_\mathrm{w})\right\}. \tag{1.135}$$

Using equation (1.54), we can then expand the last term of the right-hand side of this equation:

$$\mathbb{E}\left\{\cos^2(\phi_\mathrm{n} - \phi_\mathrm{w})\right\} = \frac{1}{2} + \frac{1}{2}\mathbb{E}\{\cos[2(\phi_\mathrm{n} - \phi_\mathrm{w})]\}. \tag{1.136}$$

As we have the independence of ϕ_n and ϕ_w, we can then evaluate the expectation on the right-hand side of this equation by integrating first the PDF of ϕ_n. But, as we deal with a stationary centered Gaussian bandpass noise, we get that ϕ_n is uniformly distributed over

$[0, 2\pi]$ according to equation (1.106). Due to this even distribution over a period of the cosine function, it follows that

$$\mathbb{E}\{\cos[2(\phi_\mathrm{n} - \phi_\mathrm{w})]\} = 0, \tag{1.137}$$

and thus that

$$P_{\mathrm{n}_\parallel} = \frac{1}{2}\frac{\mathbb{E}\left\{\rho_\mathrm{n}^2\right\}}{2} = \frac{1}{2}P_\mathrm{n}, \tag{1.138}$$

where P_n is the power of the original bandpass Gaussian noise. As exactly the same derivation can be performed for the perpendicular component $n_\perp(t)$, we finally get that

$$P_{\mathrm{n}_\parallel} = P_{\mathrm{n}_\perp} = \frac{1}{2}P_\mathrm{n}. \tag{1.139}$$

We see that whatever the characteristics of the signal such bandpass noise is added to, we recover an equal noise power over the components defined as perpendicular and parallel to the signal complex envelope. We also observe that this result highlights the derivations performed in Chapter 5 when considering the SNR improvement through nonlinearity in Sections 5.1.4 and 5.2. Indeed, in those sections we find that the fraction of the input bandpass noise corresponding to a complex envelope collinear to that of the constant amplitude signal can be canceled due to RF compression. Only the fraction of noise that corresponds to an orthogonal complex envelope succeeds in going through it. Reconsidering the above derivation, we can then understand why the SNR improvement can asymptotically reach 3 dB as the input SNR increases, as shown for instance in Figure 5.30.

1.3 Digital Modulation Examples

Let us now review some modulation schemes that are classically encountered in wireless standards and that are used as examples throughout this book. From a transceiver dimensioning perspective, we are mainly interested in the statistical properties of the modulating waveform and of the associated modulated bandpass signal we have to process in a line-up, rather than in the way such modulating waveforms are generated in practice. As a result, we review here different schemes that are representative of almost all the statistics of complex envelopes we encounter in practice, from the simple constant envelope modulation, illustrated here through the Gaussian minimum shift keying (GMSK) scheme used in the GSM standard, to the most complex waveforms as used in CDMA or OFDM based systems. However, we still need to detail the way those waveforms are generated in order to be able to derive their statistical properties and the associated constraints for transceivers.

1.3.1 Constant Envelope

Let us focus first on constant envelope modulation schemes. As the name suggests, we expect in this case to keep the instantaneous amplitude of the resulting modulated bandpass signal constant. The modulations we are referring to are thus in fact pure phase or frequency modulation schemes. This means that it is only the instantaneous phase or frequency of the resulting modulated RF bandpass signals that carries the information. To illustrate this kind of modulating waveform we can consider GMSK as defined in the GSM standard [7].

We first need to express the instantaneous phase of the resulting modulated bandpass signal as a function of the data bits. From the discussion in "Instantaneous amplitude and instantaneous frequency" (Section 1.1.3), we get that this instantaneous phase is linked to the argument of any of the complex envelopes of this bandpass signal. And due to the nature of the modulation we are considering, the polar form of such complex signal is of interest. Accordingly, let us consider the bandpass signal $s(t)$ resulting from the upconversion of the modulating complex signal $\tilde{s}(t) = e^{j\phi(t)}$ around the carrier angular frequency ω_c. It can be expressed as

$$\begin{aligned} s(t) &= \mathrm{Re}\left\{\tilde{s}(t)e^{j\omega_c t}\right\} \\ &= \mathrm{Re}\left\{e^{j(\omega_c t+\phi(t))}\right\}. \end{aligned} \tag{1.140}$$

It thus simply means that $\tilde{s}(t)$ can be further interpreted as the complex envelope, defined as centered around ω_c, of the bandpass signal $s(t)$. Here, we observe that we have assumed for the sake of simplicity a normalized modulus for $\tilde{s}(t)$ in the definition of those quantities, i.e. that $\rho = |\tilde{s}(t)| = 1$. In any case, according to equation (1.97) we get that the instantaneous frequency $f(t)$ of $s(t)$ is given by

$$f(t) = \frac{1}{2\pi}\left(\omega_c + \frac{d\phi(t)}{dt}\right). \tag{1.141}$$

In the GSM standard, the modulation is defined so that the instantaneous frequency of the resulting modulated RF bandpass signal can be written as a function of the modulating data according to

$$f(t) = \frac{\omega_c}{2\pi} + \frac{h}{2}\sum_k \alpha_k g(t-kT). \tag{1.142}$$

As a result, the argument $\phi(t)$ of $\tilde{s}(t)$ can in turn be written as

$$\phi(t) = \pi h \sum_k \alpha_k \int_{-\infty}^{t-kT} g(u)du, \tag{1.143}$$

thus leading to the expression for $\tilde{s}(t)$:

$$\tilde{s}(t) = \exp\left(j\pi h \sum_k \alpha_k \int_{-\infty}^{t-kT} g(u)du\right). \tag{1.144}$$

In equations (1.142)–(1.144), the parameter h stands for the modulation index and T for the symbol period. These parameters are respectively equal to $1/2$ and $48/13 = 3.69\,\mu$s in the standard. In the same way $g(t)$ is the pulse shaping filter that smooths the transitions of the instantaneous frequency of $s(t)$ when going from one representation of input data to the next, and α_k is the sequence of input data, which can be ± 1 here.[4]

With regard to the above expressions, it is of interest to interpret further how this modulating scheme works. For instance, when a single datum $\alpha_k = +1$ enters the modulator, we get that the instantaneous frequency signal $f(t)$ experiences a positive deviation compared to the carrier frequency $\omega_\mathrm{c}/2\pi$. This frequency offset stands for a finite duration corresponding to the length of the impulse response of the filter $g(t)$. We thus get that the impact of the datum $\alpha_k = +1$ on the final modulated signal $s(t)$ is simply a finite phase shift on its instantaneous phase compared to the average term $\omega_\mathrm{c} t$ linked to the carrier, this shift being equal to the integral of the instantaneous frequency deviation during the duration of the impulse response of $g(t)$. The magnitude of this phase shift is thus linked to the properties of the filter $g(t)$. In the GSM standard, this pulse shaping filter is a Gaussian filter defined as the convolution of the gate function $\Pi(t)$,

$$\Pi\left(\frac{t}{T}\right) = \begin{cases} \dfrac{1}{T} & \text{when } |t| < T/2, \\ 0 & \text{otherwise,} \end{cases} \tag{1.145}$$

with a Gaussian function $h(t)$ defined by

$$h(t) = \frac{1}{\delta T\sqrt{2\pi}} \exp\left(-\frac{t^2}{2\delta^2 T^2}\right). \tag{1.146}$$

Here, δ is defined by

$$\delta = \frac{\sqrt{\ln(2)}}{2\pi BT}, \tag{1.147}$$

with B the filter cut-off frequency at 3 dB, defined from the symbol duration through the relation $BT = 0.3$. After some algebra, we can express the impulse response $g(t)$ of the Gaussian pulse shaping filter as

$$\begin{aligned} g(t) &= h(t) \star \Pi\left(\frac{t}{T}\right) \\ &= \frac{1}{2T}\left\{\mathrm{Erfc}\left[\frac{1}{\sqrt{2}\delta}\left(\frac{t}{T} - \frac{1}{2}\right)\right] - \mathrm{Erfc}\left[\frac{1}{\sqrt{2}\delta}\left(\frac{t}{T} + \frac{1}{2}\right)\right]\right\}, \end{aligned} \tag{1.148}$$

where Erfc(.) stands for the complementary error function defined by

$$\mathrm{Erfc}(t) = \frac{2}{\sqrt{\pi}} \int_t^{+\infty} \mathrm{e}^{-x^2} \mathrm{d}x. \tag{1.149}$$

[4] In the GSM standard, it is in fact the differential encoded input bits that are provided to the modulator as the α_k data.

From these expressions, we can thus see that the GMSK pulse shaping filter is normalized so that $\int_{-\infty}^{+\infty} g(u)\mathrm{d}u = 1$. As a result, in the case of a single input datum α_k equal to $+1$, we get that the phase of the modulating signal given by equation (1.143) varies from 0 at $t = 0$ to $\pi/2$ rad at $t = +\infty$. And for the same reason, for a single input datum of opposite sign, we get that the phase of the signal varies from 0 at $t = 0$ to $-\pi/2$ rad at $t = +\infty$. With this behavior in mind, we can now understand that when considering a stream of constant input data all equal to $+1$, we obtain a constant phase rotation at the modulator output of $\pi/2$ rad for each symbol period, i.e. of 2π after four symbol periods. We can thus expect with such a sequence of constant input data values that the resulting modulated RF bandpass signal behaves as an almost CW signal with a frequency offset of $1/(4T) = 13 \times 10^6/(48 \times 4) = 67708.33$ Hz compared to the carrier frequency. Moreover, we understand that this value corresponds to the maximum we can achieve for the instantaneous frequency of the modulated signal, that is coherent with the plot shown in Figure 1.11. However, this maximum deviation of $\pm h/(2T) = \pm 67.70833$ kHz around the carrier frequency does not mean that the spectrum of the modulated RF signal does not spread over a wider frequency range, as shown in Figure 1.12. Indeed, we get that the final RF modulated signal is the cosine of the phase corresponding to this instantaneous frequency. The relationship between its spectrum and the spectral content of the instantaneous frequency signal is therefore not so straightforward. This topic is related to what is encountered in the derivation of the Carson bandwidth when dealing with an analog frequency modulation.

Let us now focus on the consequences on the architecture of transceivers, and more precisely of transmitters, of using such a pure phase or frequency modulating waveform. The first consequence comes from the fact that the instantaneous amplitude of the resulting RF bandpass

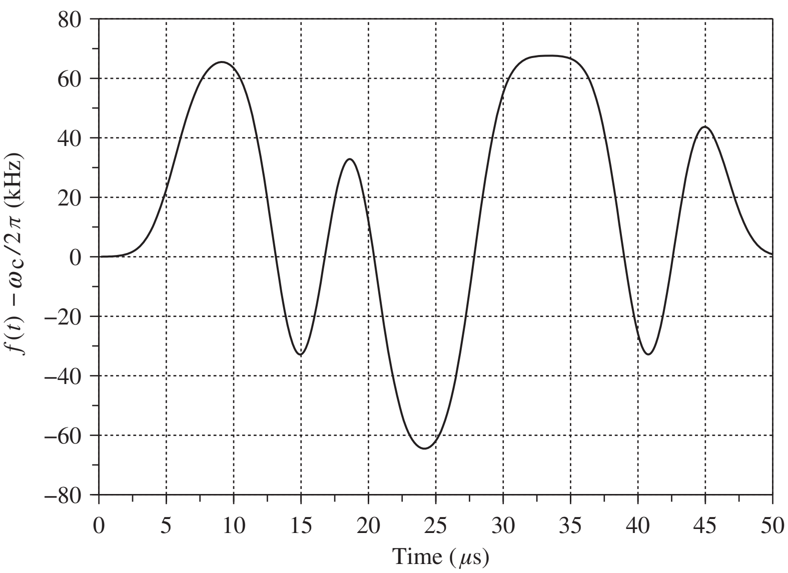

Figure 1.11 Instantaneous frequency of a GMSK modulated bandpass signal as used in the GSM standard – For the instantaneous frequency to reach the maximum theoretical value of ± 67.70833 kHz, we need at least three input data of the same polarity. In the present case, the input data sequence is $1, 1, -1, 1, -1, -1, 1, 1, 1, -1, 1$.

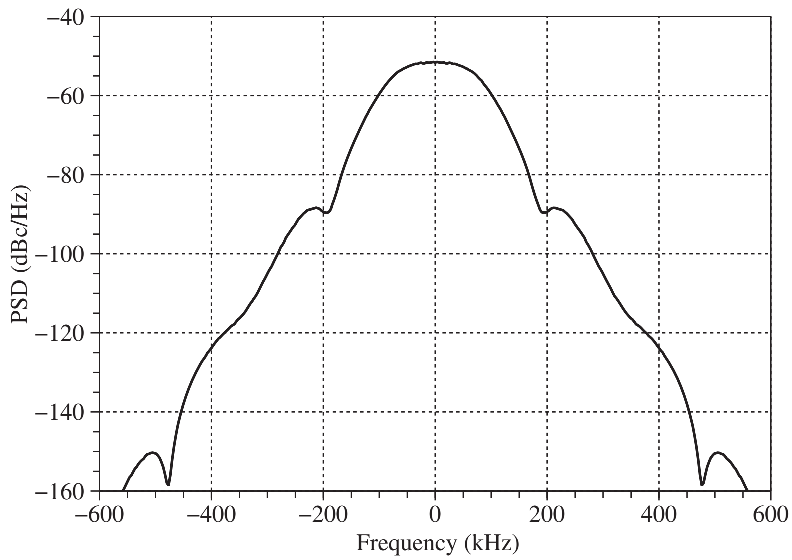

Figure 1.12 Power spectral density of a randomly modulated GMSK complex envelope as used in the GSM standard – The PSD of a randomly modulated GMSK waveform is wider than the instantaneous frequency range due to the nonlinear behavior of the cosine function and to the rate of change of the instantaneous frequency that follows the Gaussian filter response.

signal is constant. Another way to express this is to say that the PAPR of this signal, defined by equation (1.71), reduces to 1, or 0 dB. Practically speaking, this characteristic is of interest as it corresponds to RF bandpass signals that are resistant to compression, at least when considering their sideband centered around the carrier angular frequency. As discussed in Chapter 5, this allows, for instance, the use of saturated power amplifiers (PAs) that exhibit good efficiency, thus leading to an optimization of the power consumption of the transceiver implementation. Nevertheless, the counterpart of using such a constant amplitude modulating waveform is obviously a limited efficiency in terms of transmitted bit rate for a given spectrum bandwidth, as we use only one dimension out of the two available for mapping the modulation scheme.

Another interesting consequence in terms of physical implementation of using such constant instantaneous amplitude behavior can be seen when reconsidering the expression for the resulting RF bandpass signal $s(t)$ derived from the polar form of the complex modulating signal. Using equation (1.144), we get

$$\begin{aligned} s(t) &= \mathrm{Re}\left\{\tilde{s}(t)e^{j\omega_c t}\right\} \\ &= \cos\left(\omega_c t + \pi h \sum_k \alpha_k \int_{-\infty}^{t-kT} g(u)\mathrm{d}u\right). \end{aligned} \tag{1.150}$$

This expression shows that once the modulating waveform is generated, we can directly modulate the phase or frequency of the RF synthesizer that is used to generate the carrier waveform in order to directly recover the modulated RF bandpass signal. This is what allows the use of the very compact and power efficient direct phase locked loop (PLL) modulator architecture for such a transmitter, as discussed in Chapter 8. However, this does not prevent us considering a Cartesian form of the complex envelope $\tilde{s}(t)$ if required. In that case, using equation (1.144), we can write

$$p(t) = \cos\left(\pi h \sum_k \alpha_k \int_{-\infty}^{t-kT} g(u)\mathrm{d}u\right), \tag{1.151a}$$

$$q(t) = \sin\left(\pi h \sum_k \alpha_k \int_{-\infty}^{t-kT} g(u)\mathrm{d}u\right), \tag{1.151b}$$

so that we can express $s(t)$ as

$$\begin{aligned} s(t) = {} & \cos\left(\pi h \sum_k \alpha_k \int_{-\infty}^{t-kT} g(u)\mathrm{d}u\right)\cos(\omega_c t) \\ & - \sin\left(\pi h \sum_k \alpha_k \int_{-\infty}^{t-kT} g(u)\mathrm{d}u\right)\sin(\omega_c t). \end{aligned} \tag{1.152}$$

Alternatively, this last expression for the RF signal can be obtained directly from equation (1.150) using

$$\cos(\alpha + \beta) = \cos(\alpha)\cos(\beta) - \sin(\alpha)\sin(\beta). \tag{1.153}$$

Such Cartesian expansion may be required, for instance, when using a direct conversion transmitter. We then see that the real and imaginary parts of its complex envelope $\tilde{s}(t) = p(t) + \mathrm{j}q(t)$ are sinusoidal waveforms that have a CF equal to $\sqrt{2}$, i.e. 3 dB. However, we get that even if we are dealing with a final modulated bandpass signal $s(t)$ that is insensitive to RF compression when considering the sideband centered around the carrier angular frequency as mentioned above, this property is untrue for the $p(t)$ and $q(t)$ signals that are by definition lowpass. Any degradation of those Cartesian components through compression would result in a distorted RF bandpass signal that could exhibit a non-constant amplitude waveform, as originally expected. We also mention that the same behavior would result from any imbalance between those components, as illustrated in Section 6.2.2. In any case, having such non-perfect constant amplitude for $s(t)$ may be an issue if we are faced with AM-PM conversion in the final PA stage, as is frequently the case with saturated devices used for constant amplitude RF waveforms. It would thus lead to some additional distortion of the transmitted signal on top of the former non-perfect constant amplitude behavior. Here, we can thus anticipate the discussion in Chapter 8 and highlight that the generation of $s(t)$ through a direct PLL modulation would allow us to overcome this kind of limitation linked to the implementation of transmitters based on the Cartesian processing of the complex envelope of such constant amplitude signal.

We conclude with a comment on the complexity of the equations considered so far. We understand that it would be quite unrealistic to consider an analog implementation of those expressions for generating the modulating signals. This is in fact a general statement for most of the modulations used in the field of digital communication, as illustrated through the examples discussed in the forthcoming sections. It thus follows that these waveforms are almost always generated in the digital domain and then converted to analog for further processing. This therefore leads to traditional high level system block partitions in transceivers, as discussed in Section 1.4.

1.3.2 Complex Modulation

As highlighted in the previous section, the use of constant envelope modulation schemes is driven by both the potential simplicity in the generation of the corresponding modulated RF bandpass signals and their good behavior with regard to RF compression. Nevertheless, the need for increasing data rates while preserving the frequency bandwidth that is used may lead to the consideration of complex modulations. Here, by "complex" we mean a modulation scheme that effectively uses the two dimensions allowed by the complex envelope representation. Practically speaking, it thus corresponds to a modulated RF bandpass signal that is both amplitude and phase or frequency modulated. It is thus of interest to focus on the modified 8PSK modulation used in the GSM/EDGE standard. Indeed, in addition to illustrating a complex modulation in itself, this scheme gives the opportunity to highlight the way some features considered at the definition level of the modulation may or may not make realizable some particular transmit architectures as discussed at the end of this section.

Let us begin by detailing how to generate the modulating complex envelope as a function of the input data bits according to the standard specification [7]. The first step is to map the data bits into 8PSK (eight-phase shift keying) symbols. Practically speaking, the data bits are Gray mapped by groups of three bits onto eight possible symbols uniformly spread over the unit circle when represented in the complex plane. For a given sequence of input data bits, the sequence of 8PSK symbols, $\tilde{S}_k$, is in fact defined by

$$\tilde{S}_k = \mathrm{e}^{\mathrm{j}\frac{2l\pi}{8}}, \tag{1.154}$$

with l given in Table 1.1 as a function of the input data bits. Up to now, this symbol mapping corresponds to a classical 8PSK modulation. But, in the GSM/EDGE standard, the symbol mapping is slightly modified so that a continuous phase rotation of $3\pi/8$ from symbol to symbol is added to the former sequence of symbols. This results in the new sequence,

$$\tilde{S}'_k = \tilde{S}_k\,\mathrm{e}^{\mathrm{j}\frac{3k\pi}{8}}. \tag{1.155}$$

This continuous phase rotation is the reason for the epithet "modified" in the term "modified 8PSK modulation". Practically speaking, it is this simple added feature that explains the properties of the resulting modulated RF bandpass signal mentioned at the beginning of the section and further discussed at the end of the section. We can see that the final modulating waveform is obtained as the filtered version of this sequence of data symbols in order to shape the spectrum of the resulting modulated signal. Denoting this pulse shaping filter by C_0 and

Table 1.1 Symbol mapping parameter l for the GSM/EDGE modified 8PSK modulation.

Modulating bits $d_{3k}, d_{3k+1}, d_{3k+2}$	Symbol parameter l
(1,1,1)	0
(0,1,1)	1
(0,1,0)	2
(0,0,0)	3
(0,0,1)	4
(1,0,1)	5
(1,0,0)	6
(1,1,0)	7

its impulse response by $C_0(t)$, the resulting complex envelope $\tilde{s}(t) = p(t) + \mathrm{j}q(t)$ can thus be written as

$$\tilde{s}(t) = \sum_k \tilde{S}'_k C_0(t - kT + 2T), \tag{1.156}$$

so that we get

$$p(t) = \sum_k \mathrm{Re}\left\{\tilde{S}'_k\right\} C_0(t - kT + 2T), \tag{1.157a}$$

$$q(t) = \sum_k \mathrm{Im}\left\{\tilde{S}'_k\right\} C_0(t - kT + 2T). \tag{1.157b}$$

We observe that this is in fact the spectrum of both the real and the imaginary parts of the modulating complex envelope $\tilde{s}(t)$ that the C_0 filter shapes. But, referring to the discussion in "Power spectral density" (Section 1.1.3), we get that under common assumptions, those real and imaginary parts have the same spectral shape as the overall complex envelope, and thus as the final modulated bandpass signal $s(t)$. We can thus understand the importance of defining such complex modulating waveforms in their Cartesian form in order to directly control the characteristics of the transmitted output signal in terms of spectral shape. This explains why most practical complex modulations are defined in such a Cartesian way. In our present case the final modulated RF bandpass signal $s(t)$ resulting from the upconversion of this complex envelope around the carrier angular frequency ω_c can therefore be expressed as

$$s(t) = \mathrm{Re}\left\{\tilde{s}(t)\mathrm{e}^{\mathrm{j}\omega_\mathrm{c} t}\right\}, \tag{1.158}$$

or, based on the Cartesian representation of $\tilde{s}(t)$, as

$$\begin{aligned} s(t) = &\sum_k \mathrm{Re}\left\{\tilde{S}'_k\right\} C_0(t - kT + 2T)\cos(\omega_\mathrm{c} t) \\ &- \sum_k \mathrm{Im}\left\{\tilde{S}'_k\right\} C_0(t - kT + 2T)\sin(\omega_\mathrm{c} t). \end{aligned} \tag{1.159}$$

In the EDGE standard, the impulse response of this C_0 filter is defined as

$$C_0(t) = \begin{cases} \prod_{l=0}^{3} S(t+lT) & \text{when } 0 \le t \le 5T, \\ 0 & \text{otherwise,} \end{cases} \tag{1.160}$$

where T stands for the symbol period. In the EDGE standard, this period is the same as for the GMSK modulation of the GSM standard, i.e. $48/13 = 3.69\,\mu$s. In this expression, $S(t)$ is defined as[5]

$$S(t) = \begin{cases} \sin\left(\pi \int_0^t g(u)\mathrm{d}u\right) & \text{when } 0 \le t \le 4T, \\ \sin\left(\frac{\pi}{2} - \pi \int_0^{t-4T} g(u)\mathrm{d}u\right) & \text{when } 4T < t \le 8T, \\ 0 & \text{otherwise,} \end{cases} \tag{1.161}$$

with $g(t)$ given by

$$g(t) = \frac{1}{2T}\left\{ \mathrm{Q}\left(2\pi 0.3 \frac{t-5T/2}{T\sqrt{\ln(2)}}\right) - \mathrm{Q}\left(2\pi 0.3 \frac{t-3T/2}{T\sqrt{\ln(2)}}\right)\right\}. \tag{1.162}$$

In this expression, Q(.) stands for

$$\mathrm{Q}(t) = \frac{1}{\sqrt{2\pi}} \int_t^{+\infty} \mathrm{e}^{-\frac{x^2}{2}}\,\mathrm{d}x. \tag{1.163}$$

Alternatively, we can make the link between this function and the Gaussian filter defined in the previous section. For that purpose, we can express $g(t)$ using both the complementary error function, Erfc(.) defined by equation (1.149), and the δ parameter defined by equation (1.147). We obtain

$$g(t) = \frac{1}{4T}\left\{ \mathrm{Erfc}\left[\frac{1}{\sqrt{2}\delta}\left(\frac{t}{T} - \frac{5}{2}\right)\right] - \mathrm{Erfc}\left[\frac{1}{\sqrt{2}\delta}\left(\frac{t}{T} - \frac{3}{2}\right)\right]\right\}. \tag{1.164}$$

[5] In equation (1.161), the summation of the Gaussian filter transfer function $g(t)$ is done over a finite range as defined in the standard, thus resulting in $S(t)$ not being continuous for $t = 4T$ [7]. With this definition, C_0 is not exactly symmetric, whereas the main pulse in the Laurent series expansion of the GMSK modulation should be, as the original Gaussian filter is.

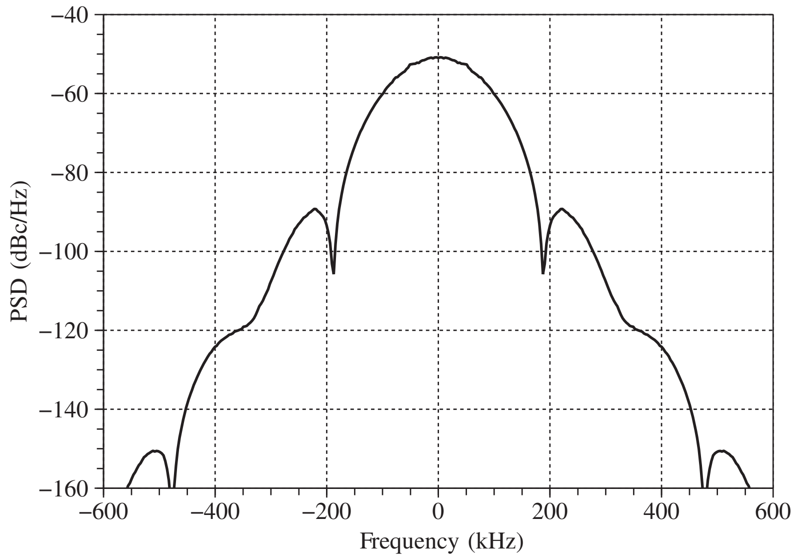

Figure 1.13 Power spectral density of a randomly modulated GSM/EDGE complex envelope – The PSD of a randomly modulated modified 8PSK waveform, as used in the GSM/EDGE standard, is comparable to that of a GMSK modulated waveform used in the GSM standard, as shown in Figure 1.12.

We thus see that $g(t)$ is nothing more than the Gaussian filter of the GMSK modulation described in the previous section, but translated around $t = 2.5T$ and with a different normalization coefficient. The reason for the correspondence is that the C_0 filter used in the present modulation scheme is nothing more than the main pulse in the Laurent series decomposition of the GMSK scheme [8]. It thus follows that the modified 8PSK scheme shaped through the use of this filter results in almost the same spectrum as the original GMSK one, as can be seen by comparing Figures 1.13 and 1.12.

Let us now focus on the statistical properties of the resulting modulating waveform. We begin with the continuous phase rotation of $3\pi/8$ added from symbol to symbol. The direct impact of this feature can be seen in Figure 1.14 where the modulating complex envelope trajectories are plotted in the two cases where the continuous phase rotation is either implemented or not. This figure clearly shows that this simple continuous rotation, easily implemented on the transmit side and compensated on the receive side, allows us to avoid any zero crossing of the modulation trajectory in the complex plane. As summarized in Figure 1.15, we get that this behavior results in interesting statistical properties, in particular the following:

(i) The dynamic range (DR) of the complex envelope magnitude $\rho(t) = |\tilde{s}(t)|$, and thus of the PAPR of the corresponding modulated bandpass signal, is minimized. This parameter can be evaluated to be 3.2 dB when this continuous rotation is used and 3.5 dB when not. This reduction of 0.3 dB can thus be directly transposed in terms of gain on the back-off regarding the saturated power to be used in order to avoid compression. Here we anticipate Section 8.1.7 where it is mentioned that this reduction can be directly transposed in terms

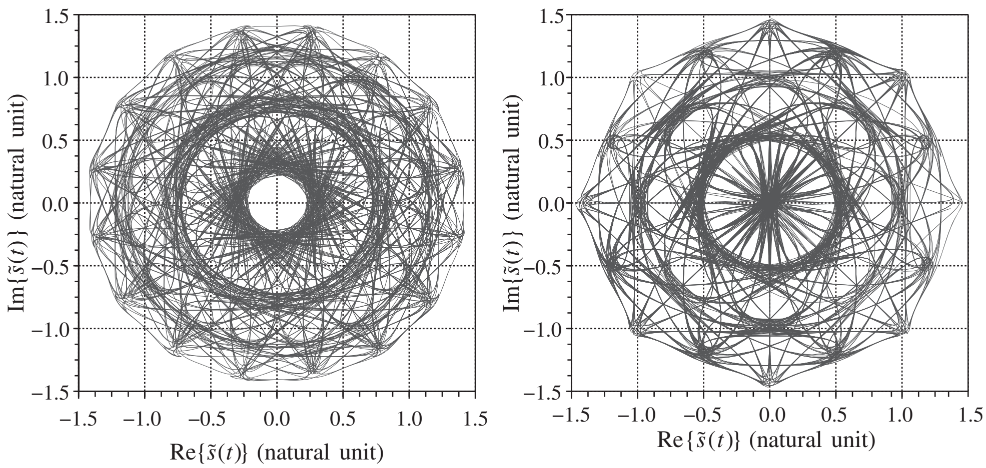

Figure 1.14 Trajectories of a randomly modulated GSM/EDGE complex envelope with and without continuous phase rotation – Compared to the case where no continuous rotation is applied (right), the trajectory of the modified 8PSK as defined in [7] exhibits no zero crossing (left).

of gain on the power consumption of the solution, at least when considering a statically polarized linear amplifier. At first glance, 0.3 dB may seem a small improvement, but we have to keep in mind that in a typical cellular system, the PA consumption can be up to hundreds of milliamperes for mobile equipment. A few tenths of a decibel on this power consumption is therefore not negligible.

(ii) A trajectory that does not vanish leads to other advantages that make simpler (and even make possible) the use of architectures such as the polar transmitter. Indeed, as discussed in Section 8.1.6, having zero crossings in the trajectory leads to important spikes in the instantaneous frequency of the resulting modulated RF bandpass signal. This is obviously due to the π shifts in the argument of the complex envelope at those instants that lead to a derivative theoretically infinite. Such important instantaneous frequency variations require, on the one hand, synthesizers with a high enough bandwidth, and, on the other hand, a very precise timing alignment between the instantaneous amplitude and the instantaneous frequency to achieve a good reconstructed modulated RF bandpass signal. In addition, having such zero crossings leads to an important DR of the modulus of the complex envelope that can theoretically reach infinity when expressed in decibels. Having an analog device that is linear over such a wide DR in order to be able to perform the amplitude modulation of an RF carrier without distortion is almost impossible. However, those problems are not too severe for the modified 8PSK modulation of the GSM/EDGE standard. We get, for instance, that the DR of the instantaneous amplitude remains within 17 dB. We thus see that a simple trick like this continuous phase rotation from symbol to symbol can make the difference between being and not being able to use a given transmit architecture.

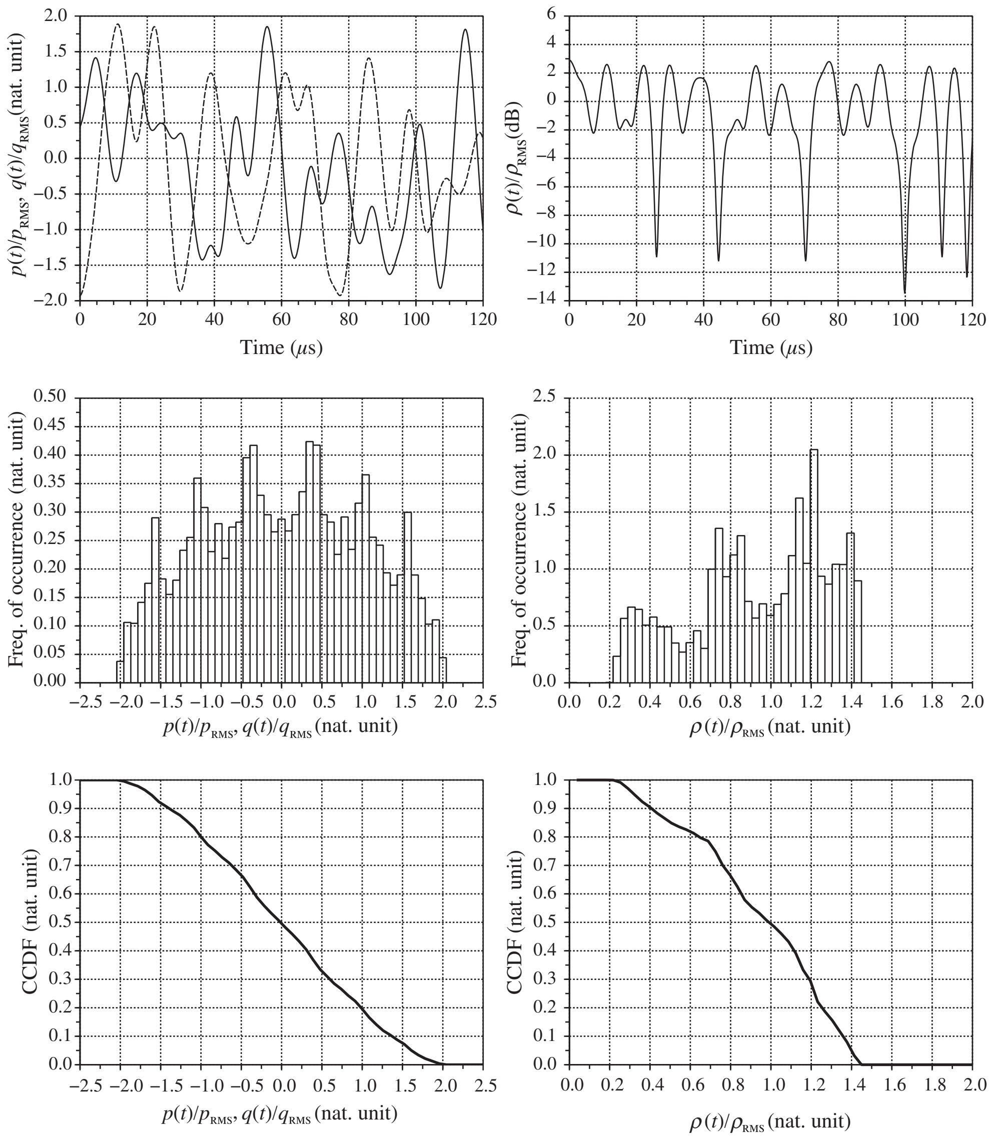

Figure 1.15 Statistical characteristics of a randomly modulated GSM/EDGE complex envelope – The real and imaginary parts $p(t)$ (top left, solid) and $q(t)$ (top left, dashed) of the GSM/EDGE complex envelope have a distribution that is bounded by ± 2 times their RMS value (middle left). Therefore their CCDF reaches 0 for $p(t) = 2p_{\text{RMS}}$ or $q(t) = 2q_{\text{RMS}}$ (bottom left). The CF of those waveforms is thus equal to 2, i.e. 6 dB. The corresponding modulus $\rho(t)$ (top right) has a bounded distribution relative to its RMS value (middle right). This upper bound of 1.4, or 3.2 dB, corresponds to the modulation PAPR as recovered on the CCDF of this parameter (bottom right).

To conclude, as can be seen in Figure 1.15, we highlight the fact that the CF of the $p(t)$ and $q(t)$ waveforms is around 6 dB, i.e. about 3 dB higher than the modulating waveform PAPR. This result is consistent with equation (1.84) and the discussion presented in "Peak to average power ratio and crest factor" (Section 1.1.3).

1.3.3 Wideband Modulation

To conclude this overview of digital modulation examples, let us now focus on wideband modulations. The problem is that the criteria used to designate a modulating waveform as wideband may depend on the point of view adopted. For instance, taking the RF implementation point of view, we may be tempted to label as wideband a modulation that leads to a modulated bandpass signal that spreads over a non-negligible frequency band with regard to the carrier frequency. Unfortunately, most of the schemes classically classified as wideband still lead to modulated signals that remain narrowband with regard to the carrier frequency in respect to RF implementation issues. Alternatively, taking the wireless mobile signal processing point of view, we may be tempted to label as wideband a modulating waveform whose spectrum is wider than the coherence bandwidth of the propagation channel according to the concept introduced in Section 2.3, the reason being that this property allows some interesting structures for the channel estimation and equalization. However, with this definition we see that even the modulating schemes reviewed in the previous sections can be considered as wideband as long as the symbol data rate is chosen high enough. In any case, this situation does not really occur in practice as the schemes leading to more efficient channel equalization when there is the possibility of using such high frequency bandwidth rely on different modulation strategies than those former ones. Moreover, in the wireless network perspective it is not necessarily of interest to have the high data rate corresponding to such high bandwidth statically allocated to a single end user. On the other hand, it may be of interest to consider the possibility of multiplexing different users over the same wideband modulating waveform in order to have the flexibility for the data rate to be dynamically allocated to any of them, as introduced in Section 3.1. In both cases, it classically results in two families of modulating waveforms that we can classify as wideband in what follows and that we can examine as such, namely those encountered in CDMA systems and in OFDM systems. As will be seen, this results in waveforms that exhibit interesting statistical properties compared to those seen up to now.

Code Division Multiple Access

Let us begin our review of wideband modulations by examining the behavior of waveforms encountered in CDMA systems. In such systems the multiplexing of the users belonging to the same network cell, as introduced in Section 3.1, or at least of the different data and logical channels of a given user, is done in the same frequency band and same time slot through the use of orthogonal codes. That said, it is of interest to remark that those codes need to have a high frequency content, at least comparable to the overall data rate of the system, in order to allow for this multiplexing. As a side effect, we then get that, from a network perspective, the modulating waveform that needs to be processed by a given receiver (RX) may potentially carry information for all the users belonging to the same cell at the same time, not just its own.[6] This deep difference with respect to the modulations reviewed in previous sections explains the fact that the modulating signals to be processed by the transceivers belonging to such a network have in most cases a much higher bandwidth than their own effective data rate, thus highlighting the label “wideband” for characterizing such modulating waveforms.

Let us consider the WCDMA standard [9, 10] as an example. In this standard, the orthogonal codes used for the multiplexing of the channels are the Walsh–Hadamard codes that can be expressed in a general form as

$$w_k(t) = \sum_{n=0}^{L-1} a_k(n)\delta(t - nT_c). \tag{1.165}$$

In this expression, T_c stands for the duration of the elementary part a_k of the code sequence, usually referred to as the chip duration. Given that this chip duration is expected to be the shortest time base of the toggling of the modulating waveform, we can expect an overall bandwidth for this signal in the region of $1/T_c$. We thus get that the choice for this chip duration is driven by the targeted bandwidth of the final modulating waveform. Then, we get that the a_k values are equal to ± 1 and are such that the scalar product between two different codes is zero. Each data symbol $\tilde{S}$ to be transmitted – which can be a QPSK symbol, a quadrature amplitude modulation (QAM) symbol, or whatever is considered in the standard – is then associated with an entire code signal $w_k(t)$. As a result, given a symbol duration equal to T, we then need to select the length of the code L, also defined as the spreading factor, such that $T = LT_c$. A sequence of data symbols $\tilde{S}_k(m)$ associated with the kth code $w_k(t)$ therefore leads to a sequence of modulating chips $\tilde{c}_k(t)$ given by

$$\tilde{c}_k(t) = \sum_m \tilde{S}_k(m) w_k(t - mT). \tag{1.166}$$

Now, supposing that we have K different users, or at least K different channels, to be multiplexed through the use of K different codes, we get that the overall sequence of modulating chips $\tilde{c}_K(t)$ is nothing more than the sum of the sequence associated with each code, i.e. $\sum_{k=1}^{K} \tilde{c}_k(t)$. Assuming for simplicity that the spreading factor L is the same for any of them, i.e. that we have the same data symbol rate for each user or channel, we can then use equations (1.165) and (1.166) to express $\tilde{c}_K(t)$ as

$$\begin{aligned} \tilde{c}_K(t) &= \sum_{k=1}^{K} \beta_k \sum_m \tilde{S}_k(m) w_k(t - mT) \\ &= \sum_{k=1}^{K} \beta_k \sum_m \tilde{S}_k(m) \sum_{n=0}^{L-1} a_k(n)\delta(t - nT_c - mT). \end{aligned} \tag{1.167}$$

[6] We leave the interested reader to think about the burden, for instance in terms of power consumption, of having a receiver that needs to demodulate and process a wideband signal that carries the information of all the users belonging to the same network cell when its own data represents only a fraction of it.

Here, β_k stands for the relative power of the kth code. This parameter depends on the data rate used with the associated code.

Practically speaking, if the characteristics of the Walsh–Hadamard codes are good in terms of orthogonality, we get that this is obviously not true in terms of autocorrelation. This can be a problem in terms of both the initial synchronization to the network, and the PSD of the resulting modulating waveform. This explains why additional scrambling codes, $\tilde{sc}$, are used in practice for that purpose. Even if not true in the considered standard, we can assume for the sake of simplicity that their length is the same as that of the channelization codes. This then leads to a modulating chip sequence $\tilde{c}(t)$ that finally takes the form

$$\tilde{c}(t) = \sum_{m} \sum_{n=0}^{L-1} \tilde{sc}(n) \sum_{k=1}^{K} \beta_k \tilde{S}_k(m) a_k(n) \delta(t - nT_\mathrm{c} - mT). \tag{1.168}$$

We observe that, in contrast to what happens for the Walsh–Hadamard codes, the $\tilde{sc}(n)$ elements of those additional scrambling codes are complex numbers. They thus scramble together the data from the real and imaginary parts of the constellation recovered after channelization. It is then of interest to mention that in the WCDMA standard, at least on the uplink side, this scrambling sequence takes a particular form in order to limit the modulated signal PAPR. This particular scheme, referred to as hybrid phase shift keying (HPSK), avoids, or at least limits, the zero crossings of the modulating waveform trajectory in the complex plane. It can thus be compared to the mechanism discussed in the previous section for minimizing the same parameter in the modified 8PSK scheme of the GSM/EDGE standard. We need not give too much detail in the present case, as the modified 8PSK scheme is already a good example of such optimization. Nevertheless, it highlights that the statistical parameters of the modulating waveform are of particular importance for the efficiency of the implementation of the RF/analog part of a transmitter at least. We can then understand why we need to consider the optimization of such parameters at the early stages of the derivation of a wireless standard.

Having derived the sequence of modulating chips $\tilde{c}(t)$ with both good orthogonality properties to allow recovery of the different data channels, and good autocorrelation properties to allow for white behavior, it remains to apply a pulse shaping filter in order to shape correctly the spectrum of the modulating waveform. In the standard being considered, this filter is a root raised cosine (RRC) filter defined by its impulse response,

$$h_\mathrm{RRC}(t) = \frac{\sin\left(\pi \frac{t}{T_\mathrm{c}}(1-\alpha)\right) + 4\alpha \frac{t}{T_\mathrm{c}} \cos\left(\pi \frac{t}{T_\mathrm{c}}(1+\alpha)\right)}{\pi \frac{t}{T_\mathrm{c}}\left(1 - \left(4\alpha \frac{t}{T_\mathrm{c}}\right)^2\right)}, \tag{1.169}$$

with

$$h_\mathrm{RRC}(0) = (1-\alpha) + \frac{4\alpha}{\pi} \tag{1.170}$$

and

$$h_{\text{RRC}}\left(\pm\frac{T_{\text{c}}}{4\alpha}\right) = \frac{1}{2}\left[\frac{4\alpha}{\pi}\sin\left(\frac{1-\alpha}{\alpha}\frac{4}{\pi}\right)\right.$$
$$\left. + (1+\alpha)\sin\left(\frac{1+\alpha}{\alpha}\frac{4}{\pi}\right) - (1-\alpha)\cos\left(\frac{1-\alpha}{\alpha}\frac{4}{\pi}\right)\right]. \qquad (1.171)$$

Here, α is the roll-off factor of the filter, set to 0.22 in the present case. Now the complex envelope of the modulating signal, $\tilde{s}(t)$, that results from the RRC filtering of equation (1.168) can be written as

$$\tilde{s}(t) = \sum_{m}\sum_{n=0}^{L-1}\tilde{sc}(n)\sum_{k=1}^{K}\beta_k\tilde{S}_k(m)a_k(n)h_{\text{RRC}}(t - nT_{\text{c}} - mT). \qquad (1.172)$$

The corresponding real and imaginary parts of $\tilde{s}(t) = p\,(t) + \mathrm{j}q\,(t)$, can therefore be expressed as

$$p\,(t) = \sum_{m}\sum_{n=0}^{L-1}\sum_{k=1}^{K}\beta_k a_k(n)\mathrm{Re}\{\tilde{S}_k(m)\tilde{sc}(n)\}h_{\text{RRC}}(t - nT_{\text{c}} - mT), \qquad (1.173a)$$

$$q\,(t) = \sum_{m}\sum_{n=0}^{L-1}\sum_{k=1}^{K}\beta_k a_k(n)\mathrm{Im}\{\tilde{S}_k(m)\tilde{sc}(n)\}h_{\text{RRC}}(t - nT_{\text{c}} - mT). \qquad (1.173b)$$

This results in the spectral shape for $\tilde{s}(t)$ shown in Figure 1.16. Alternatively, it is of interest to note that the impulse response defined by equation (1.169) has non-zero values at instants $t_s = sT_{\text{c}}$. Hence, ISI exists in the resulting modulating waveform. Nevertheless, this filter being a Nyquist filter, the self-convolution of its transfer function leads to an ISI-free signal, as illustrated in Section 4.4. This explains why this filter, used as a pulse shaping filter on the transmit side, is also implemented on the receive side of transceivers belonging to this system.

Having derived the structure of $\tilde{s}(t)$, we can now focus on the statistical properties of this modulating waveform. From equation (1.173), we can understand that the statistical characteristics of the modulating waveform obviously depend on the number of data codes that are summed together. Indeed, assuming that the data symbols are statistically independent and evenly distributed in the complex plane, we can expect that the more codes are summed, the more the distributions of the real and imaginary parts of the complex envelope $\tilde{s}(t) = p\,(t) + \mathrm{j}q\,(t)$ tend toward a centered Gaussian distribution thanks to the central limit theorem. In that case, recalling the discussion in Section 1.2, we can expect that $\rho(t) = |\tilde{s}(t)|$ tends toward a Rayleigh distribution. This behavior is indeed confirmed by comparing the simulation results shown in Figures 1.17 and 1.18 that correspond to uplink WCDMA modulating waveforms based on either one or four data codes. We see that when only one code is used, the CF of $p\,(t)$ or $q\,(t)$ is around 2, i.e. 6 dB, whereas the PAPR of the modulation is found to be 1.45, i.e. 3.2 dB. But when four codes are used, the CF on $p\,(t)$ or $q\,(t)$ attains a value of 3, i.e. 9.6 dB, whereas the PAPR is simulated to reach 2.2, i.e. 6.8 dB. In addition, we observe that even if the use of the HPSK scheme allows us to reduce the modulation PAPR, we still have

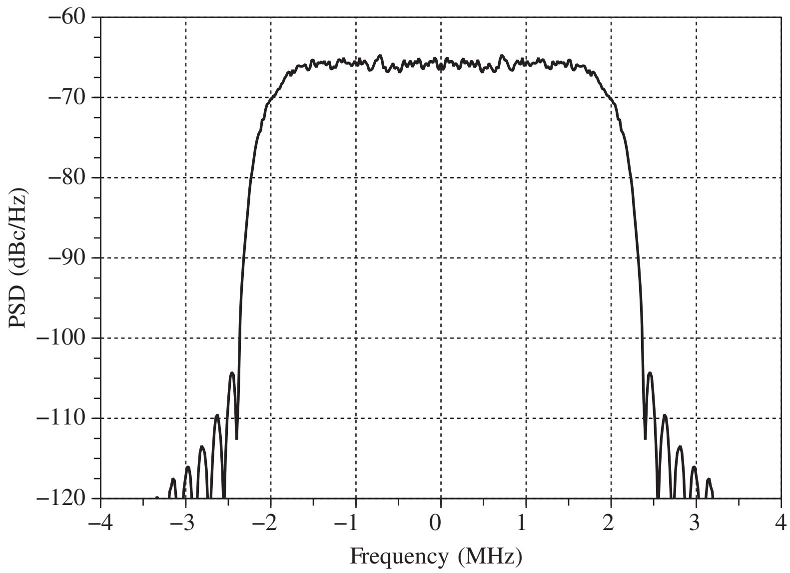

Figure 1.16 Power spectral density of a randomly modulated WCDMA complex envelope – Due to the properties of the scrambling codes defined in the standard, the spectrum of a WCDMA signal remains white within the bandwidth of the RRC filter. The spectral side lobe heights then depend mainly on the RRC filter implementation in terms of the impulse response length.

the minimum value of the modulus $\rho(t)$ of the complex envelope that can go close to 0 when the number of data codes increases. In contrast to what happens with the modified 8PSK modulation discussed in the previous section, we can expect in the present case to be faced with a huge DR for the instantaneous amplitude of the resulting modulated bandpass signal as well as wideband instantaneous frequency variations. We may thus conclude at first glance that this kind of waveform is not well suited to polar transmitter architectures, as discussed in Section 8.1.6.

OFDM

Let us now turn our attention to the modulating waveforms that can be encountered in wireless systems based on the OFDM technique. To understand their statistical properties, we first need to detail the construction of such waveforms. Practically speaking, the idea behind the OFDM is to use different subcarriers, which can be seen as orthogonal in a given sense, to multiplex the information, rather than orthogonal codes as in WCDMA systems. More precisely, the modulating waveform is constructed as the succession of slices of time domain waveforms of duration T_s, each one resulting from the superposition of $2N + 1$ subcarriers of the form $s_k(t) = \cos(2\pi f_k t)$. Here, the number of subcarriers is chosen as odd only for the sake of simplicity in our formulations. Each of those subcarriers is then in turn modulated – either in amplitude, phase, or both – in order to carry one data symbol $\tilde{S}_k$. These data symbols can result from the symbol mapping of any classical modulation scheme as a QPSK, QAM or

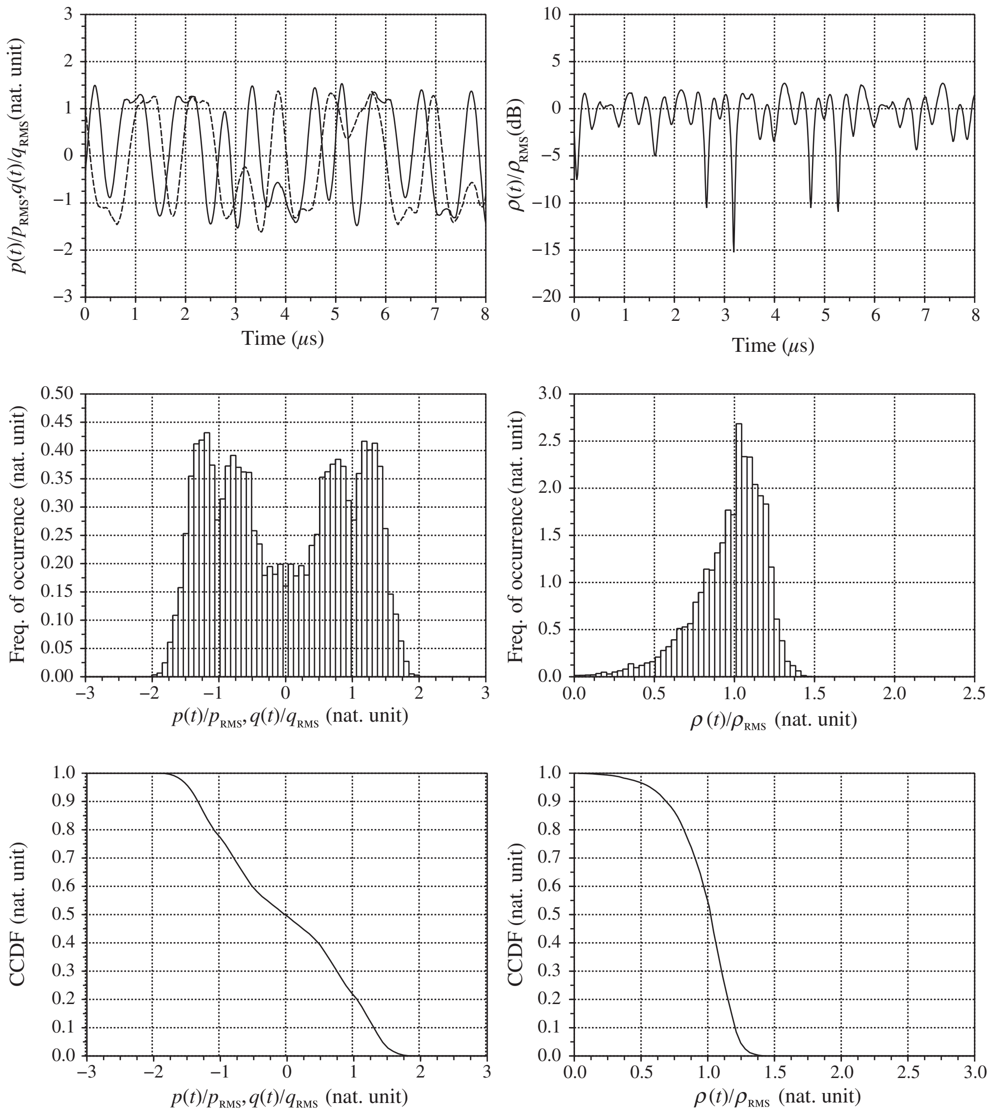

Figure 1.17 Statistical characteristics of a randomly modulated WCDMA complex envelope in the case of a single data code – The real and imaginary parts $p(t)$ (top left, solid) and $q(t)$ (top left, dashed) of the WCDMA uplink complex envelope when one data code is used have a distribution that is bounded by ± 2 times their RMS value (middle left). Therefore their CCDF reaches 0 for $p(t) = 2p_{\text{RMS}}$ or $q(t) = 2q_{\text{RMS}}$ (bottom left). The CF of those waveforms is thus equal to 2, i.e. 6 dB. The corresponding modulus $\rho(t)$ (top right) can reach 1.45 or 3.2 dB above its RMS value (middle right). This upper bound for $\rho(t)$ corresponds to the modulation PAPR as recovered on the CCDF of this parameter (bottom right).

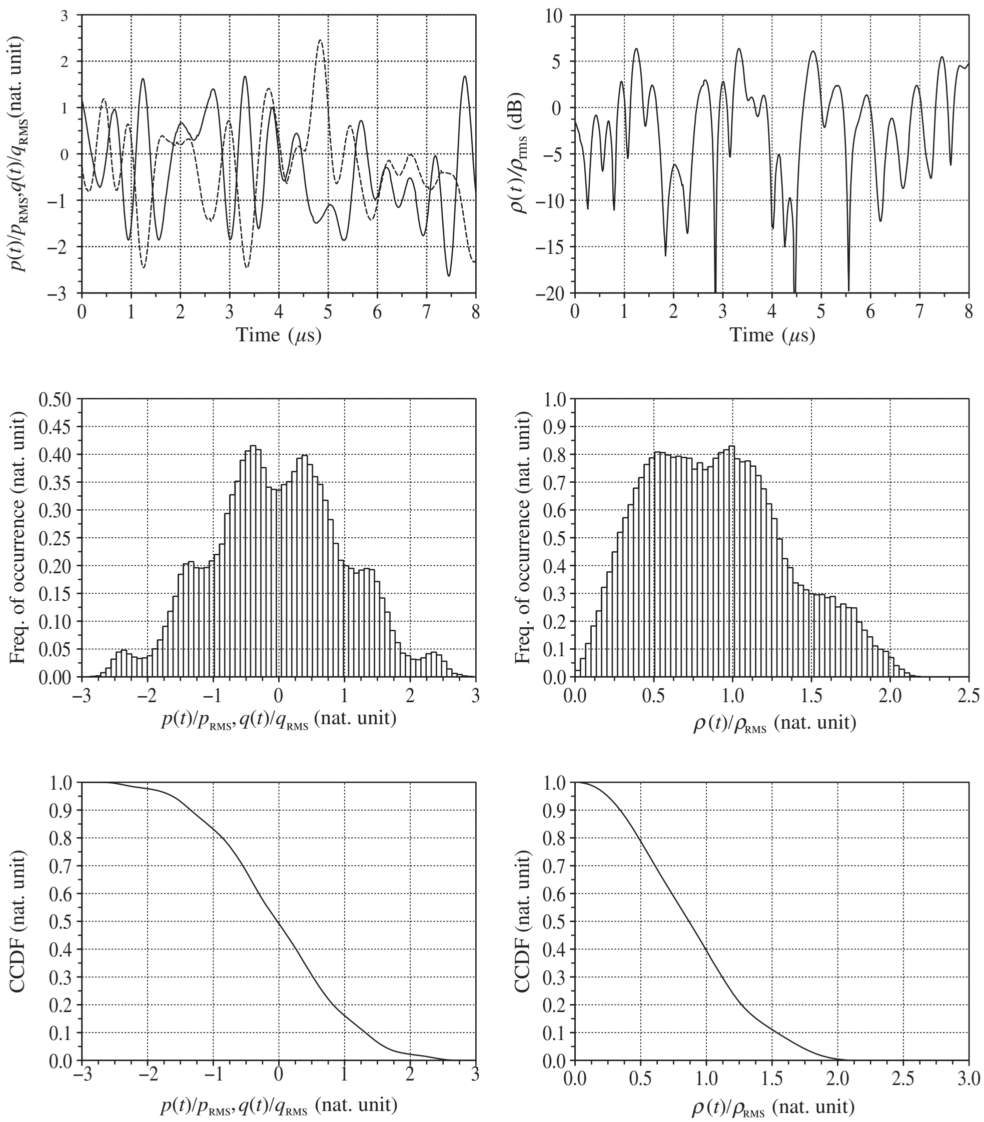

Figure 1.18 Statistical characteristics of a randomly modulated WCDMA complex envelope in the case of four data codes – The real and imaginary parts $p(t)$ (top left, solid) and $q(t)$ (top left, dashed) of the WCDMA uplink complex envelope when four data codes are used have a distribution that is bounded by ± 3 times their RMS value (middle left). Therefore their CCDF reaches 0 for $p(t) = 3p_{RMS}$ or $q(t) = 3q_{RMS}$ (bottom left). The CF of those waveforms is thus equal to 3, i.e. 9.6 dB. The corresponding modulus $\rho(t)$ (top right) can reach 2.2 or 6.8 dB above its RMS value (middle right). This upper bound for $\rho(t)$ corresponds to the modulation PAPR as recovered on the CCDF of this parameter (bottom right).

JWST466-c01 JWST466-Baudin Printer: Yet to Come September 19, 2014 11:56 Trim: 244mm × 170mm

whatever. Such a slice of modulating waveform is then called an OFDM symbol, and thus T_s represents the OFDM symbol duration. In addition, the subcarriers $s_k(t)$ are chosen so that their frequencies f_c are equally distributed on each side of the carrier. With our present assumptions, these frequencies are thus of the form $f_k = f_c + k\delta f$ with $k = -N, \dots, N$. This periodicity in the frequency domain in fact allows us to achieve the orthogonality we were referring to, as can be understood when examining the expression for the complex envelope $\tilde{s}_l(t)$ of the modulated bandpass signal carrying the lth OFDM symbol. Assuming that we are dealing with complex envelopes defined as centered around the carrier frequency, we can refer to the definitions given in Section 1.1.2 to see that the corresponding complex envelope of the kth subcarrier $s_k(t) = \cos(2\pi f_k t)$ can be directly written as $e^{j2\pi k\delta f t}$. Thus, given that all the complex envelopes we are dealing with are defined as centered around the same frequency, we can immediately write $\tilde{s}_l(t)$ as the sum of the complex envelopes of the N subcarriers,

$$\tilde{s}_l(t) = [\mathrm{U}((l-1)T_s) - \mathrm{U}(lT_s)] \sum_{k=-N}^{N} \tilde{S}_{k,l}\, e^{j2\pi k\delta f t}. \tag{1.174}$$

Here, U(.) stands for the Heaviside step function and $\tilde{S}_{k,l}$ represents the data symbols carried by the kth subcarrier during the lth OFDM symbol. We then observe that due to the periodicity in the subcarrier spacing, the transposition of this expression in the sampled time domain leads to a discrete Fourier transform that links the values of the data symbols carried by each subcarrier to the values of the time domain samples of the corresponding OFDM symbol. In that case we get that the OFDM symbol duration T_s is inversely proportional to the subcarrier frequency spacing δf, thus leading to the orthogonality between vectors composed of the sample of each subcarrier. Finally, the complex envelope $\tilde{s}(t)$ of the overall modulated signal carrying the succession of OFDM symbols can be written as

$$\tilde{s}(t) = \sum_{l} \tilde{s}_l(t). \tag{1.175}$$

Having derived the structure of $\tilde{s}(t)$ for a general OFDM signal, we can now focus on its characteristics. We will use a concrete example by way of illustration. We examine the 10 MHz bandwidth long-term evolution (LTE) downlink signal that corresponds in the configuration considered to an OFDM modulation composed of 600 useful subcarriers separated by a frequency offset of 15 kHz. This results in a complex envelope signal whose spectrum is spread over the band $[-4.5, 4.5]$ MHz. Obviously, the first consequence of summing subcarriers that are evenly distributed in the frequency domain and carry the same power on average is that the PSD of the resulting complex envelope is expected to be almost flat. This is indeed confirmed by inspecting the spectrum shown in Figure 1.19. Nevertheless, we observe that in the present case, even if not visible in the figure, a non-negligible amount of power necessarily leaks in the adjacent channels through the secondary lobes of the sinc function resulting from the lack of time domain windowing of the OFDM symbols. But due to the orthogonality resulting from the discrete Fourier transform approach, this leakage can be made visible only through an oversampling of the corresponding waveforms, which is obviously not done here.

Let us now focus on the statistical characteristics of such modulating waveform. Practically speaking, in most of the standards based on an OFDM technique, the number of subcarriers

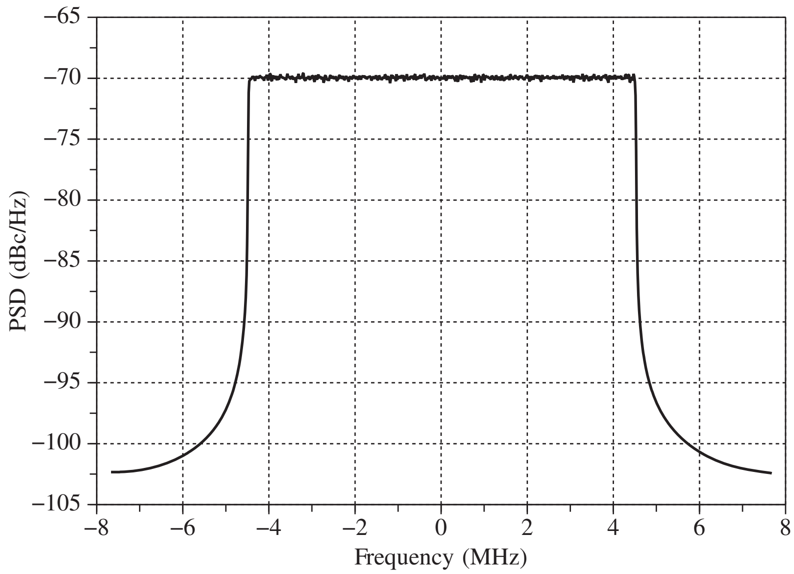

Figure 1.19 Power spectral density of a randomly modulated OFDM complex envelope – An LTE downlink waveform using 600 useful subcarriers separated by a frequency offset of 15 kHz exhibits a PSD that spreads over the band $[-4.5, 4.5]$ MHz.

involved in the generation of the modulating waveforms is important, as illustrated by our LTE example. Thus, referring to equation (1.174), we see that the real and imaginary parts of the complex envelope $\tilde{s}(t) = p(t) + \mathrm{j}q(t)$ result from the summation of a great number of data symbols. Thus, as long as they can be considered as evenly distributed in the complex plane and statistically independent, both $p(t)$ and $q(t)$ tend to have a centered Gaussian distribution according to the central limit theorem. In that case, from the discussion in Section 1.2.1, we can also expect that the modulus $\rho(t)$ of $\tilde{s}(t)$ tends to have a Rayleigh distribution. Those behaviors are confirmed by the simulations shown in Figure 1.20. There is indeed an obvious fit between the histograms of those waveforms and the theoretical Gaussian and Rayleigh distributions displayed in the same graphs. Nevertheless, even if there is such a good agreement, the fact is that the summation of the subcarriers remains finite in the definition of $\tilde{s}(t)$. This means that the maximum values of the modulating waveforms remain well defined and cannot reach infinity. Practically speaking, those values can be used to derive the CF and PAPR of the modulating waveforms as defined in “Peak to average power ratio and crest factor” (Section 1.1.3). As an example, we can reconsider our former 10 MHz bandwidth LTE downlink signal. In that case, time domain simulations lead to both a CF for $p(t)$ and $q(t)$ of around 5, i.e. 14 dB, and a PAPR of around 3.6, i.e. 11.1 dB. We observe that these numbers are larger than what could be expected when considering the complementary cumulative distribution function (CCDF) curves shown in Figure 1.20. The reason for this behavior is that the exact maximum values reached by the waveforms during such a time domain simulation correspond to a very low probability of occurrence. This justifies having a statistical definition for the CF and the PAPR that reflects this behavior. Obviously, the exact thresholds to be considered

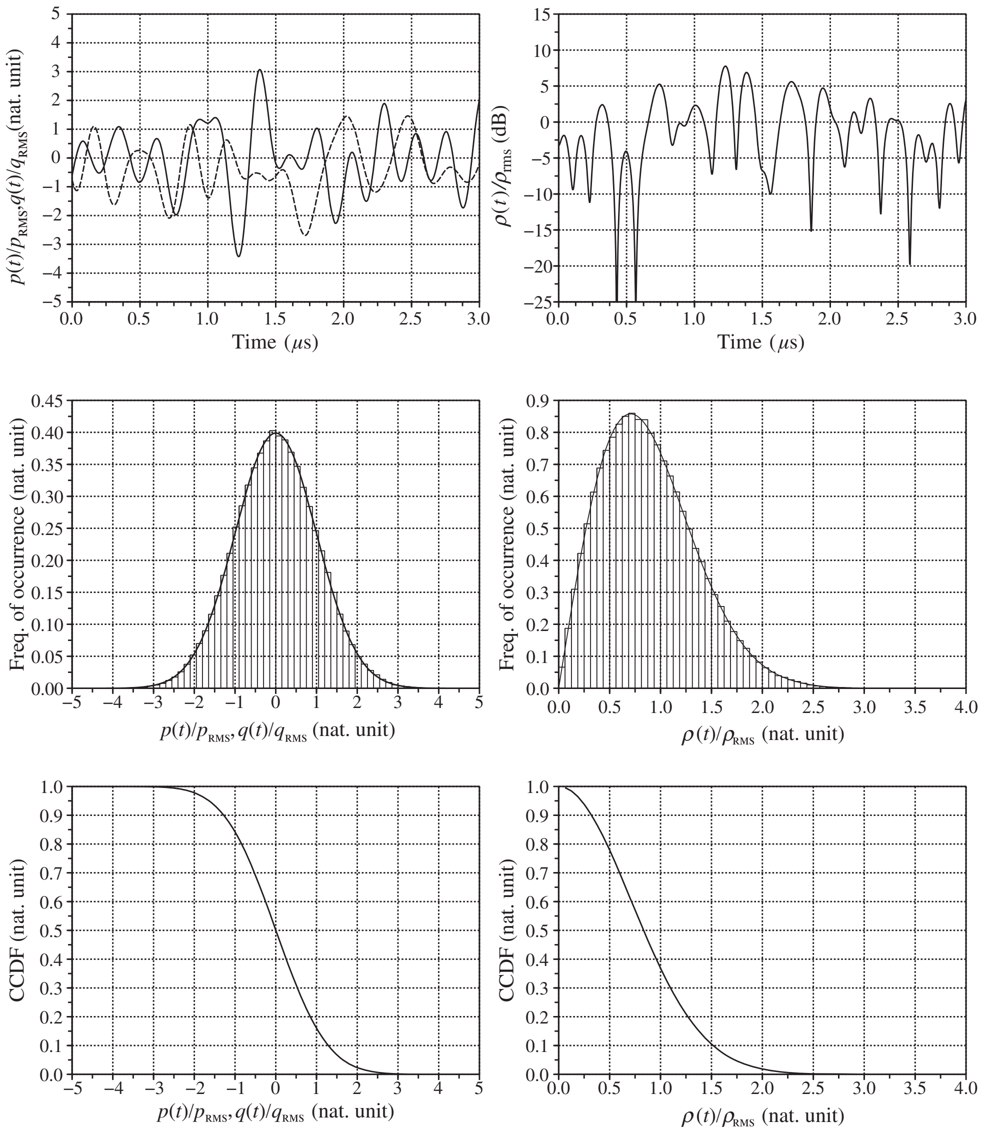

Figure 1.20 Statistical characteristics of a randomly modulated OFDM complex envelope – The real and imaginary parts $p(t)$ (top left, solid) and $q(t)$ (top left, dashed) of an OFDM complex envelope tend to have a Gaussian distribution (middle left), but with a deterministic maximum value due to the finite summation of the subcarriers. Using the statistical definition for the maximum values, their CCDF reaches 0.001 for $p(t) = 3.1p_{\text{RMS}}$ or $q(t) = 3.1q_{\text{RMS}}$ (bottom left). The CF of those waveforms thus reaches 9.8 dB. The modulus $\rho(t)$ (top right) follows a Rayleigh distribution and can reach 2.2 times its RMS value (middle right). This corresponds to the modulation PAPR as recovered on the CCDF of $\rho(t)$ (bottom right).

to decide whether or not a frequency of occurrence has negligible impact on the average performance of a line-up should be refined. It is realistic to define the peak value of those waveforms as the value for which their CCDF reaches 0.001. In other words, we can define the peak value of $p(t)$ or $q(t)$ as the upper bound below which those waveforms are 99.9% of the time. Applying this definition to $p(t)$, for instance, we get that its peak value p_{pk} is defined from equation (1.75) such that

$$F_{\text{c}}(p_{\text{pk}}) = 0.001. \tag{1.176}$$

Assuming a Gaussian distribution for this parameter, we get that its CCDF is given by

$$F_{\text{c}}(p_{\text{pk}}) = \frac{1}{2}\text{Erfc}\left(\frac{1}{\sqrt{2}}\frac{p_{\text{pk}}}{p_{\text{RMS}}}\right), \tag{1.177}$$

with Erfc(.) the complementary error function defined by equation (1.149). It then follows that the CF of $p(t)$, defined as the ratio $p_{\text{pk}}/p_{\text{RMS}}$, is approximately equal to 3.1, or 9.8 dB, for such a Gaussian waveform. This is in line with the values that can be deduced from the CCDF shown in Figure 1.20 and should be compared to the 14 dB derived previously. We thus see more than a 4 dB reduction in the evaluation of the CF, merely by considering a realistic upper bound that takes into account the frequency of occurrence of the peak values. The same can obviously be done for the modulating waveform PAPR. Recall that, according to equation (1.84), the PAPR must remain around 3 dB lower than the CF of the $p(t)$ or $q(t)$ waveforms. This then results in a direct estimation of this quantity in the region of 7 dB, i.e. 2.2 in natural units. Here again, this is in line with the CCDF of $\rho(t)$ displayed in Figure 1.20.

To conclude this review, we highlight that even when taking into account the low probability of occurrence of the peak values of the waveforms in the dimensioning of a line-up, we get that such OFDM signals still exhibit really high PAPR. This is one of the main reasons for the use of a slightly different modulation scheme for the uplink in the LTE standard. For that scheme, chosen modulation is indeed based on the single carrier frequency division multiple access (FDMA) scheme rather than a pure OFDM one. The idea behind this is to introduce some correlation terms between the symbols used to modulate each subcarrier so that their sum no longer tends toward a normal distribution as would be the case if they were statistically independent. This correlation, introduced through the use of an extra discrete Fourier transform, is enough in practice to quite significantly reduce the PAPR of the modulated signal compared to the case of a pure OFDM scheme. In that sense, this approach can be related to what has already been encountered in both the modified 8PSK scheme of the GSM/EDGE standard and in the HPSK scheme of the WCDMA. This is thus another example of an optimization of a modulation scheme that allows for greater efficiency in the physical implementation of the transmit side.

1.4 First Transceiver Architecture

Based on what we have done so far in this chapter, we can already derive first block diagrams for transceiver architectures based on the signal processing functions involved in the modulation and demodulation of an RF bandpass signal. Here we continue with the general case of a complex modulation. These structures, which can be seen as the minimal ones that enable transceiver functionality, are then further completed in the subsequent chapters by taking into account the constraints linked to other aspects of wireless systems as well as the limitations of their physical implementation. This will lead to the practical architectures discussed in Chapter 8.

When considering this minimum set of functions derived from the communication theory, it is hard to totally get rid of additional constraints linked to their physical implementation if we want to keep the approach realistic. Despite this, we try to stay as much as possible at a theoretical level at this first stage.

1.4.1 Transmit Side

Let us focus for now on the architectures that can be derived from the signal processing involved in the generation of a complex modulated RF bandpass signal as encountered on the transmit side. Based on the foregoing, we understand that the signal processing we are referring to reduces on the one hand to the generation of the modulating waveform in itself, and on the other hand to the modulation of an RF carrier according to this complex lowpass signal in order to obtain the expected modulated RF bandpass signal. From the discussion in Section 1.1.2, we see that there are basically two different approaches for achieving such a modulation process, depending on the chosen representation of the complex lowpass modulating waveform. Here, by "representation", we mean either Cartesian or polar. We can thus expect two different families of transmit architectures, depending on the chosen representation.

Let us first suppose that we are dealing with a Cartesian representation of the complex lowpass modulating waveform $\tilde{s}(t) = p\,(t) + \mathrm{j}q\,(t)$. By equation (1.28a), the resulting modulated bandpass signal $s(t)$ can be expressed as

$$\begin{aligned} s(t) &= \mathrm{Re}\left\{\tilde{s}(t)\mathrm{e}^{\mathrm{j}\omega_{\mathrm{c}}t}\right\} \\ &= p\,(t)\cos(\omega_{\mathrm{c}}t) - q\,(t)\sin(\omega_{\mathrm{c}}t). \end{aligned} \tag{1.178}$$

Starting from this equation, as highlighted above, we then need to take into account a minimum set of constraints linked to the physical implementation of the corresponding signal processing functions in order to derive a realistic overview of the line-up. For instance, recalling the examples of modulating waveforms reviewed in Section 1.3, we can understand that the complexity associated with the mathematical operations required for their generation leads to having those operations implemented in the digital domain. As a result, we then need to consider the generation of digital samples $p\,[k] = p\,(kT_{\mathrm{s}})$ and $q\,[k] = q\,(kT_{\mathrm{s}})$ of the real and imaginary parts of the complex modulating signal. These samples are then necessarily converted at a given point in the analog domain. In the present case, we can assume this is done through the use of a digital to analog converter (DAC) that delivers analog baseband signals. Anticipating Section 4.6.2, we observe that such conversion requires in most practical implementations the use of a reconstruction filter in order to cancel the copies still present, even if attenuated, at the output of the DAC. At this stage, we then achieve the generation of analog $p\,(t)$ and $q\,(t)$ signals. It thus remains to achieve the modulation of the RF carrier through the implementation of the operation corresponding to the above equation.

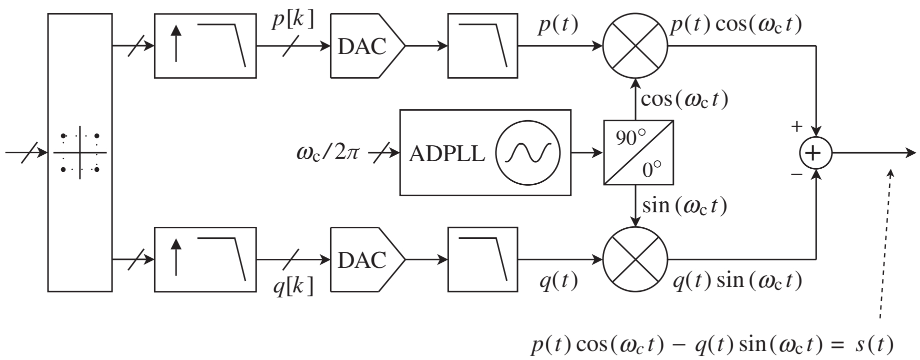

Figure 1.21 Modulated RF bandpass signal generated through the direct upconversion of the complex modulating waveform – Using the Cartesian representation of a complex lowpass modulating waveform $\tilde{s}(t) = p(t) + jq(t)$, we can derive an implementation for the generation of the corresponding modulated RF bandpass signal through a direct complex frequency upconversion of the modulating signal. This structure is thus referred to as the direct conversion transmitter.

For that purpose, we obviously need to generate the two LO signals in quadrature, $\cos(\omega_c t)$ and $\sin(\omega_c t)$. This can be done through the use of an RF synthesizer, classically implemented as a PLL that locks the oscillating frequency of an RF oscillator to that of an accurate low frequency reference, as discussed in Section 4.3.1. In the present case this reference is not represented in Figure 1.21 for the sake of simplicity, and the PLL is assumed to be an all digital one [11]. Having generated the LO signals, we can then achieve the generation of the modulated bandpass signal we are looking for through their multiplication by the lowpass signals $p(t)$ and $q(t)$, using RF mixing stages for instance, and then subtracting the result. All this results in the structure shown in Figure 1.21. Practically speaking, this structure is a simplified view of a direct conversion, or (zero intermediate frequency, or ZIF), transmitter. This widespread architecture is discussed in more depth in Section 8.1.1, and taken as an example in Chapter 7.

Turning now to a polar representation of the complex lowpass modulating waveform $\tilde{s}(t) = \rho(t)e^{j\phi(t)}$, the resulting modulated bandpass signal $s(t)$ can be expressed according to equation (1.28b) as

$$\begin{aligned} s(t) &= \mathrm{Re}\left\{\tilde{s}(t)e^{j\omega_c t}\right\} \\ &= \rho(t)\cos(\omega_c t + \phi(t)). \end{aligned} \tag{1.179}$$

However, in the present case we again need to take into account a minimum set of constraints linked to the physical implementation of the signal processing functions we are considering for the derivation of a realistic block diagram. Thinking back to the examples reviewed in Section 1.3, we observe that most of the practical modulating waveforms we are dealing with are defined through their generation in a Cartesian way. As discussed in more depth in Section 8.1.6, there are obviously good reasons for that. In our present polar approach a Cartesian to polar conversion is necessary in order to generate the samples $\rho[k]$ and $\phi[k]$ from the Cartesian $p[k]$ and $q[k]$. We observe that the constant amplitude part of $s(t)$, i.e. $\cos(\omega_c t + \phi(t))$, can be seen as a pure carrier signal, but with a angular frequency that is varying according to the phase modulation term $\phi(t)$. As a result, even if it should obviously be refined, this signal can be generated through the modulation of the PLL that delivers the carrier signal according to the expected instantaneous frequency $f(t)$. Practically speaking, we get from equation (1.97) that $f(t)$ is linked to the carrier frequency and to the argument of the modulating complex envelope through

$$f(t) = \frac{1}{2\pi}\left(\omega_{\mathrm{c}} + \frac{\mathrm{d}\phi(t)}{\mathrm{d}t}\right). \tag{1.180}$$

As a result, we need to differentiate $\phi(t)$ in order to be able to generate the samples $f[k]$ of $f(t)$ that are further provided to the PLL. Once this is done, it then simply remains to apply the instantaneous amplitude to the constant amplitude signal flowing from the PLL to obtain the expected modulated RF bandpass signal. This can be achieved, for instance, through the use of a variable gain amplifier (VGA), or through a mixing stage that uses this constant amplitude waveform as an LO signal to upconvert the instantaneous amplitude signal $\rho(t)$. As this multiplication is performed in the analog domain, $\rho(t)$ can be reconstructed from the samples $\rho[k]$ through a DAC and a reconstruction filter. The resulting structure shown in Figure 1.22 is a simplified view of the polar transmit architecture that is discussed in more depth in Section 8.1.6.

1.4.2 Receive Side

Let us now focus on the architectures that can be derived from the signal processing corresponding to the recovery of the complex envelope $\tilde{s}(t)$ of a bandpass RF signal $s(t)$ as involved on the receive side. Following the discussion in Section 1.1.2, we get from equation (1.23)

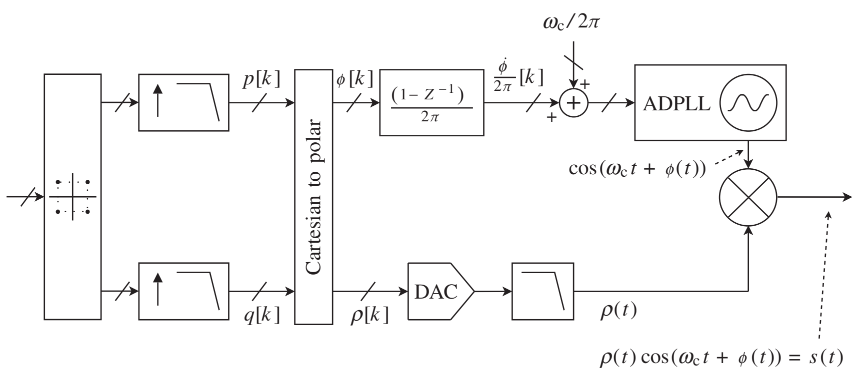

Figure 1.22 Modulated RF bandpass signal generated through a direct instantaneous frequency and amplitude modulation – Using the polar representation of a complex lowpass modulating waveform $\tilde{s}(t) = \rho(t)\mathrm{e}^{\mathrm{j}\phi(t)}$, we can derive an implementation for the generation of the corresponding modulated RF bandpass signal based on the direct modulation of its instantaneous frequency and amplitude. This structure is referred to as a polar transmitter.

that the real and imaginary parts of $\tilde{s}(t) = p(t) + jq(t)$ can be recovered through the use of a Hilbert transform of $s(t)$ and of dedicated mixing stages using LO signals at the carrier angular frequency. Nevertheless, even if such a Hilbert transform can be implemented for bandpass signals using a pure $\pi/2$ phase shifter as discussed in that section, this approach is not the easiest way forward from the physical implementation perspective. Moreover, it requires a double mixing stage for its correct implementation.

Alternatively, the complex envelope $\tilde{s}(t)$ can be obtained through the use of a complex frequency downconversion followed by a lowpass filtering, as detailed in Chapter 6. With such an approach, we are faced with a situation symmetrical to that encountered on the transmit side when considering the frequency upconversion of the complex modulating waveform expressed in its Cartesian form. Transposed to the present receive case, it results in the simplified view shown in Figure 1.23. Anticipating the discussion in the following chapters, we observe that the signal being processed in a receiver is often composed of both the wanted signal and of unwanted ones linked to the coexistence with other users. As a result, the lowpass filtering dedicated to the cancellation of the unwanted sideband of the wanted signal in the signal processing approach associated with the complex frequency downconversion is also used in practice to cancel, or at least attenuate sufficiently, the unwanted signals. In that sense, it also behaves as an anti-aliasing filter prior to the analog to digital converter (ADC) stage according to the arguments of Section 4.6.1. Such conversion to the digital world is indeed required in practice due to the complexity of the signal processing associated with channel equalization, in particular in a mobile environment, as highlighted in Chapter 2. Here again, we can thus make the link with what was encountered on the transmit side with the complexity of the generation of practical modulating waveforms used in the field of digital communication. Furthermore, we may also mention the interest there is in using the integration capabilities of modern silicon processes for digital logic. The resulting structure shown in Figure 1.23 is a simplified view of a direct conversion, or ZIF receiver. As was the case for its counterpart on the transmit side, this receive architecture is also in widespread use for low cost integrated solutions. As such, it is discussed in more depth in Section 8.2.1, and taken as an example in Chapter 7.

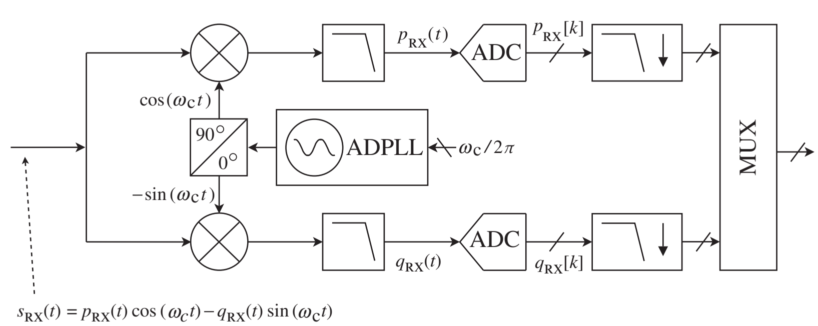

Figure 1.23 Complex envelope recovery using a direct complex frequency downconversion of a modulated bandpass RF signal – The use of a complex frequency downconversion associated with a lowpass filtering on the two branches allows the recovery of the real and imaginary parts of a modulating complex envelope.

To conclude, we observe that we could alternatively imagine recovering the instantaneous frequency and amplitude of the received RF bandpass signal using a sort of polar demodulator that would be the symmetric implementation of the polar transmitter. However, because of various problems this kind of structure is not necessarily considered in practice except in the notable case of a pure frequency modulation. In that case, a PLL can indeed be used to directly recover the instantaneous frequency of the received signal, thus leading to a very compact solution. Such a PLL demodulation scheme is discussed in Section 8.2.4.